Author: J. C. Benedyk

Composition limits of H-13 based on the AISI/UNS (T20813) standards are (mass %): 0.32-0.45 C, 0.20-0.50 Mn, 0.80-1.20 Si, 4.75-5.50 Cr, 0.30 max Ni, 1.10-1.75 Mo, 0.80-1.20 V, 0.250 max Cu, 0.03 max P, and 0.03 max S. Where specified, as resulfurized H-13, sulfur may be increased to 0.06-0.15% to improve machinability.

Besides the standard H-13 grade, various modified, premium, and superior grades of H-13 are available from hot work steel producers, usually with limiting phosphorus and/or sulfur levels that are below the standard composition limits to improve toughness and thermal fatigue resistance and containing principle alloying elements in particular ranges that may be outside the T20813 standard. Also, the premium grades of H-13 within T20813 composition limits are generally produced by special refining and metallurgical practices to control microstructure and especially carbide size and distribution.

1.0 General

This medium alloy, martensitic, air hardening, ultrahigh-strength steel is similar to H-11 and H-11 Mod in composition, heat treatment, and many properties. The steels H-11, H-11 Mod, and H-13 exhibit several properties that are important in airframe and landing gear applications, including the ability to be heat treated to an ultimate tensile strength of 300 ksi while having excellent thermal shock resistance. These grades are typically hardened by austenitizing and cooling in air, flowing inert gas, oil, or hot salt bath. Upon tempering, they show secondary hardness maxima in their tempering curves and, upon being double or triple tempered at 1050-1100F, typically develop the combination of high hardness (44-48 R_c) and high room temperature ultimate tensile strength (220-250 ksi) combined with good fracture toughness and maximum fatigue strength at room and elevated temperatures. H-13 steel is not as commonly used as H-11 Mod as a constructional steel in ultrahigh-strength applications, although it can be substituted for H-11 Mod in cases where availability or the slightly better wear resistance and other characteristics of H-13 offer advantages.

All these steels are susceptible to hydrogen embrittlement and, in structural applications, must be protected with a corrosion-resistant coating, even in mild atmospheric environments. Similarly, they must be protected against oxidation if exposed to air for prolonged periods of time at temperatures above 750F.

The main compositional difference between H-13 and H-11 Mod is higher vanadium content in H-13, which leads to a greater dispersion of vanadium carbides and higher wear resistance. The H-13 steel also has a slightly wider range of the other principal alloying elements, allowing producers flexibility in tailoring mechanical properties for given heat treatments and applications. Premium and superior grades of H-13 have carefully controlled compositions with low levels of sulfur and phosphorus and are produced by special melting, refining, and hot forging/rolling schedules primarily to achieve a fine microstructure and improve toughness and thermal fatigue resistance over conventionally produced H-13 grades. In a few cases, some H-13 producers employ long term, high temperature, homogenization techniques with controlled cooling to refine the carbide distribution and produce a more isotropic microstructure. Powder/particle metallurgy grades of H-13 are available with significantly refined distributions of carbides and sulfides (for the high sulfur, free machining grade) to improve toughness and thermal fatigue and wear resistance relative to conventional H-13 steel that is normally produced by ingot metallurgy. Careful consideration of H-13 supply will assure a cost effective selection of steel grade for a given application.

	Fe
5.0	Cr
1.5	Mo
1.0	V
0.35	C

Due to its good temper resistance and ability to maintain high hardness and strength at elevated temperatures, H-13 is one of the most widely used hot work die and mold materials for nonferrous and ferrous casting and hot forming operations or for molding of plastics. Dies and tools made of H-13 can withstand working temperatures of 1000F or more. The steel has deep hardening characteristics, thereby allowing large sections to be cooled in still or fan stirred air or by pressurized inert gas from austenitizing temperatures. It is the preferred material for aluminum and magnesium die casting dies as well as for many other hot work die and tooling applications, e.g., extrusion tools and containers, hot forging and stamping dies, hot shear blades, and plastic molds, where good thermal fatigue, hot erosion and wear resistance, and ability to maintain hot hardness during operations at temperatures up to 1000F or higher are important. Due to the good thermal shock resistance of H-13 in hardened tempers, dies and tools may be

internally water cooled in service to prevent undue softening. In many cases, H-13 hot work dies are nitrided or hard coated by other means to improve wear resistance. (Refs. 1–2)

1.1 Commercial Designations

H-13
H13 (Alternatively)
AISI H-13
Premium AISI H-13
ASTM H-13
SAE H-13
Material No. 1.2344
40CrMoV5
Cast Grade CH-13
GX40CrMoV5-1
X40CrMoV5

1.2 Other Designations

ESR H-13 (ESR – Electroslag Remelted)
8407 SUPREME (Assab)
8407 2M (Assab)
Orvar® Superior (Bohler-Uddeholm)
Orvar® 2M (Bohler-Uddeholm)
W302 SUPERIOR® (Bohler Uddeholm)
ISOBLOC® (Bohler Uddeholm)
No. 883® (Carpenter)
Extendo-Die® (modified H-13 composition by Carpenter)
Pyrotough® 78 (modified H-13 composition by Carpenter)
Nu-Die® V (Crucible Specialty Metals)
Nu-Die® XL (Crucible Specialty Metals)
Nu-Die® ESR (Crucible Specialty Metals)
DH2F (International Mold Steel)
MTEK T90813 (MetalTek)
THYROTHERM® 2344 EFS (ThyssenKrupp Specialty Steels)
THYROTHERM® 2344 EFS SUPRA (ThyssenKrupp Specialty Steels)
THYROTHERM® 2367 SUPRA ESR (ThyssenKrupp Specialty Steels)
THYROTHERM® 2344 ESR MAGNUM (ThyssenKrupp Specialty Steels)
VDC® H-13 (Timken Latrobe Steel. Timken sold Latrobe in December 2006, and it is now Latrobe Specialty Steels)
TLS® H-13 PQ (TLS – Timken Latrobe Steel. Timken sold Latrobe in December 2006, and it is now Latrobe Specialty Steels)
LSS® H-13 (Latrobe Specialty Steels)
LSS® H-13 PQ (Latrobe Specialty Steels)

1.3 Specifications

ASTM E45 Method A
ASTM E114
ASTM A388
ASTM A597
ASTM A681
SAE J437a
SAE J438b
SAE J467
UNS T20813
CAST UNS T90813
FED-QQ-T570
UNE 36072/2
BS 4659 BH-13 (UK)
BS 4659 H-13 (UK)
EN ISO 4957: 2000 XCrMoV5-1
AFNOR NFA35-590 Z 40 CVD 5 (France)
DIN 1.2344 (Germany)
DIN 17350 (Germany)
JIS SKD61 (Japan)
UNI X 35 CrMoV 05 KU (Italy)
SS 2242 (Sweden)
DC-9999-1 (GM Powertrain Group)
AMTD-DC2010 (FORD Advanced Manufacturing Technology Development)

1.4 Composition

The composition of H-13 can vary depending on the grade selected and particular offerings of specialty steel suppliers, who typically produce standard H-13 but may also produce premium and superior grades of H-13 that have lower than minimum levels of phosphorus and sulfur, are specially refined, usually by vacuum arc remelting (VAR), to reduce segregation and inclusions, lower gas (N, O, H) levels, and spheroidize non-metallics. Special forging practices are used on H-13 steel to break up coarse alloy carbides and achieve a fine microstructure. Modified versions of H-13 are also available from different H-13 steel producers with some alloying elements falling outside of the standard T20813 H-13 composition range in order to impart special properties for particular applications (Refs. 4–21).

As H-13 steel is so widely used in die casting dies, which require high die life to reach break-even costs, the North American Die Casting Association (NADCA) has specified compositions for both premium and superior grades of H-13 in their steel acceptance criteria and permissible limits of microcleanliness (Table 1.4.2). (Ref. 4) However, requirements for other applications are not as critical, and the standards for H-13 steel

acceptance for hot work dies and tooling differ depending on the industry.

1.4.1 *[Table]* Standard AISI/UNS chemical composition of H-13 steel and typical compositions of specially produced commercial grades of H-13 steel available from specialty steel companies (Refs. 1–21)

1.4.2 *[Table]* Chemical composition (weight %) of critical alloying elements and impurities in premium and superior quality grades of H-13 steel (Ref. 4)

1.4.3 *[Table]* Maximum allowable limits of nonmetallic inclusions according to ASTM E45 Method A for H-13 steel for premium and superior quality grades of H-13 steel (Ref. 4)

1.5 Heat Treatment and Microstructure

1.5.1 Normalizing

Normalizing is unnecessary and not recommended for H-13. (Ref. 3)

1.5.2 Annealing

Annealing must be done after hot working and before hardening or rehardening. Most H-13 material that is to be used for dies and tools that require machining is purchased in the annealed or soft condition at a typical annealed hardness of 192-235 HB. Annealing of H-13 is done by heating slowly and uniformly to 1575-1650F in a vacuum furnace, a controlled atmosphere furnace, or in a protective annealing pack to prevent decarburization. Holding time varies from one hour for thin sections and small furnaces to ten hours for heavy sections and large charges. For pack annealing, hold time is one hour per inch of cross section thickness. Upon removal from the furnace, H-13 should be cooled slowly (at 50F/h maximum) to about 1000F, then cooled at a faster rate to room temperature without affecting hardness. (Ref. 3)

This annealing treatment should result in a fully spheroidized microstructure with a grain size from ASTM 1 to ASTM 3. However, the microstructure of annealed H-13 steel varies, depending on previous metallurgical processing, and several microstructural standards have been established, including the often followed NADCA (North American Die Casting Association) acceptance microstructures for annealed H-13 steel used for die casting dies. Figure 1.5.2.1 shows acceptable (AS1-AS9) and unacceptable annealed microstructures (AS10-AS18) for H-13 steel according to NADCA specifications for H-13 tool steel used in die casting dies. Acceptable annealed microstructures consist of a ferritic matrix with a homogeneous distribution of spheroidized carbides when viewed at 500x after etching with 5% Nital. The numbering of the acceptable annealed microstructures from AS1 to AS9 does not denote a quality ranking, but shows typical variations within thick die blocks of H-13 steel. (Ref. 4)

Banding microsegregation, indicative of alternating layers of different composition aligned in the direction of primary hot working, is also typically monitored in annealed H-13 steel blocks, and excessive banding microsegregation is cause for rejection for sizes above four inches in thickness. Figure 1.5.2.2 shows acceptable and unacceptable banding microstructures according to NADCA specifications for H-13 tool steel used in die casting dies. (Ref. 4)

It should be noted that outside of NADCA and die casters, other major users of H-13 tool steel in hot work die/tooling applications or high-temperature structural components do not specify annealed microstructure of H-13 steel; rather chemical composition and hardness of the annealed H-13 steel are most commonly specified.

1.5.2.1 *[Figure]* Annealed quality "AS" microstructure chart for annealed H-13 steel showing acceptable (AS1-AS9) and unacceptable (AS10-AS18) microstructures according to NADCA—all microstructures at 500x and etched with 5% Nital (Ref. 4)

1.5.2.2 *[Figure]* Banding microsegregation chart for annealed H-13 steel blocks showing acceptable and unacceptable microstructures according to NADCA—all microstructures at 50x and etched with Villella's reagent (Ref. 4)

1.5.3 Stress Relieving

Stress relieving of annealed H-13 steel after rough machining and prior to finish machining and hardening is optional but is sometimes done to minimize distortion during hardening, especially for dies or tools with complex shapes. This is done by heating to 1200–1250F, holding for one hour per inch of cross section (minimum of one hour), then cooling slowly in air or in the furnace to about 400F then in air to room temperature. (Ref. 3)

Electro-discharge machining (EDM), commonly used in finish machining of die insert cavities made from hardened H-13 steel, can leave surface effects such as unwanted residual stresses that seriously affect tool life. Before stress relieving EDM-processed H-13 materials, the white layer should be removed by stone or sand blasting before stress relieving. Stress relieving after finish machining is done by heating to 1000-1050F (or 50F below the highest tempering temperature), holding for one hour per inch of cross section or

for two hours minimum, then cooling in still air to room temperature. (Refs. 20–21)

1.5.4 Hardening

Hardening heat treatment for H-13 steel by austenitizing and quenching, usually followed by tempering, is a critical factor in the performance of this material and must be carefully planned for optimal results. H-13 steel experiences very little dimensional changes and shape distortion upon quenching and tempering.

1.5.4.1 *[Figure]* Schematic of NADCA—recommended austenitizing, quenching, and tempering heat treatment cycle for H-13 steel (Ref. 4)

1.5.5 Austenitization/Quenching

For austenitizing, typically done at 1850–1900F and sometimes higher, surface protection against oxidation and decarburization is necessary by utilizing vacuum or controlled atmosphere furnaces, salt baths, or pack protection. Preheating of H-13 die blocks or tools for austenitizing can be done in open furnaces at temperatures below 500F. Pack containers with H-13 parts can be safely heated in a furnace to 1000F. Once workpieces or containers have reached temperature, they should be heated slowly in a protective atmosphere or vacuum to 1500F at 200F/h maximum, held for one hour per inch of thickness or per inch of pack container, then austenitized at 1850–1900F for 15–40 min, with longer times for thicker sections. Quenching is normally done in still or fan-blown air or in special pressurized inert gas quench chambers that are mounted within vacuum furnaces. Sections greater than five inches in thickness require accelerated cooling in forced air, pressurized gas, or interrupted oil quenching. In oil quenching H-13, the part should be removed when black at about 900F, then cooled in still air to 150–125F. Quenching can also be done in hot salt baths at 950–1050F followed by air cooling. Too rapid quenching induces distortions, which may offset critical dimensions in dies and tools. However, to obtain optimum properties, H-13 steel must be quenched from austenitizing temperature at a minimum rate of 50F/min to below 1000F. (Refs. 3–21)

Austenitizing of H-13 has been commonly done at 1850F for many years since this steel was developed; however, as early as 1969, research done at Case Western Reserve University (CWRU) on thermal fatigue of H-13 steel (see 3.7.1) had shown that austenitizing temperatures of 1950F and even 2050F greatly improved thermal fatigue resistance. This was determined to be due to the increase in resistance to softening under thermal stress cycling conditions simulative of aluminum die casting, in spite of the larger grain size that results from high temperature austenitizing. (Refs. 22–25)

Prior to the CWRU work, which caused a paradigm shift in metallurgical thinking about hardening hot work tool steels, it was generally assumed that austenitizing of H-13 steel at temperatures of 1900–2050F would result in a decrease in fracture toughness relative to austenitizing at 1850F due to an increase in grain size (Figure 1.5.5.4). Subsequent research has established that austenitizing H-13 at 1950–2050F does not affect fracture toughness and may actually increase it, while significantly decreasing softening at high temperatures due to better carbide dissolution (Figure 1.5.5.5), thus explaining the increase in H-13 die life in many hot working applications after high temperature austenitization. The greater degree of dissolution of carbides at higher austenitizing temperatures generally results in higher as-quenched hardness of H-13 steel, depending on component cross section influencing the quench rate (Figure 1.5.5.6). (Refs. 22–28)

Due to its high hardenability, quenching of small section sizes of H-13 components in still air from austenitization temperatures is often adequate to achieve a martensitic structure throughout and to avoid carbide precipitation at grain boundaries. Most accepted standards for achieving proper H-13 microstructures require cooling rates of >30F/min to produce proper microstructures and mechanical properties. H-13 parts must be cooled below 1300–1350F in less than 15–20 min in order to avoid grain boundary carbide precipitation, which can reduce toughness if excessive (Figure 1.5.5.7). Once past this range, cooling can be interrupted at 1050–700F for a period of time to equalize temperature gradients in large and intricate sections without degrading mechanical properties.

For large section sizes of H-13, portions may enter into the bainitic region upon quenching (Figures 1.5.5.2, 1.5.5.3, and 1.5.5.8), resulting in reduced toughness upon tempering; in H-13, the toughness of tempered bainite has been shown to be inferior to that of tempered martensite due to the presence of interlath carbides formed during the slow quench following austenitizing. At an austenitizing temperature of 1870F (1020C), H-13 steel has a transformation into the bainitic range starting at higher cooling rates than H-11 steel, probably as a result of the higher molybdenum content of H-13; however, at the higher austenitizing temperature of 1975F (1080C) for H-13, the bainitic transformation starts at slower cooling rates that are similar to those for H-11 (Figure 1.5.5.3). (Refs. 4, 28–29)

1.5.5.1 *[Figure]* Isothermal phase transformation diagram for H-13 steel (0.40 C, 1.05 Si, 5.00 Cr, 1.35 Mo, 1.10V) austenitized at 1850F (Ref. 3)

1.5.5.2 *[Figure]* Time-temperature transformation diagram for premium grade H-13 steel (Thyrotherm 2344 ESR Magnum, ThyssenKrupp Specialty Steels, Inc.) austenitized at 1870–1920F (Refs. 17, 18)

1.5.5.3 *[Figure]* Kinetics of bainite transformation for H-13 and H-11 steels compared at given austenitizing temperatures (Ref. 29)

1.5.5.4 *[Figure]* ASTM grain size versus austenitizing temperature for H-13 steel and air cooled for 0.5-in. cube samples soaked at temperature for 25–80 minutes (Ref. 28)

1.5.5.5 *[Figure]* Volume % carbide (95% confidence interval) in the as-quenched condition of air cooled (AC) small sections and larger 6- and 12-in rounds of H-13 steel as a function of austenitizing temperature for given soak times (Ref. 28)

1.5.5.6 *[Figure]* As-quenched hardness as a function of austenitizing temperature of air cooled (AC) small sections and larger 6- and 12-in rounds of H-13 steel for given soak times (Ref. 28)

1.5.5.7 *[Figure]* As-Quenched microstructure for H-13 steel showing moderate carbide precipitation at grain boundaries and finely dispersed carbides in matrix (Ref. 30)

1.5.5.8 *[Figure]* Continuous cooling transformation diagram for H-13 steel austenitized at 1970F showing cooling curves A through E (Ref. 30)

1.5.6 Critical Temperatures (Ref. 31)

Heating @ 100F/h:

Ac_1 – 1544F (temperature at which austenite begins to form)

Ac_3 – 1634F (temperature at which ferrite to austenite transformation is complete)

Cooling @ 50F/h:

Ar_3 – 1475F (temperature at which austenite begins to transform to ferrite)

Ar_1 – 1418F (temperature at which transformation of austenite to ferrite or to ferrite + cementite is complete)

1.5.7 Stabilizing

Stabilizing is optionally done, sometimes on complex shapes, to remove residual stresses and to convert some of the residual austenite that may have formed in quenching H-13 from austenitizing temperatures. In stabilizing H-13 steel, a brief stress relief/stabilizing temper is conducted at 300 to 320F, followed by refrigeration at -150 to -320F. The steel may be used in this condition if a high hardness is required. Normally, to reduce hardness, tempering is done immediately after stabilizing after the part reaches room temperature. (Ref. 3)

1.5.8 Tempering

Tempering of H-13 steel components can begin as soon as they reach 120 to 200F upon quenching from austenitizing temperature, i.e., assuming no stabilizing treatment is used. There is little change in as-quenched hardness with tempering treatments up to 1000F, although a secondary hardness peak occurs at ~950F caused by transformation of retained austenite and formation of complex carbides. At temperatures above 1000F, hardness drops and toughness increases. Thus, tempering of H-13 is usually done at temperatures of 1000 to 1200F, and preferably double tempering or triple tempering (cooling to room temperature between each temper) to convert residual austenite that may have formed in quenching from austenitizing temperature and also to control final temper hardness. Convection air tempering furnaces are used to heat large H-13 dies and tools at a moderate rate. Salt baths are acceptable for small parts but not for large or intricate shaped dies and tools, as they might crack due to thermal shock. Tempered hardness depends on austenitizing temperature, increasing with increasing austenitizing temperature as seen in Figures 1.5.8.2–1.5.8.4. (Ref. 3)

Tempering is usually done in cycles at a selected temperature for one hour per inch of thickness, cooling to room temperature, and retempering using the same time at temperature. The second temper is essential, and a third temper is beneficial (Figure 1.5.4.1). Final temper hardness is 53 to 40 HRC, depending on initial austenitizing temperature and total tempering temperature and time.

The relationship of hardness of quenched and tempered H-13 depends on tempering temperature and time, often expressed by the Hollomon-Jaffe parameter or master tempering parameter (MTP):

MTP = (Temperature, F + 460) x (20 + Log Time, Hours) (Ref. 4)

The relationship of hardness of H-13 steel on the MTP is shown in Figure 1.5.8.5. For example, to achieve 46 HRC in a small H-13 steel tool after austenitizing at 1850F, tempering may be conducted at 1080F for four hours, while a large tool soaked for 24 hours at 1025F to attain uniform temperature should also achieve 46 HRC, as the MTP in both cases is 31,727. (Ref. 4)

Another method based on the MTP for predicting hardness of tempered H-13 steel, assuming average composition and adequate quenching from an austenitizing temperature of 1875F, is

diagramed in Figure 1.5.8.6. The upper part of this diagram is applicable for a one hour tempering period, while the effect of longer tempering time on hardness is determined by following the slanted lines to a particular time in question and then vertically into the upper part where hardness can be read. For example, the diagram shows a tempered hardness of 47 HRC after tempering at 1130F for 3 h, then tempering for 3 h more for a total of 6 h gives a hardness of 43.5 HRC, while still another 3 h temper totaling 9 h further reduces the hardness to 42 HRC, etc. The higher the tempering temperature, the greater the sensitivity of H-13 steel to an increase in tempering time, as indicated by the MTP above. (Ref. 32)

After austenitization, air quenching, and double or triple tempering, H-13 steel should exhibit a tempered martensitic microstructure with varying amounts of tempered bainite along with very fine undissolved carbides distributed in the matrix (Figures 1.5.8.7 and 1.5.8.8). In Figure 1.5.8.7, the variations are typical of those that occur within different sections of a heat treated block of H-13 steel that had the different acceptable annealed and banded microstructures shown in Figures 1.5.2.1 and 1.5.2.2. (Refs. 4, 30)

The microstructural changes that occur on tempering cause some slight dimensional changes in blocks of H-13 steel, and these may need to be compensated in the finishing of dies and tools that have tight dimensional tolerances. (Figure 1.5.8.9 and Table 1.5.8.10). (Ref. 3)

1.5.8.1 *[Figure]* Hardness variation with tempering temperature for H-13 steel air cooled from 1875F and tempered 2 h at temperature (Ref. 1)

1.5.8.2 *[Figure]* Hardness as a function of tempering temperature for H-13 steel austenitized at 1850F and 1800F, air cooled, and double tempered (Ref. 3)

1.5.8.3 *[Figure]* Hardness as a function of tempering temperature for H-13 steel austenitized at 1950F and 1800F, air cooled, and tempered for 2 h (Ref. 3)

1.5.8.4 *[Figure]* Tempering curve (double tempered 2 h + 2 h) for H-13 steel after air quenching (AC) 0.5-in. square samples from 1875, 1950, and 2050F (Ref. 28)

1.5.8.5 *[Figure]* Master tempering parameter curve for H-13 steel hardened by austenitizing at 1750–1950F and quenching (Ref. 4)

1.5.8.6 *[Figure]* Time-temperature tempering diagram for H-13 steel hardened by austenitizing at 1875F (Ref. 32)

1.5.8.7 *[Figure]* Acceptable microstructures (500x, 5% Nital etch) of H-13 steel properly heat treated by austenitizing, quenching, and tempering as per NADCA acceptance criteria (numbering HS1-HS9 does not denote a quality ranking as all are acceptable) (Ref. 4)

1.5.8.8 *[Figure]* Typical microstructure from the center of a six-inch-thick H-13 steel die hardened commercially in a vacuum furnace at 1850F and double tempered (2 h at 1050F + 2 h at 1100F) (Ref. 30)

1.5.8.9 *[Figure]* Dimensional change of H13 steel in a 1 x 2 x 6 in. block versus tempering temperature (Ref. 3)

1.5.8.10 *[Table]* Typical dimensional changes in hardening and tempering H-11 and H-13 steels (Ref. 2)

1.5.9 Stress Accelerated Tempering

H-13 steel, like other H-series steels in hot work tooling and dies, is often exposed to temperatures just below the standard tempering temperatures of heat treatment and relatively high stresses imposed by either the pressures imposed by hot working, thermal stresses imposed by sharp temperature gradients during casting or hot working, or both. Thus, it is likely that these stresses acting at high temperatures affect tempering mechanisms, hardness changes, and even die and tool failure mechanisms in H-13 steel components. These effects were noted initially in the work of Benedyk, et al., first in relation to the mechanism of thermal fatigue failure and stress accelerated hardness change of H-13 steel (see 3.7.1) and later in relation to the mechanism of creep rupture. (Refs. 22-24)

The work done at the Illinois Institute of Technology Research Institute (IITRI) on the investigation of stress accelerated tempering in creep of H-13 steel utilized a variable section test specimen (Figure 1.5.9.1) tested to failure at temperatures of 1000–1100F with hardness determined over the range of cross sectional areas, representing a 10:1 difference in applied stress. In this work, the H-13 steel was supplied as annealed 1-in. round bar, reduced by forging and rolling from a cast 6-in. square billet. The variable section test specimens were heat treated by austenitizing at 1850F, oil quenching, tempering at 1100F for 2 h, air quenching to room temperature, and retempering as before. The original hardness of the specimens after heat treatment was 46 Rockwell C, and the standard tempering curves showing further hardness change as a function of time at 1000, 1050, and 1100F with no imposed stress are shown in Figure 1.5.9.2. Hardness changes due to stress

accelerated tempering at stress levels of 25-80 ksi were measured in the sectioned variable cross section of specimens as a function of time during creep testing at 1000, 1050, and 1100F, and the results are presented in Figures 1.5.9.3–1.5.9.5. (Ref. 25)

1.5.9.1 *[Figure]* Variable section creep specimen used to study stress accelerated tempering of H-13 steel as reported in Figures 1.5.9.2–1.5.9.5 (Ref. 25)

1.5.9.2 *[Figure]* Tempering curves for H-13 steel constructed from unstressed section of test specimen shown in Figure 1.5.9.1 (Ref. 25)

1.5.9.3 *[Figure]* Hardness change (microhardness surveys converted to Rockwell C) in H-13 steel measured along variable section creep specimen shown in Figure 1.5.9.1 due to stress accelerated tempering at 1000F (Ref. 25)

1.5.9.4 *[Figure]* Hardness change (microhardness surveys converted to Rockwell C) in H-13 steel measured along variable section creep specimen shown in Figure 1.5.9.1 due to stress accelerated tempering at 1050F (Ref. 25)

1.5.9.5 *[Figure]* Hardness change (microhardness surveys converted to Rockwell C) in H-13 steel measured along variable section creep specimen shown in Figure 1.5.9.1 due to stress accelerated tempering at 1100F (Ref. 25)

1.5.10 Retained Austenite

Retained austenite in H-13 steel that has been quenched from austenitizing temperatures can result in the formation of untempered martensite in operation, which will produce concentrated local stresses that promote brittle failure. Due to its low carbon content (~0.40%) and consequently high M_S (martensitic start) temperature, H-13 steel has small quantities (~1%) of retained austenite after austenitizing and quenching. With double or triple tempering treatments, any minor amount of residual austenite is basically converted to tempered martensite. (Ref. 33)

1.5.11 Nitriding

Nitriding of H-13 is done after finish machining and final heat treatment to produce an especially hard and wear resistant surface that is resistant to the softening effect of heat at temperatures up to the nitriding temperature. Nitriding also induces surface compressive stresses, thereby improving fatigue life. Since nitriding is normally carried out at 50F below the normal tempering temperature, the nitriding step can serve as the last temper in a double or triple tempering heat treatment. Before nitriding, the surfaces should be clean and free of decarburization.

Gas nitriding is most common, although liquid bath nitriding, pack, and ion or plasma nitriding are also done. Nitrided case depth (outer "white" brittle layer and more ductile diffusion layer) is a function of time and temperature, e.g., gas nitriding at 950F for 10–12 h results in a case depth of 0.004–0.005 in., while for 40–50 h, a case depth of 0.012–0.016 in. is obtainable. The diffusion layer is 10–30 times thicker than the "white" layer, depending on the type of nitriding process (Figure 1.5.11.1 and Table 1.5.11.2). The outer "white" nitrided layer is brittle and its thickness must be optimized to achieve best results. The demarcation of the "white" layer may not always be clear, as grain boundary networks of nitride may be present throughout the tempered martensitic case of H-13 steel (Figure 1.5.11.3).

1.5.11.1 *[Figure]* Cross-sectional optical micrographs of gas nitrided, ion nitrided, and salt bath nitrided H-13 steel after austenitization at 1890F and triple tempering (70X magnification) (Ref. 34)

1.5.11.2 *[Table]* Thickness of surface layers of nitrided H-13 steel after austenitization at 1890F and triple tempering depending on nitriding treatment (Ref. 34)

1.5.11.3 *[Figure]* Gas nitrided case (24 h at 975F) produced on H-13 steel that was austenitized at 1890F, triple tempered at 950F, and surface activated in manganese phosphate (300X magnification) (Ref. 35)

1.6 Hardness

1.6.1 Room Temperature Hardness

Annealed hardness characteristics of H-13 steel are similar to those of H-10, H-11, and H-12 steels and typically are measured by the Brinell hardness (HB) test, which for these annealed steels ranges from 192 to 229 HB. Rockwell C (HRC) hardness measurements, typically used to gauge the quality of austenitization and tempering heat treatments, range from 42 to 56 HRC, depending on composition and heat treatment conditions. Vickers hardness (HV), Knoop hardness (KHN or KH), and 15N Rockwell tests are used to evaluate the superficial hardness of H-13 steel in order to establish a comparison of surface and subsurface hardening (nitriding, carburization, nitrocarburizing, or other treatment) or softening (decarburization). Conversions of HV, Knoop, and 15N Rockwell readings to HRC are readily available from standard tables.

The hardness of austenitized H-13 steel sections depends on several factors that include austenitizing temperature, section size, and rate of quenching (Figure 1.5.5.6 and Table 1.6.1.1). The measurement of room temperature HRC, determined as a function of austenitizing and tempering temperatures for specific times, gives

a measure of the resistance to tempering of the hardened steel (Figures 1.5.8.1–1.5.8.6, Tables 1.6.1.2–1.6.1.4).

Hardened and tempered H-13 steel decreases in hardness upon heating in service and exposure to high temperature (at or near tempering temperatures) for various times. The ability of H-13 steel hardened under different conditions to maintain its tempered hardness in service, sometimes called "red hardness", can be measured by exposing hardened and tempered samples to high temperatures for different periods of time (Figure 1.6.1.5). However, it should be noted, that this does not always give a good indication of the combined effects of exposure to stress and temperature in service (see 1.5.7).

1.6.1.1 *[Table]* Effect of oil and air quenching on room temperature hardness of small H-13 steel test pieces (1 in. round x 2 in. long) cut from annealed bars austenitized for six minutes at indicated temperatures and quenched in oil or still air (Ref. 31)

1.6.1.2 *[Table]* Effect of tempering on room temperature hardness of small H-13 test pieces (1 in. round x 1 in. long) austenitized at 1800, 1850, 1900, and 1950F, quenched in still air, and tempered for two hours at indicated temperatures (Ref. 31)

1.6.1.3 *[Table]* Effect of tempering on room temperature hardness of large H-13 test pieces (4 x 4 x 4 in.) ground on two saw-cut ends, preheated at 1500F for one hour, austenitized at 1850F for one hour in a controlled atmosphere, quenched in oil or still air, and tempered for three hours at indicated temperatures (Ref. 31)

1.6.1.4 *[Table]* Resistance to tempering for H-13 steel austenitized at either 1800 or 1850F and double tempered (3 + 3 h) at indicated temperatures (Ref. 36)

1.6.1.5 *[Figure]* Room temperature hardness or "red hardness" of H-13 steel hardened and tempered as indicated after exposure to elevated temperatures for 4-100 h (Ref. 36)

1.6.1.6 *[Figure]* Tempering curves of H-13 steel air quenched after austenitizing at 1750, 1850, and 2050F showing hardness (R_c or HRC) as a function of time at a tempering temperature of 1100F (Ref. 22)

1.6.1.7 *[Figure]* Tempering curves for H-13 steel air quenched after austenitizing at 1750, 1850, and 2050F, tempering to 45 HRC, and showing hardness (R_c or HRC) as a function of time at a tempering temperature of 1000F (Ref. 22)

1.6.2 Hot Hardness

Hot hardness of H-13 is the actual hardness of the steel measured by a penetrator at a given temperature for controlled amounts of time of application of the indentation load. Samples are normally held for 30 min. at the testing temperature before testing. The longer the indentor is in contact with the steel under load, the softer the steel appears due to creep deformation. Thus, hot hardness determinations are typically made in the minimum time to apply the indentor load. Hot hardness gives an indication of strength at the high temperature at which H-13 steel is used, and again it depends on heat treatment conditions.

1.6.2.1 *[Figure]* Typical hot hardness of H-13 steel for specimens oil quenched from 1850F and double tempered 2 + 2 h at indicated tempering temperature (Ref. 37)

1.6.2.2 *[Table]* Brinell hot hardness of H-13 steel samples (1 in. round x 7/8 in. long) hardened by oil quenching from 1850F and tempering for two hours at 1050F or test temperature if higher (Ref. 31)

1.6.2.3 *[Table]* Rockwell C hot hardness of H-13 steel heat treated to indicated room temperature hardness levels (Ref. 36)

1.6.2.4 *[Figure]* Effect of temperature on hot Brinell hardness (HB) of hardened (austenitized and quenched, untempered) H-13 steel (Ref. 44)

1.6.3 Nitrided Case Hardness

Microhardness testing, usually Vickers hardness (HV) or Knoop hardness (KHN or HK), or 15N Rockwell superficial hardness are used to measure nitrided case hardness. A typical nitrided H-13 surface has a hardened surface or case of about 0.004 in. thickness and exhibits a case hardness of about 1, 000–1, 250 HV or 69–72 HRC (converted from HV using standard hardness conversion tables).

1.6.3.1 *[Table]* Case and core hardness on ½-in. square test pieces of nitrided H-13 steel hardened at 1850F and tempered at 1050F, ground, and nitrided as indicated (Ref. 31)

1.7 Forms and Conditions Available

H-13 steel in conventional, premium, and superior grades (Table 1.4.1) is most commonly available in wrought form as bar, rod, billet, and forgings in the annealed or pre-hardened condition. However, it is also available as wire, sheet, and plate. Round bar stock is supplied in sizes of 0.50 to 25 in. diameter; square bar stock is supplied in sizes of 8 to 24 in. or more. Surface finish and dimensional tolerances on bar stock

vary and are specified. Die blocks for die cast and hot work tooling are supplied in annealed or pre-hardened (austenitized and tempered) conditions as rounds of as much as 36 in. in diameter and flats in a range of sizes up to 20 in. x 40 in. in area or more with a varying thickness to accommodate die and tooling sizes and with special orders of shape and size available. Typically, the cost of the material used for die casting and hot work dies represents 10–15% of the total die cost. (Refs. 5–19)

Cast H-13 steel (designated as CH-13) billets and ingots and even shapes are available in the annealed condition. (Ref. 40)

H-13 tool steel powders (predominantly spherical shape) of varying compositions and particle size distributions (1–250 microns), used for powder metallurgy, metal injection molding, and cladding applications, are also available. (Ref. 41)

1.8 Melting and Casting Practice

H-13 steel is most commonly air arc melted (AAM) in an electric furnace in heat lots of 25–50 tons. The AAM H-13 melt is then degassed by one of several techniques and often followed by vacuum arc remelting (VAR) or electroslag remelting (ESR). Alternatively, vacuum induction melting (VIM) followed by VAR or ESR is used for heat lots of up 5–15 tons. After melting and solidification, the next operation before hot working by forging or rolling is soaking pit practice or homogenization, conducted at temperatures at or near 2000F, in order to level the microsegregation and relieve the thermal residual stresses that accompany solidification. This is followed by long holding and slow cooling to hot working temperature for ingots that undergo immediate hot working or to room temperature for ingots to be stored. Hot working by rolling or forging is important in refining the cast metallurgical structure; however, the larger the ingot size, open die forging is commonly done because standard hot rolling pressures do not refine the internal portions of large ingots in applications slated for production of large H-13 block sizes. (Ref. 42)

For production of premium and superior grades of H-13 steel, ESR or VAR processes are necessary. In fact, some specifications for die materials only make exceptions in cases where availability of ESR or VAR material is wanting for small stock such as rounds of less than three inches diameter. (Ref. 20)

2.0 Physical and Environmental Properties

2.1 Thermal Properties

2.1.1 Melting Range

The melting temperature of H-13 steel ranges from 2500F to 2700F and depends on composition, mainly carbon content, i.e., the melting point decreases with increasing carbon content within the specified range.

2.1.2 Phase Changes

Critical temperatures of ferrite to austenite and austenite to ferrite or ferrite and cementite transformations on heating and cooling are given in 1.5.6. Generally, the amount of retained austenite in H-13 after austenitizing and quenching is minimal (~1% or less) and is transformed upon double and triple tempering (1.5.10).

The two major types of carbides formed in H-13 steel upon heat treatment are the V-rich MC type and the Cr-rich M_7C_3/$M_{23}C_6$ types. The composition of these carbides in H-13 steel varies widely, and the size and distribution of these carbides in annealed microstructures depends greatly on prior metallurgical processing and austenitizing/quenching/tempering conditions. (Refs. 26–28)

2.1.3 Thermal Conductivity

2.1.3.1 *[Table]* Thermal conductivity of H-13 steel as a function of temperature (Ref. 2)

2.1.3.2 *[Table]* Thermal conductivity of Thyrotherm 2344 ESR Magnum premium grade AISI H-13 steel at indicated temperatures (Ref. 18)

2.1.4 Thermal Expansion

2.1.4.1 *[Table]* Average linear thermal expansion coefficient of H-13 steel over indicated temperature range (Ref. 44)

2.1.4.2. *[Table]* Average thermal expansion coefficient of Nu-Die V (Crucible Steel) and VDC (Timken Latrobe Steel) H-13 steel from room temperature (RT) to indicated temperature (Refs. 12, 16)

2.1.4.3 *[Table]* Average thermal expansion coefficient of Thyrotherm 2344 ESR Magnum premium grade AISI H-13 steel over indicated temperature range (Ref. 18)

2.1.4.4 *[Table]* Average thermal expansion coefficient of Crucible CPM® Nu-Die® EZ patented H-13 particle metallurgy sulfurized steel from room temperature (RT) to indicated temperature (Ref. 43)

2.1.5 Specific Heat

The mean specific heat of H-13 steel over the temperature range 32–212F is 0.11 Btu/lb-F.

Values of specific heat (heat capacity) of H-13 steel increase linearly with temperature, from 0.125 at 212F to 0.148 Btu/lb-F at 1300F. (Refs. 17, 18, 44)

2.1.6 Thermal Diffusivity

Thermal diffusivity (α) of H-14 steel can be derived from physical properties (k = thermal conductivity, ρ = density, and c = specific heat) utilizing the general equation $\alpha = k/\rho c$.

2.2 Other Physical Properties

2.2.1 Density/Specific Gravity

Room temperature density of H-13 steel is 0.28 lb/in^3. Room temperature specific gravity of H-13 steel is 7.761.

2.2.1.1 *[Table]* Density of Thyrotherm 2344 ESR Magnum premium grade AISI H-13 steel over the temperature range 70–1200F (Ref. 18)

2.2.2 Electrical Properties

Electrical Properties are similar to H-11; refer to the H-11 chapter (Code 1218) for this information.

2.2.3 Magnetic Properties

This steel is highly magnetic, but becomes nonmagnetic at temperatures of 1400–1500F (Curie temperature) and above. Induction heating is disturbed by heating above the Curie temperature, thereby drastically reducing the induction heating rate above that temperature.

2.2.4 Emittance

Emittance is similar to H-11; refer to the H-11 chapter (Code 1218) for this information.

2.2.5 Damping Capacity

2.3 Chemical Environments

2.3.1 General Corrosion

The general corrosion resistance of H-13 steel is low and surface protection is required. For H-13 dies and tooling, temporary protection during storage is recommended by first cleaning the surfaces and then coating with oil or corrosion inhibiting solvent or water-base solutions. During hot working service, H-13 dies and tooling are often coated repeatedly with emulsions and lubricants that protect the surface from general corrosion. Nitriding or nitrogen implantation into the surface of H-13 steel has been shown to increase its corrosion resistance in salt water (Figure 2.3.1.1). As shown in 2.3.1.1, H-13 specimens treated by nitrogen PIII (plasma immersion ion implantation) exhibited passive regions under polarization conditions in salt water, with a corrosion potential as low as -0.42 V for a PIII H-13 nitrided specimen against -0.52 V for the untreated specimen. Also, the passive region current density of PIII nitrided H-13 was as much as two orders of magnitude lower than for untreated H-13, indicating a higher corrosion resistance for the PIII treated H-13.

2.3.1.1 *[Figure]* Potentiodynamic polarization curves of AISI H-13 steel measured in a 3.5% NaCl solution at pH = 6 on an (…) untreated sample, (----) nitrogen plasma immersion ion implantation (PIII) processed sample (T=300C, t=12 h), and (—) nitrogen PIII processed sample (T=450C, t=9 h) (Ref. 45)

2.3.2 Stress Corrosion

H-13 steel, although it has good stress corrosion resistance in comparison to other high strength steels due to its high chromium and molybdenum content, will still fail prematurely when exposed under stress to corrosive media. Use of premium and superior grades of H-13 steel and appropriate heat treatment (higher tempering temperature to lower yield strength) improve stress corrosion resistance.

2.3.3 Oxidation Resistance

The chromium content of H-13 steel improves its oxidation resistance over steels with lower alloy content. In service, at temperatures at or below the tempering temperature, H-13 steel oxidizes in still air at low rates. However, the oxidation rate of uncoated H-13 steel climbs as a function of temperature above 1000F and is severe at austenitizing temperatures, necessitating a vacuum or endothermic atmosphere to prevent excessive oxidation and the decarburization and loss in surface hardness that accompanies oxidation of carbon steels. Nitrided H-13 steel surfaces also oxidize when heated for long periods in air furnaces and ovens, commonly done on dies and tools to facilitate production, thereby losing their hardness and protective surface properties.

Oxidation has been implicated as one of the mechanisms of crack propagation in thermal fatigue, with the lower density oxide acting to wedge open the crack; EDS (electron dispersion spectral) analysis of the oxide within the thermal fatigue cracks of an H-13 steel specimen has indicated that it is predominantly iron oxide with a chromium oxide layer at the metal-oxide interface. (Ref. 22)

Not all oxidation of H-13 steel components is bad, since properly prepared oxide films on H-13 steel dies and tooling are beneficial with respect to preventing soldering of molten metal to the dies and tooling during casting and to prevent sticking of solid workpiece metal during hot metalworking. Dense oxide films on H-13 dies and tooling, prepared by careful heating in air furnaces (often with proprietary atmospheres) at

temperatures below the lowest tempering temperature, are beneficial in preventing soldering and sticking of metal during casting or metalworking. Oxide films prepared for such purposes have "blue", "blue-black", or "black" surface coloration and not only prevent soldering and sticking but also act to reduce the surface heat transfer coefficient. (Ref. 22)

2.3.3.1 *[Figure]* Comparative oxidation resistance of H-13 and maraging steels at 1000F (Ref. 46)

2.3.3.2 *[Figure]* Cross sectional view of oxide buildup in thermal fatigue crack in hardened H-13 steel specimen: (a) 50x, nital etch and (b) 500x, nital etch (Ref. 22)

2.3.4 Hydrogen Resistance

A few parts per million of hydrogen dissolved in steel can cause hairline cracking and loss of tensile ductility. In casting dies for aluminum in particular, soldering and washout of H-13 steel often results in die failure due to the high velocity of impinging molten aluminum. In the hardened condition, H-13 steel is most susceptible to hydrogen embrittlement. Resistance to hydrogen embrittlement decreases as strength increases, particularly when the strength level exceeds 150–180 ksi, and the effects of hydrogen embrittlement increase as strain rate decreases. Prevention of failure due to hydrogen damage, especially in structural applications in mild atmospheric environments, involves protection with a corrosion-resistant coating and/or imparting compressive residual stresses on the surface by shot peening or other means. If H-13 steel parts are welded, the welding rods should be kept dry in storage and during welding, as adsorbed water is a major source of hydrogen. (Ref. 55)

2.3.5 Corrosion/Erosion by Molten Metal

Corrosion/erosion (washout) by molten aluminum, zinc, or other metals that react with H-13 steel is accelerated by turbulence and increase in melt temperature. In aluminum die casting dies in particular, soldering and washout of H-13 steel often result in die failure due to the high velocity of impinging molten aluminum. Immersion tests conducted in molten aluminum have shown that the dissolution of H-13 steel decreases significantly with nitrided coating thickness Figure 2.3.5.1). (Ref. 47)

In an accelerated die washout test conducted on H-13 steel test pins (Figure 2.3.5.2 and 2.3.5.3) impinged by molten A356 aluminum alloy at 1350F, various types of PVD (physical vapor deposition) coatings on H-13 steel pins have significantly increased washout resistance (Figure 2.3.5.3). Among the various PVD coatings tested, a CrC PVD coating was especially effective. (Ref. 48)

2.3.5.1 *[Figure]* Variations in corroded/eroded depth of immersion test specimens of hardened and tempered H-13 steel as heat treated and machined and separately nitrided by gas or ion nitriding maintained in a molten Al-Si-Cu (KS ALDC) aluminum alloy at 1300F for 43 h (Ref. 47)

2.3.5.2 *[Figure]* Schematic diagram of accelerated washout testing arrangement at Case Western Reserve University (CWRU) with molten aluminum alloy injected into die cavity at ~70 in/s (Ref. 48)

2.3.5.3 *[Figure]* Test pin design and position within die cavity of CWRU accelerated washout test arrangement shown in Figure 2.3.5.2 (Ref. 48)

2.3.5.4 *[Figure]* Microstructural cross sections (500x) PVD coated pin specimens tested in CWRU accelerated washout arrangement shown in Figure 2.3.5.2 (Ref. 48)

2.3.5.5 *[Figure]* Effect of various types of PVD coatings shown in Figure 2.3.5.4 on washout resistance of H-13 steel die casting core pins in CWRU accelerated washout test shown in Figures 2.3.5.2 and 2.3.5.3 (Ref. 48)

2.3.6 Liquid Metal Induced Embrittlement Resistance

Liquid metal induced embrittlement (LMIE) is the catastrophic brittle failure of a normally ductile metal when coated with a thin film of a liquid metal while stressed in tension. In most cases, the stress needed to initiate and propagate cracks occurs instantly, with fracture propagating at 4–40 in/sec through the entire test specimen. As with other types of high strength steels, H-13 steel in the heat treated condition can be embrittled by various liquid metals, notably lead, antimony, cadmium, zinc, and others. (Ref. 49)

U-bend liquid metal embrittlement tests (Figure 2.3.6.1) of heat treated H-13 steel recently conducted in pure zinc melts at the TPTC (Thermal Processing Technology Center) of Illinois Institute of Technology (IIT) indicate a low resistance to LMIE in this medium. Results are shown in Figure 2.3.6.2 for embrittlement tests conducted in molten zinc baths maintained at either 970 or 1050F for hardened H-13 steel plates in the longitudinal and transverse rolling direction after austenitizing and air quenching at 1750, 1850, or 1950F, with some specimens triple tempered (2 + 2 +2 h at 1100F — #9 and #11), and some specimens single tempered for the same period (6 h at 1100F); as a control, a single tempered specimen was tested in a neutral molten salt bath (#12) and exhibited no failure. (Ref. 50)

2.3.6.1 *[Figure]* Schematic drawing of TPTC U-bend liquid zinc embrittlement test procedure conducted on H-13 steel plate specimens: original annealed specimen bent into U-shape, heat treated, bent to an incipient plastic flow condition at a displacement of Δd (left), displacement held by fastener, and immersed in a molten zinc bath (right) (Ref. 50)

2.3.6.2 *[Figure]* Liquid zinc embrittlement TPTC U-bend test data (Y-axis: time to fracture in hours; X-axis: test conditions as shown in Figure 2.3.6.1) conducted on H-13 steel plate specimens (Ref. 50)

2.3.7 Solid Metal Induced Embrittlement Resistance

Embrittlement can occur in heat treated H-13 steel below the melting temperature of the solid in certain liquid-metal embrittlement couples; this type of failure is known as solid metal induced embrittlement (SMIE). The severity of SMIE generally increases with temperature, with a sharp and significant increase in severity at the melting point of the embrittling metal. Above the melting point, the embrittlement has all the characteristics of liquid metal embrittlement. Many high strength steels such as heat treated H-13 steel have experienced failures due to SMIE. (Ref. 51)

SMIE has been identified as a failure mechanism in extrusion dies made of hot work steels such as SKD61 (Japanese steel similar to H-12 steel) and H-13 steel for the extrusion of Al-4.75Zn-1.25Mg alloy hollows, thus implicating the zinc in the alloy as the embrittling agent. (Refs. 52-53)

In analyzing SMIE and LMIE transport mechanisms, Gordon determined that bulk liquid metal flow penetrating the tips of sharp cracks is the likely transport mechanism in LMIE, but surface self diffusion is the likely transport mechanism in SMIE. (Ref. 54) As the melting point of zinc is 787F and it has a high vapor pressure and short vapor transport time at its melting point, the hot metalworking of an aluminum alloy with high zinc content may under certain conditions contribute to brittle failure. (Ref. 54)

2.4 Nuclear Environment

Neutron irradiation of H-13 steel at low and moderate strength levels leads to an increase in the ductile to brittle transition temperature (DBTT) and a decrease in energy above the DBTT as determined by Charpy V-notch impact tests. The degree of damage caused by a nuclear environment depends on neutron dose, neutron spectrum, irradiation temperature, and steel composition and properties. Vacuum degassing and control of phosphorus content helps to reduce susceptibility to neutron embrittlement. (Ref. 56)

3.0 Mechanical Properties

3.1 Specified Mechanical Properties

3.1.1 NADCA H-13 207-97 H-13 Steel Acceptance Criteria (Ref. 4)

Acceptance criteria fo H-13 steel used in casting dies for aluminum have been established by NADCA and involve impact capability testing of all mill product forms with a thickness greater than 2.5 in. The specimen blanks should be removed from the short transverse orientation (base of Charpy V notch parallel to the longitudinal direction of the parent block, slab, or bar) in the center of the parent block of steel as per ASTM A370. The blanks should be heat treated by austenitizing at 1885F for 30 min, oil quenching, double tempering at 1000F for 2 h minimum each temper (air cooled between each temper) to achieve a final hardness of 44–46 HRC, and machining to final Charpy V impact specimen size per ASTM A370. Acceptance criteria, based on five specimens tested at room temperature with values of highest and lowest specimens discarded are as follows for the remaining three results:

Premium Quality H-13 – 8 ft-lb average with 6 ft-lb single minimum value

Superior Quality H-13 – 10 ft-lb with 8 ft-lb single minimum value

3.1.2 Other H-13 Steel Acceptance Criteria (Refs. 5–21, 40, 41)

H-13 steel in its various wrought product forms is typically purchased on the basis of H-13 steel producer or user specifications that not only include mechanical properties but also forging and heat treatment procedures.

3.2 Mechanical Properties at Room Temperature

3.2.1 Tension Stress-Strain Diagrams and Tensile Properties

3.2.1.1 *[Table]* Typical longitudinal room temperature mechanical properties of H-13 steel bar oil quenched from an 1850F austenitizing temperature and tempered at different temperatures (Ref. 1)

3.2.1.2 *[Table]* Transverse mechanical properties at room temperature of air melted and electroslag remelted (ESR) H-13 steel large section bars oil quenched from 1850F and double tempered (2 + 2 h) at 1090F to a final hardness of 48 HRC (Ref. 1)

3.2.1.3 *[Figure]* Room temperature tensile properties of H-13 steel in relation to hardness and Charpy V-notch impact energy (Ref. 44)

3.2.1.4 *[Table]* Room temperature tensile properties of annealed and heat treated H-13 steel (Ref. 16)

3.2.2 Compression Stress-Strain Diagrams and Compression Properties

Compression yield strength of H-13 steel is equivalent to tensile yield strength at room and high temperatures. Tensile yield strength data are commonly used to estimate compressive yield strength of H-13 steel components in service.

3.2.3 Impact

To achieve maximum impact toughness in service, H-13 steel specimens should be quenched from austenitizing temperatures at a minimum rate of 50F/min and preferably at 25F/min to below 1000F (see 1.5.5). The preferred method for determining impact toughness of H-13 steel is Charpy V-notch testing, and an average Charpy V-notch toughness in the short transverse direction of 8 ft-lb or more at room temperature is considered the standard for high quality H-13 steel (see 3.1.1). However, it is difficult to characterize the impact resistance of H-13 steel from room temperature tests alone, especially considering that this steel is most often used at temperatures up to 1000F and higher (see 3.3.3 and 3.3.9).

3.2.3.1 *[Table]* Longitudinal Charpy V-notch impact properties at room temperature of H-13 bar air cooled from an 1850F austenitizing temperature and tempered at different temperatures (Ref. 1)

3.2.3.2 *[Table]* Transverse Charpy V-notch impact toughness at room temperature of various grades of H-13 steel at 45–46 HRC (Ref. 43)

3.2.3.3 *[Table]* Izod impact properties at room temperature of H-13 steel specimens machined from ½-in. square bar stock to 0.394-in. square, preheated to 1500F, austenitized at 1850F, oil quenched, and tempered at indicated temperatures for 2 h (Ref. 31)

3.2.4 Bending

3.2.5 Torsion and Shear

3.2.6 Bearing

3.2.7 Stress Concentration

3.2.7.1 Notch Properties

Sharp notches can significantly reduce the ability of H-13 steel to withstand impact and shock loads.

3.2.7.1.1 *[Figure]* Effect of notch radius on the impact strength of Izod type specimens of H-13 steel heat treated to 48 Rockwell C and tested at room temperature (Ref. 61)

3.2.7.2 Fracture Toughness

Plane strain fracture toughness (K_{Ic}) test results for heat treated (austenitized, air cooled, and tempered) H13 steel at room temperature are given in Table 3.2.7.2.1 and Figure 3.2.7.2.2. (Refs. 58, 28) As mentioned in 1.5.5, decreased quenching rates of H13 steel sections from austenitizing temperature can result in the formation of upper bainite along with preferential precipitation of carbides along prior austenitic grain boundaries, which decreases toughness in the heat treated component (Figure 3.2.7.2.3 and 3.2.7.2.4). (Ref. 76)

Correlations have been made between K_{Ic}, Charpy-V notch (CVN), and HRC test data for heat treated H13 and H11 steels. (Ref. 77) For these steels, having room temperature yield strength (σ_{ys}) in the range 150–230 ksi and hardness in the range 40–56 HRC, the correlation between $(K_{Ic}/\sigma_{ys})^2$ and CVN/σ_{ys} is given in Figure 3.2.7.2.5 Linear regression analysis of K_{Ic}, HRC, and CVN at room temperature for H13 and H11 steels shows the following relationship:

$$K_{Ic}\,(\text{estimated}) = 4.53(CVN)^{1.11}(HRC)^{-0.135}$$

for which experimental and calculated values of K_{Ic} are plotted in Figure 3.2.7.2.6. (Ref. 77)

3.2.7.2.1 *[Table]* Longitudinal plane strain fracture toughness of H-13 steel air cooled from 1920F and tempered two hours at temperature (Ref. 58)

3.2.7.2.2 *[Figure]* Room temperature plane strain fracture toughness (K_{Ic}) of small and large size specimens of H-13 steel versus austenitizing temperature (a) and tempered hardness (b) after all specimens were double tempered at 1100F (2 + 2 h) for austenitizing soak times and cooling conditions given (25 min soak and air quench for small specimens and 50 and 60 min soak and simulated laboratory quench for 6- and 12-in. rounds) (Ref. 28)

3.2.7.2.3 *[Figure]* Variation of room temperature plane strain fracture toughness K_{Ic} of heat treated H13 steel, austenitized at 1870F for 30 min, quenched at various rates, and tempered to 44 HRC, as a function of quench rate (Ref. 76)

3.2.7.2.4 *[Figure]* Charpy V-notch (CVN) impact values of H13 steel quenched at

various rates after austenitizing at 1870F for 30 min and tempered to 44 HRC (Ref. 76)

3.2.7.2.5 *[Figure]* Correlation between $(K_{Ic}/\sigma_{ys})^2$ and CVN/σ_{ys} at room temperature for H13/H11 steels (Ref. 77)

3.2.7.2.6 *[Figure]* Experimental values of K_{Ic} at room temperature compared with values of K_{Ic} calculated from CVN and HRC data at room temperature (see linear regression relationship in 3.2.7.2) for H13 and H11 steels (Ref. 77)

3.3 Mechanical Properties at Various Temperatures

3.3.1 Tensile Properties

3.3.1.1 *[Figure]* Effect of elevated temperature on tensile strength of H-13 steel heat treated to room temperature Rockwell C (HRC) hardness values given (Ref. 44)

3.3.1.2 *[Figure]* Effect of elevated temperature (C x 1.8 + 32 = F) on tensile and 0.2 yield (creep limit) strength (N/mm^2 x 0.145 = ksi) and reduction in area of H-13 steel heat treated to room temperature strength level given (Ref. 17)

3.3.1.3 *[Figure]* Flow stress (determined from modified Johnson-Cook model of flow stress and tuned by OXCUT computer program and experimental data from lathe machining experiments) of H-13 steel at temperatures of 800–1200C (1472-2192F) and strain rates of $6 \times 10^3 - 9 \times 10^5$ 1/s for H-13 steel originally at 46 Rockwell C (HRC) hardness (MPa x 0.145 = ksi) (Ref. 57)

3.3.1.4 *[Table]* Elevated temperature tensile properties of heat treated H-13 steel (Ref. 16)

3.3.2 Compression Stress-Strain Diagrams and Compression Properties

Compression yield strength of H-13 steel is approximately equivalent to tensile yield strength at room and high temperatures. Tensile yield strength data are commonly used to estimate compressive properties of H-13 steel components in service.

3.3.3 Impact

3.3.3.1 *[Table]* Charpy V-notch (CVN) properties of Nu-Die V (AISI H13) steel air cooled to room temperature from 1825/1875F, and double tempered (two hours minimum) to original room temperature hardness (Rockwell C or HRC) indicated and tested at elevated temperatures (Ref. 58)

3.3.3.2 *[Figure]* Longitudinal Charpy V-notch impact resistance versus austenitizing temperature for H-13 steel specimens austenitized for treatment times given, air quenched (small size specimens) or cooled to simulated quenching of 6- and 12-in. rounds, double tempered at 1000F (2 + 2 h), and subsequently tested at room temperature and 800F (Ref. 28)

3.3.3.3 *[Figure]* Longitudinal Charpy V-notch impact resistance versus austenitizing temperature for H-13 steel specimens austenitized for treatment times given, air quenched (small size specimens) or cooled to simulated quenching of 6- and 12-in. rounds, double tempered at 1100F (2 + 2 h), and subsequently tested at room temperature and 800F (Ref. 28)

3.3.3.4 *[Figure]* Longitudinal Charpy V-notch impact resistance versus austenitizing temperature for H-13 steel specimens austenitized for treatment times given, air quenched (small size specimens) or cooled to simulated quenching of 6- and 12-in. rounds, double tempered at 1150F (2 + 2 h), and subsequently tested at room temperature and 800F (Ref. 28)

3.3.3.5 *[Figure]* Longitudinal Charpy V-notch impact resistance versus tempered hardness for H-13 steel specimens austenitized at 1875, 1950, and 2025F for soak times given, air quenched (small size specimens) or cooled to simulated quenching of 6- and 12-in. rounds, tempered, and subsequently tested at 800F (Ref. 28)

3.3.4 Bending

3.3.5 Torsion and Shear

3.3.6 Bearing

3.3.7 Stress Concentration

3.3.7.1 Notch Properties

3.3.7.2 Fracture Toughness

Plane strain fracture toughness (K_{Ic}) measurements were made at temperatures up to 800F on four types of high strength steels, including H13 steel, for the purpose of developing a drill bit used in tricone roller drill bits capable of sustained operation at the temperatures encountered in drilling geothermal wells. (Ref. 78) Short rod (chevron-notch) fracture toughness (K_{Iv}) tests (Figure 3.3.7.2.1) were conducted on H13 steel specimens cut from blanks of 0.5-in. diameter by 0.75-in. length, originally cut from a 4.13-in. diameter x 3.54-in. forging using stock close to the forging surface. (Ref. 79) The specimen axes were parallel to the forging axis. The H13 specimens were heat treated by austenitizing at 1825F, air quenching, and double tempering at 1000F (2+2 h), resulting in an average room temperature

yield strength of 238 ksi and elongation of 9%. After heat treatment, the chevron-notch slots were ground as shown in Figure 3.3.7.2.1.

It should be noted that, for high strength steels, the minimum specimen diameter of a short rod fracture toughness specimen to give size independent test results that meet the requirements of a valid plane strain fracture toughness (K_{Ic}) measurement, i.e., $K_{Iv} \sim K_{Ic}$, was estimated to be $<4.6(K_{Ic}/\sigma_y)^2$ where σ_y is the yield strength, a condition that was adequately met in these experiments. Values of $K_{Iv} \sim K_{Ic}$ are presented as a function of temperature for heat treated H13 steel and other heat treated tool steels in Figure 3.3.7.2.2 with heat treatments and room temperature properties listed in Table 3.3.7.2.3. (Ref. 78)

Due to the difficulty of obtaining high temperature K_{Ic} data for high strength materials such as H13 steel, an attempt has recently been made to develop a relationship between high temperature K_{Ic} and high temperature CVN (Charpy V-notch) and HRC hardness values. The relationship developed assumes that the correlation should be of the same form as that obtained from regression analysis of room temperature data for K_{Ic} as a function of CVN and HRC. Utilizing values of CVN and HRC at high temperature of H13 steel samples originally heat treated to different room temperature hardness values (56-42 HRC) by tempering at temperatures of 932–1112F (Figure 3.3.7.2.4), a quadratic fit of data is assumed to give a fair correlation between the ratios of K_{Ic}/HRC and CVN/HRC at test temperatures equal to the temperatures at which values of CVN and HRC were obtained (Figure 3.3.7.2.5). (Ref. 80)

3.3.7.2.1 *Figure]* Short rod (chevron-notch) fracture toughness specimen used to obtain data shown in Figure 3.3.7.2.2 with shaded area denoting crack advance increment (Refs. 78, 79)

3.3.7.2.2 *[Figure]* Temperature dependence of K_{Ic} ($K_{Iv} \sim K_{Ic}$) of H13 steel, VASCO MA ultrahigh strength steel, M 50 high temperature bearing steel, and S 2 tool steel used for drill bit bearings (SOLAR STEEL) (heat treatment and room temperature property data on these steels presented in Table 3.3.7.2.3) (Ref. 78)

3.3.7.2.3 *[Table]* Heat treatments and room temperature properties of H13 and other steels tested for temperature dependence of K_{Ic} with data as shown in Figure 3.3.7.2.2 (Ref. 78)

3.3.7.2.4 *[Figure]* Variation of HRC hardness and CVN Charpy V-notch values of heat treated H13 steel as a function of test temperature: H13 steel samples austenitized, quenched, and tempered to a room temperature hardness of 56–42 HRC at tempering temperatures given in insert (Ref. 80)

3.3.7.2.5 *[Figure]* Regression analysis showing quadratic fit of K_{Ic}, HRC, and CVN room temperature data for H13 steel heat treated by austenitizing, quenching, and tempering at various temperatures to a room temperature hardness of 56–42 HRC—assumed to hold at high temperatures if high temperature values of HRC and CVN are used instead (Ref. 80)

3.3.8 Combined Loading

3.3.9 Ductile to Brittle Transition Temperature

As with other ferritic and martensitic tool steels, H-13 steel exhibits a ductile to brittle transition temperature (DBTT), i.e., the temperature at which its impact fracture surface exhibits at least 50% ductile fracture. The toughness below and above the DBTT is called the lower and upper shelf respectively. (Ref. 56)

The DBTT of H-13 steel is approximately 350F, hence the need to preheat hot working and casting dies above this temperature carefully in service. The actual Charpy V-notch value of H-13 steel at the DBTT is a function of composition and microstructure and, as seen in Figure 3.3.9.1, an overlap can occur in the lower shelf of high and low quality H-13 steel, although this overlap disappears as test temperature is raised. (Ref. 60)

3.3.9.1 *[Figure]* Representation of DBTT curves based on Charpy V-notch (CVN) tests of low quality and high quality H-13 tool steels heat treated as per NADCA 207-97 (3.1.1) (Ref. 60)

3.4 Creep and Creep Rupture Properties

3.4.1 *[Figure]* Creep characteristics of H-13 steel heat treated to 216 ksi room temperature tensile strength (~44–46 HRC): strain duration in h (to 1% creep limit – left or creep rupture – right) as a function of stress (N/mm^2 x 0.145 = ksi) at temperatures (C x 1.8 + 32 = F) indicated (Ref. 17)

3.5 Fatigue Properties

3.5.1 High-Cycle Fatigue

The better the microstructural homogeneity of H-13 steel, the higher the fatigue strength. This is shown in the comparison of fatigue strength of electric arc air melted (AAM), electroslag remelted (ESR), and ESR-Isodisc (a patented H-13 microstructural control process of Böhler Edelstahl GmbH) in Figure 3.5.1.1. (Ref. 38) Axial or tension-tension fatigue tests conducted on heat treated longitudinal H-13 steel specimens also have shown the benefits of ESR H-13 over electric arc air melted H-13 steel (Figure 3.5.1.2). However, in fully reversed or tension-compression fatigue tests, while no significant differences were noted between longitudinal specimens of ESR and air melted H-13 steel, a significantly better life was noted in the transverse ESR H-13 steel specimens (Figure 3.5.1.3). (Ref. 62)

A general formula for estimating fatigue properties of most metallic materials including H-13 steel is based on the universal slopes method developed by Manson and coworkers at NASA Lewis:

$$\Delta\varepsilon_t = (3.5\sigma_u/E)N_f^{-0.12} + D^{0.6}N_f^{-0.6}$$

where $\Delta\varepsilon_t$ is the total strain range and the mechanical properties σ_u, E, and D are the ultimate tensile strength, modulus of elasticity, and true ductility (determined from the % reduction in area (RA) by ln(100/(100-RA), and N_f is fatigue life in number of cycles. The universal slopes equation is relatively accurate for estimating room temperature fatigue behavior in small laboratory specimens. It basically indicates that strength predominates over ductility for good high-cycle fatigue life at low values of total strain range. When applied to estimating high-cycle fatigue life at high temperatures, values for σ_u, E, and D are selected at the high temperature of interest at moderate strain rates used in tensile testing. (Ref. 63)

3.5.1.1 *[Figure]* Fatigue strength (N/mm^2 x 0.145 = ksi) of smooth and notched specimens tested at room temperature in fully reversed tension-compression (R = -1) of hardened H-13 steel in relation to microstructural homogeneity achieved by electric arc air melted, ESR, and special treatment (patented Isodisc process) (Ref. 38)

3.5.1.2 *[Figure]* Tension-tension (R = +0.2) fatigue curves determined at 60 Hz for longitudinal specimens of air melted (△) and ESR (❍) heats of H-13 steel in the hardened condition (austenitized at 1850F, oil quenched, and double tempered 2 + 2 h at 1090F to 48 HRC hardness) (Ref. 62)

3.5.1.3 *[Figure]* Fully reversed tension-compression (R = -1) fatigue curves determined at 60Hz for longitudinal (❍ – ESR, △ – air melted) and transverse (● – ESR, ▲ – air melted) H-13 steel in the hardened condition (austenitized at 1850F, oil quenched, and double tempered 2 + 2 h at 1090F to 48 HRC hardness) (Ref. 62)

3.5.2 Low-Cycle Fatigue

Low-cycle fatigue is an important failure mode, especially in dies and tooling subjected to complex stress states over a range of temperatures. The universal slopes equation developed by Manson (3.5.1) for estimating low-cycle fatigue life indicates that true ductility is more important than ultimate strength in low-cycle fatigue at high levels of total strain range, although for low-cycle fatigue it has been found to only work well for estimating room temperature low-cycle fatigue behavior in small laboratory specimens. At relatively high temperatures and levels of total strain, it overestimates N_f significantly due to creep effects that induce time dependent failures. In cases of combined fatigue and creep-rupture damage, when taking values for σ_u, E, and D at the high temperature of interest at moderate strain rates used in tensile testing, a cycle-reduction factor called the "10% rule" (fatigue life N_f is taken as 10% less of that predicted by the universal slopes equation) offers a good approximation of low-cycle fatigue life for H-13 steel. Manson and Halford have developed a more accurate method of estimating low-cycle fatigue life at high temperatures and low frequencies of loading for cases when the cycle-reduction factor is less than 10% and $N_f < 10^5$ that takes greater account of the creep rupture damage that may occur in such cases and have applied it successfully to hot work tool steels such as H-13 and other high temperature alloys. (Ref. 64)

3.6 Elastic properties

3.6.1 Poisson's Ratio

The room temperature Poisson's ratio of H-13 steel is 0.28, but it increases with temperature in a nonlinear fashion, approaching 0.30 at 1000F and 0.33 at 1400F.

3.6.2 Modulus of Elasticity

3.6.2.1 *[Table]* Modulus of elasticity of Thyrotherm 2344 ESR Magnum premium grade H-13 steel as a function of temperature (Ref. 18)

3.6.2.2 *[Table]* Modulus of elasticity of VDC H-13 steel as a function of temperature (Ref. 16)

3.6.3 Modulus of Rigidity

3.6.4 Tangent Modulus

3.6.5 Secant Modulus

3.7 Thermal Fatigue Properties

Thermal fatigue differs from conventional fatigue at high temperatures in that the stresses that produce thermal fatigue failure are induced by repeated temperature gradients at the surface (thermal stresses). Thermal fatigue failures typically initiate at the surface in a multiple crack pattern that gradually deepens, a phenomenon called heat checking in dies and tooling, which eventually causes failure. Thermal fatigue is one of the main causes of heat checking in H-13 steel dies and tools used in die casting and hot working, with cracks deepening every cycle to the point where the dies and tools are useless and must be replaced. Heat checking due to thermal fatigue is the main limiting factor, for example, in die life in aluminum die casting. Various thermal fatigue tests have been developed to assess thermal fatigue or heat checking resistance of H-13 steel using thermal cycles that attempt to simulate those that occur in service; however, the results of these tests do not necessarily correlate well with each other. Only relative comparisons of H-13 variables (H-13 steel grade, heat treatment, coatings, etc.) in a particular thermal fatigue or heat checking test seem to be relevant.

3.7.1 CWRU Thermal Fatigue Test

The thermal fatigue test developed at Case Western Reserve University (CWRU) in the 1960s has become the standard of comparison of H-13 steel and other die materials for the aluminum die casting industry (Figure 3.7.1.1). The CWRU square specimen, water cooled from the inside, results in thermal fatigue cracking along each of the four corners, and all the cracks are measured periodically as a function of number of cycles, then averaged. This test was developed to simulate specifically the thermal fatigue behavior that causes heat checking in aluminum die casting dies. In the initial work done in testing H-13 steel in this test, the discovery was made of the unexpected advantages of high temperature austenitizing of H-13 steel in significantly raising its thermal fatigue and heat checking resistance (see 1.5.5 and Figure 3.7.1.2) and the role of stress accelerated softening as an important mechanism in thermal fatigue failure (see 1.5.9). (Ref. 4, 22-25) The CWRU test has been very useful in isolating quality of H-13 steel in terms of thermal fatigue and heat checking resistance. For example, the test has clearly distinguished various qualities of H-13 steel (Table 3.7.1.5) against the standard heat of base H-13 steel, obtained from an argon degassed melt that was forged into a 5 x 20 in. block from a 32-in. square ingot, and established an order of merit (Figure 3.7.1.3); the poor thermal fatigue resistance of a particular heat of vacuum remelted H-13 (vac. remelt #1) was found to be due to an inadequate forging reduction of the ingot. Thermal fatigue testing at CWRU of H-13 steel with various coatings and of competitive high temperature materials continues today. (Ref. 48)

3.7.1.1 *[Figure]* Schematic drawing of CWRU thermal fatigue test used in studying H-13 thermal fatigue and heat checking resistance showing apparatus used to dip specimen into molten A380 aluminum at 1300F (upper) and water cooled H-13 steel test specimen (lower) (Refs. 22–24, 48)

3.7.1.2 *[Figure]* Thermal cycle used in determining thermal fatigue resistance of H-13 steel in the CWRU test for different austenitizing temperatures (Figure 3.7.1.3) and various types and grades of H-13 steel (Figure 3.7.1.4) (Refs. 22–24)

3.7.1.3 *[Figure]* Thermal fatigue behavior in the CWRU test (Figure 3.7.1.1) of H-13 steel austenitized at 1750, 1850, 1950, and 2050F, air quenched, and all tempered to 45 R_c (HRC) showing average maximum crack length in microns (μ) (upper) and summation of total crack area (lower) as a function of number of cycles (Refs. 22–24)

3.7.1.4 *[Figure]* Thermal fatigue behavior in the CWRU test (Figure 3.7.1.1) of various types and grades of H-13 steel austenitized at 1850F, air quenched, and all tempered at 1100F to 45 R_c (HRC) showing average maximum crack length in microns (μ) (upper) and summation of total crack area (lower) as a function of number of cycles (Refs. 22–24)

3.7.1.5 *[Table]* Chemical composition and inclusion ratings of H-13 steel materials tested for thermal fatigue resistance in the CWRU test (Figure 3.7.1.1) (Refs. 22–24)

3.7.2 IITRI Thermal Fatigue Test

The thermal fatigue test developed at IITRI (the former Illinois Institute of Technology Research Institute) utilized a stack of disc shaped specimens with a peripheral fin that were subjected to alternating heating and cooling cycles in fluidized beds (Figure 3.7.2.1). The material tested was machined from 2.5-in. diameter bar stock forged from induction air melted and cast 6-in. ingots of H-13 steel. The IITRI results confirmed some of the observations made in the CWRU test regarding effects of composition, inclusion level, and hardness of hardened H-13 steel on thermal fatigue resistance. Also, as in the CWRU thermal fatigue tests, stress accelerated tempering

occurred in the IITRI thermal fatigue tests conducted on hardened H-13 steel. (Refs. 25, 66)

Stress accelerated tempering was also noted in the thermal fatigue tests conducted at IITRI. The effect of the length of the thermal cycle between 1100 and 400F was also determined. Besides the short cycle shown in Figure 3.7.2.1, a long thermal cycle was used (Figure 3.7.2.4), and the results were compared (Figure 3.7.2.5). The hardness noted in the highly stressed fin section was always less than that to be expected from standard temperature-time tempering data in unstressed pieces of H-13 steel hardened and tempered to the same initial condition. (Ref. 25)

3.7.2.1 *[Figure]* Heating and cooling curves for H-13 steel during a short cycle of thermal cycling between 1100 and 400F in the IITRI thermal fatigue test (Refs. 25, 66)

3.7.2.2 *[Table]* Influence of initial tempered hardness of H-13 steel on thermal fatigue resistance measure in the IITRI thermal fatigue test according to the cycle shown in Figure 3.7.2.1 (Ref. 66)

3.7.2.3 *[Figure]* Number of cycles to crack initiation of H-13 steel in IITRI thermal fatigue test according to the cycle shown in Figure 3.7.2.1 as a function of cleanliness of the steel as rated by the number of +4 mm oxide inclusions at 320x magnification in 40 random fields (Ref. 66)

3.7.2.4 *[Figure]* Heating and cooling curves for H-13 steel during a long cycle of thermal cycling between 1100 and 400F in the IITRI thermal fatigue test (Ref. 25)

3.7.2.5 *[Figure]* Tempering of IITRI thermal fatigue fins (HRC hardness noted on fins) during short and long thermal cycling for 250–16,000 cycles (Ref. 25)

3.7.3. Thermal Fatigue Tests of H-13 Steel Suppliers

Various thermal fatigue tests have been devised by H-13 steel suppliers and even a few users in order to be able to distinguish quality of the steel in relation to thermal fatigue resistance and to optimize metallurgical processing accordingly. These tests differ significantly in method of heating and cooling; however, the comparative data are useful in assessing effects due to microstructure and processing, especially if care is taken to duplicate the thermal fatigue conditions in service.

For example, the comparative thermal fatigue data in Figure 3.7.3.1, generated by Crucible Steel Co. in their thermal fatigue test show the following order of merit for similarly hardened H-13 steel: (1-best) CPM Nu-Die EZ powder metallurgy produced resulfurized H-13 steel, (2) premium H-13 steel/Nu-Die XL, and (3-worst) conventional resulfurized H-13 steel. This test also indicates the deleterious effect of the EDM'd (electrodischarge'd machined) surface on thermal fatigue of H-13 steel. (Ref. 12, 43).

EWK-GmbH and ThyssenKrupp Specialty Steels NA have developed a thermal fatigue test based on high frequency induction heating and water quenching (Figure 3.7.3.3) to evaluate heat checking of H-13 steel and modified versions of H-13 steel. A comparison was made of the thermal fatigue resistance of a superior grade of H-13 steel of standard composition (Thyrotherm 2344 EFS Supra) with a modified version of H-13 steel (Thyrotherm 2367 EFS Supra) having a variation in the content of Si (lower), Mo (higher), and V (lower) than the standard AISI H-13 composition. The modified H-13 composition (see Table 1.4.1) had a significantly better thermal fatigue resistance relative to the standard superior grade H-13 composition (Figures 3.7.3.4 and 3.7.3.5) upon evaluation of crack patterns over 2, 000–8, 000 heating and cooling cycles. (Ref. 68)

3.7.3.1 *[Figure]* Thermal fatigue data from Crucible Steel Co. test (alternate immersion of square specimens in molten A380 aluminum at 1250F and quenching in a water bath at 200F with examination for cracks every 10, 000 cycles) (Ref. 43)

3.7.3.2 *[Table]* Thermal fatigue/heat checking comparison of AISI H-13 and premium H-13 steel specimens (1.75 x 2.38 in.) heat treated to 47 HRC tested at 1,500 cycles of alternating heating at 1300F and quenching into hot water (Ref. 67)

3.7.3.3 *[Figure]* Thermal fatigue testing apparatus of EWK/Thyssen Krupp Specialty Steel: Ar atmosphere to avoid corrosion, induction heating to 1200F, water bath maintained at or near room temperature and at a pH = 10.5 to improve wetting, 2 x 2 x 0.40 in. H-13 steel samples cut from 30 x 8 in. forged slabs in transverse direction and rough machined, samples were hardened and tempered to 44–46 HRC and ground to a fine finish (Ref. 68)

3.7.3.4 *[Figure]* Total crack length measured on samples of a superior grade of AISI H-13 (Thyrotherm 2344 EFS Supra) and a modified grade of H-13 (Thyrotherm 2367 EFS Supra) heat treated to 44–46 HRC and tested in the EWK/ Thyssen Krupp Specialty Steel thermal fatigue apparatus shown in Figure 3.7.3.3 (Ref. 68)

3.7.3.5 *[Figure]* Microscopic evaluation at 200x of some thermal fatigue cracks developed in samples (Figure 3.7.3.4) from the EWK/Thyssen Krupp Specialty Steel thermal fatigue test (Figure 3.7.3.3) (Ref. 68)

4.0 Fabrication

4.1 Forming

In the fully annealed condition, H-13 steel can be formed to a limited extent by most common methods.

4.1.1 Hot Working

Forging

H-13 steel is normally forged in open or closed dies at 1900–2200F and should not be forged below 1500–1600F. A typical forging practice consists of heating slowly to about 1500F and then more rapidly to the forging range of 1900–2200F. After forging, the H-13 workpiece should be cooled slowly and annealed as soon as possible. (Refs. 17, 31)

Conventional grades of H-13 do not have a specification on prior hot forging reductions or practice, although inadequate hot forging reduction and practice may compromise some physical and mechanical properties, e.g., thermal fatigue (see 3.7.1) and elevated temperature impact resistance. Premium and superior grades of H-13 steel typically have been forged from three directions (triaxial forging) in order to minimize longitudinal, transverse, and thickness property differences. Forging reductions that assure a minimum ratio of 5:1 in each direction are necessary to obtain optimum physical and mechanical properties. Should there be a need to reforge the as-received material, the original physical and mechanical properties may no longer apply.

4.2 Machining and Grinding

Rough machining (usually, turning, milling, and/or drilling) is generally performed on H-13 steel in the fully annealed condition, in which its machinability is considered fair, somewhat less than the A steels and better than the D steels. Fully annealed H-13 steel has an average machinability rating of about 70% of the rating for annealed 1% C tool steel or about 45% of that for B1112, which is used as a standard reference steel for machinability ratings. Nominal speeds for milling of annealed H-13 steel (200-250 HB) with HSS and carbide cutters at standard cutter feeds of 0.001-0.003 in./tooth are 70-75 sfm for rough milling and 95-100 sfm for finish milling; for hardened H-13 steel (48-50 HRC) under the same conditions the nominal speeds for rough and finish milling are 30 and 35 sfm respectively. Grindability of H-13 steel decreases as hardness increases and is a function of vanadium and chromium content, both of which adversely affect grindability; however, use of cubic boron nitride superabrasive wheels with a resinoid or vitrified matrix and in metal-plated monolayer CBN (cubic boron nitride) wheels can significantly increase H-13 steel removal rates as well as wheel life. (Ref. 69)

Electric discharge machining (EDM) is widely used for production of hardened H-13 steel dies and tools. However, EDM generates a harmful "white layer" of martensite on the surface, which must be removed by careful grinding, stoning, or polishing. After removal of the "white layer", a double temper at 50F below the highest tempering temperature used in hardening is sometimes recommended in order to stress relieve the surface. (Ref. 70) Although a "white layer" does not usually form during conventional machining operations at normal machining speeds, a "white layer" can form on the surface during the high speed turning of H-13 steel bars in the hardened condition (54–56 HRC) using CBN cutting tools. (Ref. 71)

On H-13 extrusion dies with complex configurations and passages, abrasive flow machining (AFM) is often used to finish surfaces and edges by extruding viscous abrasive media through or across the die. AFM is used to deburr, polish, radius, and remove the "white layer" produced by EDM on H-13 steel surfaces and edges. (Ref. 72)

Sulfurized H-13 steel with sulfur additions of about 0.20% has a much better machinability rating than standard H-13 compositions (~75% of that for B1112). For the same turning and milling conditions, machining of sulfurized H-13 requires about 30% less time. In grinding operations, sulfurized H-13 steel in annealed or hardened conditions has much better grindability than H-13 with standard limits on sulfur (<0.03%). However, the long, non-uniformly distributed sulfides that are found in conventionally sulfurized H-13 steel can be detrimental to the performance of tools and dies (see 3.7.1.4, 3.7.1.5, and 3.7.3.1) not only in resistance to fracture in service but also in relation to polishability. The sulfurized grade of H-13 produced by Crucible Material Corporation utilizing particle metallurgy processing (Crucible CPM® Nu-Die® EZ) results in a very fine distribution of uniformly distributed sulfides with no detrimental effects on tool performance. It is supplied in a prehardened condition at HRC 40–44 and can be readily machined to finish dimensions without further heat treatment. (Ref. 43)

4.3 Joining

H-13 steel can be welded in an annealed or hardened condition if necessary. Die casting and hot work dies are often welded to make changes in them before they enter service or for repair;

however, welding of H-13 steel dies involves risks such as cracking. Thus, several guidelines have been established for proper welding of H-13 steel. (Ref. 4-20)

For welding annealed H-13 steel, the part should be preheated to 650–1000F, preferably in a furnace to assure a uniform temperature. Uncoated H-13 steel filler rod (0.10–0.17 in. diameter) with tungsten inert gas (TIG) welding at 100–150 A D.C. using Ar protective gas should be used. The temperature of the part should be kept above 600F, with reheating applied as required until welding is complete. Slow cooling after welding can be achieved in an insulating medium. As-welded hardness is typically 48–52 HRC. After slow cooling, the part then is given a full anneal.

For welding hardened H-13 parts, such as dies or tooling, the same procedure that is used for welding annealed H-13 may be used, preferably using a preheating temperature close to 1000F. It is recommended that the welded part be placed in a furnace kept at the preheat temperature and furnace cooled to room temperature. To further relieve welding stresses and make the hardness in the weld zone come closer to the base metal, the welded part should be tempered at 30–50F below the original tempering temperature.

4.4 Surface Treating

Gas, salt bath, fluidized bed, or ion nitriding and ferritic nitrocarburizing are all effective procedures for nitriding H-13 steel and producing a hard, abrasive resistant surface having a case hardness of 60–70 HRC (see 1.5.11 and 1.6.3). For hot working dies and tools, deep nitriding to a case depth of >0.010 in. is not recommended. H-13 parts that have been deep nitrided need to be lapped or surface ground to remove the thin, outer brittle layer. Also, dies with sharp corners or critical projections may not benefit from nitriding and may actually have shortened lives due to breakage. Selective nitriding can also be done to produce a hard nitrided case only where needed. Copper plating is preferred for stopping off areas that do not need nitriding. Stop-offs that contain lead should not be used, as lead embrittles H-13 steel. (Refs. 1–3) The Aluminum Extruders Council has made several recommendations for nitriding H-13 steel aluminum extrusion dies and promoted the benefits of re-nitriding them to increase life substantially. (Ref. 73)

Physical vapor deposited (PVD) and chemical vapor deposited (CVD) coatings have been used on H-13 dies and tools to protect H-13 steel against corrosion/erosion of molten aluminum (2.3.5) and to improve its wear resistance in hot metalworking dies and tools. Duplex coatings involving plasma nitrided pretreatment and either a PVD or plasma-assisted CVD or PVD coatings have been successful in prolonging H-13 steel die life in aluminum extrusion dies compared to conventional nitriding. (Refs. 74–75)

References

1. *Metals Handbook Ninth Edition. Volume 1. Properties and Selection: Irons and Steels*, American Society for Metals (now ASM International), 1978, pp. 437–39.
2. *Metals Handbook Ninth Edition. Volume 3. Properties and Selection: Stainless Steels, Tool Materials and Special-Purpose Metals,* American Society for Metals (now ASM International), 1980, pp. 421–69.
3. *HEAT TREATER'S GUIDE: Practices and Procedures for Irons and Steels*, ASM International, 2nd Ed., 1998, pp. 600-605.
4. *Premium and Superior Quality H-13 Steel and Heat Treatment Acceptance Criteria for Pressure Die Casting Dies: NADCA #207-2003,* North American Die Casting Association (NADCA), River Grove, Illinois, 2003.
5. Allegheny Ludlum H-13 Tool Steel, UNS T20813, DATA SHEET.
6. Assab Steels 8407 SUPREME Hot Work Steel, DATA SHEET.
7. Bohler-Uddeholm ORVAR H-13 Hot Work Tool Steel, DATA SHEET.
8. Bohler-Uddeholm SUPERIOR H-13 Hot Work Tool Steel, DATA SHEET.
9. Bohler-Uddeholm ISOBLOC H-13 Hot Work Tool Steel, DATA SHEET.
10. Carpenter Pyrotough® 78 Hot Work Die Steel. DATA SHEET.
11. Carpenter No. 883® Hot Work Die Steel (Red-Tough) (AISI H-13), DATA SHEET.
12. Crucible Nu-Die® XL (Premium Quality AISI H-13) Tool Steel, DATA SHEET.
13. International Mold Steel DH2F Pre-Hardened H-13-Type Mold Steel, DATA SHEET.
14. International Mold Steel Premium H-13 Hot Work Die and Mold Steel, DATA SHEET.
15. Latrobe LSS® H-13 Tool Steel, DATA SHEET.
16. Latrobe VDC® H-13 Tool Steel, DATA SHEET.
17. ThyssenKrupp Specialty Steels THYROTHERM 2344, DATA SHEET.
18. ThyssenKrupp Specialty Steels THYROTHERM 2344 ESR MAGNUM, DATA SHEET.
19. ThyssenKrupp Specialty Steels THYROTHERM 2367 SUPRA ESR, DATA SHEET.
20. Premium Grade H-13/Hot Work Tool Material Standard Specification: Die Insert and Heat Treating Specification, Spec. No. DC-9999-1, GM Powertrain Group, 6-29-2001.
21. Die Insert Material and Heat Treatment Performance Requirements: General Applications, Spec. No. AMTD-DC2010, FORD Advanced Manufacturing Technology Development, 17 February 2003.
22. Benedyk, J. C., Thermal Fatigue Behavior of H-13 Die Steels, Ph.D. Thesis, Case Western Reserve University, January, 1969.
23. Benedyk, J. C., Moracz, D. J., and Wallace, J. F., "Thermal Fatigue Behavior of Die Materials for Aluminum Die Casting, " Paper No. 111, 6th SDCE (Society of Die Casting Engineers) International Die Casting Congress, November 16–19, 1970.
24. Dunn, R. P., "Thermal Fatigue Behavior of H-13 Steel & Other Die Materials for Aluminum Die Casting, " Report of the Task Group on Materials & Surface Treatments for Dies, Die Casting Research Foundation 1969 Annual Meeting, October 8, 1969.
25. Nolen, R. K., Benedyk, J. C., and Howes, M. A. H., Investigation of Strain Softening Occurring during Thermal Fatigue, Internal Research and Development Project Final Report on Project B1051, IIT Research Institute, October 23, 1969.
26. Purohit, S. and Tszeng, C., "Carbide Dissolution in H-13 Tool Steel during Austenitization, " TPTC (Thermal Processing Technology Center, Illinois Institute of Technology) Project Review, 2003.
27. Pacyna, J. and Mazur, A., "The Influence of Grain Size upon the Fracture Toughness of the Hot-Work Tool Steel, " *Scandinavian J. of Metallurgy*, No. 12, 1983, pp. 22–28.
28. Schmidt, M. L., "Effect of Austenitizing Temperature on the Structure and Mechanical Property Behavior of Laboratory Treated Specimens and Large Section Sizes of H-13 Tool Steel, " Paper No. G-T87-006, 14th SDCE (Society of Die Casting Engineers) International Die Casting Congress, May 11–14, 1987.
29. Stuhl, J. H. and Schindler, A. M., "New Materials Study of 5% Chromium Type Steels for Use in Die Casting Dies, " Paper No. G-T75-053, 8th SDCE (Society of Die Casting Engineers) International Die Casting Congress, May 17–20, 1975.
30. Conybear, J. A., "Vacuum Hardening of H-13 Die Steels: Experience with Convective Assisted Heating and Isothermal Holding in Regard to Distortion and Metallurgical Properties, " reprinted from Industrial Heating, August, 1993.
31. Alloy Tool Steel SPEC FACTS A.I.S.I. H-13, DATA SHEET.
32. Thelning, K. E., "How Far Can H-13 Die Casting Die Steel Be Improved, " Paper No. 114, 6th SDCE (Society of Die Casting Engineers) International Die Casting Congress, November 16–19, 1970.

33. Huffman, D. D. "Avoiding Retained Austenite in Tool Steels, " Source Book on Heat Treating: Vol. II – Production and Engineering Practices, American Society for Metals (now ASM International), December, 1974, pp. 276–79.

34. Y.-M. Rhyim, et al., "Effect of Surface Treatment on the Life of AISI H-13 Steel Core Pin for Die Casting, " *Key Engineering Materials*, Vols. 326–28, 2006, pp. 1181–84.

35. *Metals Handbook Ninth Edition. Volume 9: Metallography and Microstructures*, American Society for Metals (now ASM International), 1985, p. 228.

36. Cremisio, R. S., Pridgeon, J. W., and Mills, D. W, Hot Work Materials Processing and Metallurgy for Hot-Extrusion Applications, AJAX Forging and Casting Co., Allegheny Ludlum Industries Co., Ferndale, MI, 1977, pp. 24–25.

37. *Metals Handbook Ninth Edition. Volume 1. Properties and Selection: Irons and Steels*, American Society for Metals (now ASM International), 1978, p. 440.

38. Schindler, A. M., Kulmberg, A., and Stuhl, J. H., "Thermal Fatigue of H-13 in Die Casting Applications, " Paper No. G-T77-065, 9th SDCE (Society of Die Casting Engineers) International Die Casting Congress, June 6–9, 1977.

39. *Metals Handbook Ninth Edition. Volume 9: Metallography and Microstructures*, American Society for Metals (now ASM International), 1985, p. 271.

40. MetalTek MTek T90813 H-13 Tool Steel, DATA SHEET.

41. Osprey Metals H-13 Tool Steel Powder Grades, DATA SHEETS.

42. Cremisio, R. S., Pridgeon, J. W., and Mills, D. W, Hot Work Materials Processing and Metallurgy for Hot-Extrusion Applications, AJAX Forging and Casting Co., Allegheny Ludlum Industries Co., Ferndale, MI, 1977, pp. 4–13.

43. Crucible CPM® Nu-Die® EZ, DATA SHEET, Issue #2.

44. *Engineering Properties of Steel: Hot Work Tool Steels*, ASM International, 1982, pp. 457–62.

45. da Silva, L. L. G., Ueda, M., and Nakazato, R. Z., "Enhanced Corrosion Resistance of AISI H13 Steel Treated by Nitrogen Plasma Immersion Ion Implantation, " *Surf. Coat. Techn.*, 201, 2007, pp. 8291–94.

46. Hamaker, J. C. and Yates, D. H., "A Forward Look at the New Die Steels, " Paper No. 1201, 4th SDCE (Society of Die Casting Engineers) International Die Casting Congress, November 14–17, 1966.

47. Youn, K.-T., et al., "An Evaluation of Thermal Fatigue Cracking and Chemical Reaction in Die Casting Mould, "*Key Engineering Materials*, Vols. 345-346, 2007, pp. 701–04.

48. Test data and review of latest research on H-13 steel kindly provided by Prof. J. Wallace of CWRU.

49. Kamdar, M. H., "Liquid-Metal Embrittlement, " *Metals Handbook. Volume 11. Failure Analysis and Prevention*, ASM International, 1986, pp. 225–38.

50. Kim, T., et al., "Liquid Zinc Embrittlement Study of H-13 Steel in Various Austenitized and Tempered Conditions, " TPTC Confidential Report for Industrial Client (data kindly provided with permission), 2008.

51. Kamdar, M. H., "Embrittlement by Solid-Metal Environments, " *Metals Handbook. Volume 11. Failure Analysis and Prevention*, ASM International, 1986, pp. 239–44.

52. Takao, et al., "Crack Initiation and Propagation Mechanism of Die for Extruding 7000 Series Alloy, " *Keikinzoku Fakkai Koen Gaiyo*, 1993, Vol. 84, pp. 275–76 (in Japanese).

53. Benedyk, J., et al., "Literature Survey on H-13 Extrusion Die Failure (I), " TPTC Confidential Report for Industrial Client, 2003.

54. Gordon, P., "Metal-Induced Embrittlement of Metals – An Evaluation of Embrittler Transport Mechanisms, " *Met. Trans. A*, V. 9A, Feb., 1978, pp. 267–73.

55. Kim, C. D, "Hydrogen-Damage Failures, " *Metals Handbook. Volume 11. Failure Analysis and Prevention*, ASM International, 1986, pp. 245–51.

56. Rosenfield, A. R. and Marshall, C. W., "Ductile-to-Brittle Fracture Transition, " *Metals Handbook. Volume 11. Failure Analysis and Prevention*, ASM International, 1986, pp.69, 100.

57. Shatla, M., Kerk, C., and Altan, T., "Process Modeling in Machining. Part I: Determination of Flow Stress Data, " *International J. of Machine Tools & Manufacture*, Vol. 41, 2001, pp. 1511–34.

58. Crucible Nu-Die® V (AISI H-13) Tool Steel, Issue #13, DATA SHEET.

59. *Plane Strain Fracture Toughness (K_{Ic}) Data Handbook for Metals*, Army Materials and Mechanics Research Center, Watertown, MA, December, 1973.

60. Brada, G., "Effects of Quench Rate and Impact Test Temperature on the Toughness and Microstructure of H13, " *Die Casting Engineer*, May, 2002, pp. 22–24.

61. Huffman, D. D., "Aluminum Extrusion Tooling: Where Do We Stand?, " International Extrusion Technology Seminar, 1969, paper no. 23.

62. Philip, T.V., "ESR: A Means of Improving Transverse Mechanical Properties in Tool and Die Steels, " *Metals Technology*, Dec., 1975, p. 554.

63. Manson, S. S., Thermal Stress and Low-Cycle Fatigue, McGraw-Hill, 1966, pp. 125–91.

64. Manson, S. S. and Halford, G., "A Method of Estimating High-Temperature Low-Cycle Fatigue Behavior of Materials, " NASA Lewis Research Center, Cleveland, Ohio, January, 1967.

65. Barrow, B. J., "The Thermal Fatigue Resistance of H-13 Die Steel for Aluminum Die Casting Dies, " NASA Technical Memorandum 83331, NASA Lewis Research Center, Cleveland, Ohio, August, 1982.

66. Rostoker, W., et al., The Metallurgy of Thermal Fatigue: Summary Report IV on Thermal Fatigue Resistance of Martensitic Steels, IITRI-B879-20, July 17, 1967.

67. Alloy Tool Steel SPEC FACTS Premium Grade H-13, DATA SHEET.

68. Ehrhardt, R., et al., "Improving the Heat Checking Characteristics of AISI H13 by Modification of the Chemical Composition, " *Die Casting Engineer*, Nov., 2003, pp. 30–37.

69. *Metals Handbook Ninth Edition. Vol. 16. Machining*, ASM International, 1989, pp. 712–26.

70. *Metals Handbook Ninth Edition. Vol. 16. Machining*, ASM International, 1989, pp. 557–64)

71. Bosheh, S. S. and Mativenga, P. T., "White Layer Formation in Hard Turning of H13 Tool Steel at high Cutting Speeds Using CBN Tooling, " *International J. of Machine Tools & Manufacture*, Vol. 46, 2006, pp. 225–33.

72. *Metals Handbook Ninth Edition. Vol. 16. Machining*, ASM International, 1989, pp. 514–19)

73. *Extrusion Dies & Tooling Manual: Recommended Handling and Maintenance*, Aluminum Extruders Council, pp. 16-17.

74. Björk, T., Westergård, R., and Hogmark, S., "Wear of Surface Treated Dies for Aluminium Extrusion – A Case Study, " *Wear*, Vol. 249, 2001, pp. 316–23.

75. Müller, K. B., "Deposition of Hard Films on Hot Working Steel Dies for Aluminium, " *J. of Materials Processing Technology*, Vols. 130-131, 2002, pp. 423–37.

76. Okuno, T., "Effect of Microstructure on the Toughness of Hot Work Tool Steels, H13, H10, H19," *Tran. ISIJ, Research Article*, Vol. 27, 1987, pp. 51–59.

77. Leskovšek, V., "Correlation Between the K_{Ic}, the HRC and the Charpy V-Notch Test Results for H11/H13 Hot-work Tool Steels at Room Temperature," *Steel Research Int.*, Vol. 79, No. 4, 2008, pp. 306–13.

78. Barker, L. M. and Leslie, W. C.," Short Rod K_{Ic} Tests of Several Steels at Temperatures to 700K," *Fracture 1977*, Vol. 2, ICF4, Waterloo, Canada, June 19–24, 1977, MS311, pp. 305–11.

79. ASTM E 1304: Standard Test Method for Plane-Strain (Chevron-Notch) Fracture Toughness of Metallic Materials.

80. Qamar, S. Z., et al., "Regression-based CVN-K-$_{Ic}$ Models for Hot Work Tool Steels," *Mater. Sci. and Eng.*, Vol. A 430, 2006, pp. 208–15.

Table 1.4.1 Standard AISI/UNS chemical composition of H-13 steel and typical compositions of specially produced commercial grades of H13 steel available from specialty steel companies (Refs. 1–21)

H-13 Type	Mass %									
	C	Mn	Si	Cr	Ni	Mo	V	Cu	P	S
Standard H13 Tool Steel AISI/UNS (T20813)	*0.32-0.45*	*0.20-0.50*	*0.80-1.20*	*4.75-5.50*	*0.30 max*	*1.10-1.75*	*0.80-1.20*	*0.25 max*	*0.03 max*	*0.03 max*
H13 Tool Steel (Allegheny Ludlum)	0.37	--	1.00	5.00	--	1.35	1.00	--	--	--
Nu-Die V H13 (Crucible)	0.40	0.35	1.00	5.20	--	1.30	0.95	--	--	--
No. 883 (Red Tough) H13 (Carpenter)	0.41	0.35	1.00	5.35	--	1.40	0.90	--	--	--
LSS H13 (Latrobe Specialty Steel)	0.40	0.40	1.00	5.25	--	1.35	1.00	--	--	--
THYROTHERM 2344 EFS (ThyssenKrupp)	0.40	--	1.00	5.30	--	1.40	1.00	--	--	--
DH2F H13* (International Mold Steel)	0.32-0.42	1.50	1.50	4.50-5.50	--	1.00-1.50	0.40-1.20	--	--	--
Nu-Die XL** (Crucible)	0.40	--	1.00	5.20	--	1.30	0.95	--	--	0.003 max
LSS H13 PQ** (Latrobe Specialty Steel)	0.40	0.40	1.00	5.25	--	1.35	1.00	--	--	0.001
Premium H13** (International Mold Steel)	0.40	0.40	1.00	5.25	--	1.35	1.00	--	--	<0.03 max
THYROTHERM 2344 ESR MAGNUM** (ThyssenKrupp)	0.40	--	1.00	5.30	--	1.40	1.00	--	0.020 max	0.003 max
W302 SUPERIOR** (Bohler-Uddeholm)	0.39	0.40	1.10	5.20	--	1.40	0.95	--	--	0.003 max
ISOBLOC** (Bohler-Uddeholm)	0.39	0.40	1.10	5.20	--	1.40	0.95	--	--	0.003 max
THYROTHERM 2367 SUPRA ESR*** (ThyssenKrupp)	0.37	--	0.40	5.00	--	3.00	0.60	--	0.020 max	0.003 max
Extendo-Die*** (Carpenter)	0.44	0.45	1.00	6.00	--	1.90	0.80	--	--	0.005 max
Pyrotough 78*** (Carpenter)	0.40	0.45	1.00	4.45	--	2.05	0.80	--	--	0.005 max
CPM Nu-Die EZ**** (Crucible)	0.36	0.35	1.00	5.50	--	1.60	0.85	--	--	0.17
GM Powertrain Group (Spec. No. DC-9999-1)	0.37-0.42	0.20-0.50	0.80-1.00	5.00-5.50	--	1.20-1.75	0.80-1.20	--	0.020 max	0.003 max
FORD Advanced Manufacturing Technology Department (Spec. No. AMTD-DC2010)	-Specific to H13 steel supplier-									

* Modified H-13 steel grade.

** Premium grade of electro-slag remelted (ESR) or specially melted and refined H-13 steel.

*** Premium grade and modified AISI H13 steel.

**** Patented AISI H13 resulfurized steel made by Crucible particle metallurgy (CPM) process.

Table 1.4.2 Chemical composition (weight %) of critical alloying elements and impurities in premium and superior quality grades of H13 steel (Ref. 4)

Elements	Premium Grade H13		Superior Grade H13	
	Min.	Max.	Min.	Max
C	0.37*	0.42*	0.37	0.42
Mn	0.20	0.50	0.20	0.50
P	--	0.025*	--	0.015**
S	--	0.005*	--	0.003**
Si	0.80	1.20	0.80	1.20
Cr	5.00*	5.50*	5.00	5.50
V	0.80	1.20	0.80	1.20
Mo	1.20	1.75*	1.20	1.75

*Modifications from ASTM A681 for premium quality

** Modifications from NADCA premium quality for superior quality

Table 1.4.3 Maximum allowable limits of nonmetallic inclusions according to ASTM E45 Method A for H13 steel for premium and superior quality grades of H13 steel (Ref. 4)

	Premium Grade H13		Superior Grade H13	
Inclusion Type	**Thin**	**Heavy**	**Thin**	**Heavy**
A (sulfide)	1.0	0.5	0.5*	0.5
B (aluminide)	1.5	1.0	1.5	1.0
C (silicate)	1.0	1.0	0.5*	0.5*
D (globular oxides)	2.0	1.0	1.5*	1.0

*Modifications from NADCA premium quality for superior quality

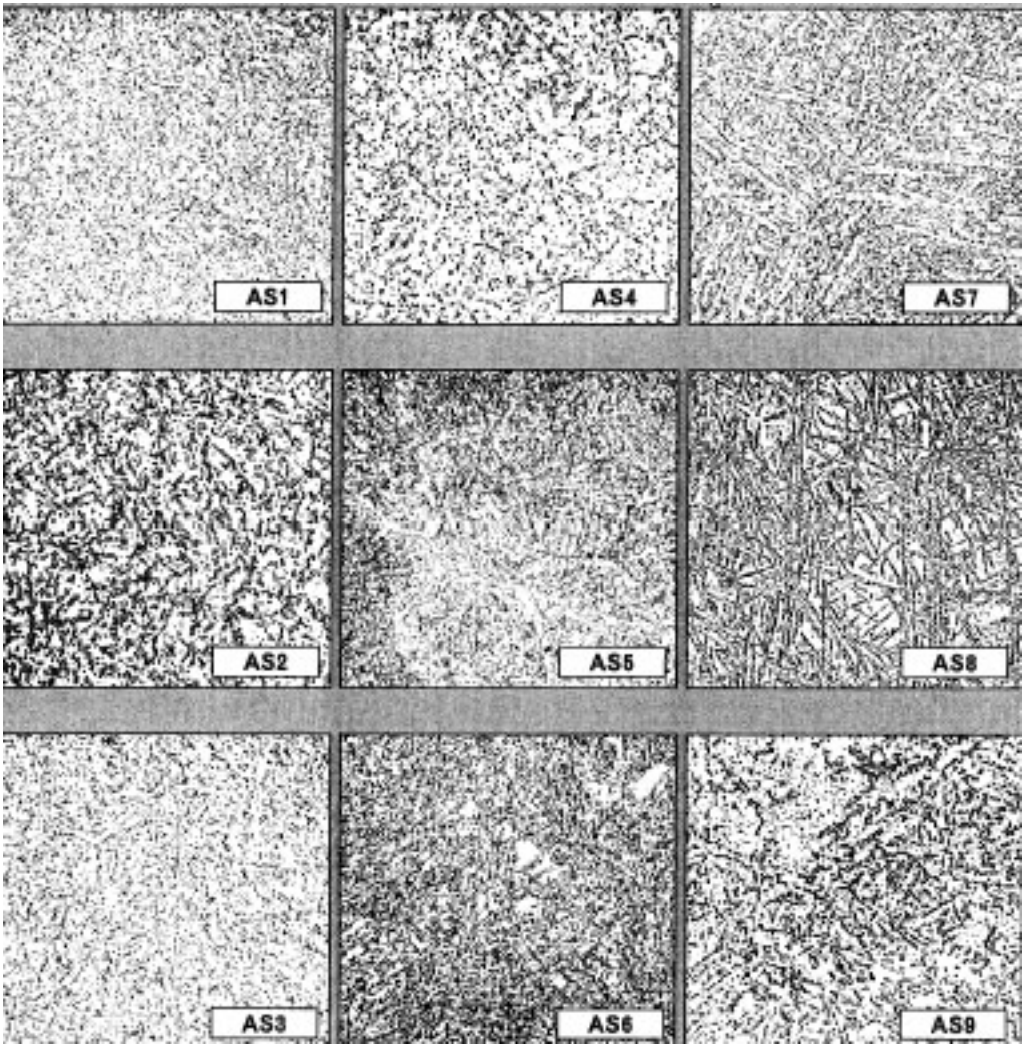

Figure 1.5.2.1 Annealed quality "AS" microstructure chart for annealed H-13 steel showing acceptable (AS1-AS9) and unacceptable (AS10-AS18) microstructures according to NADCA—all microstructures at 500x and etched with 5% Nital (Ref. 4)

continued

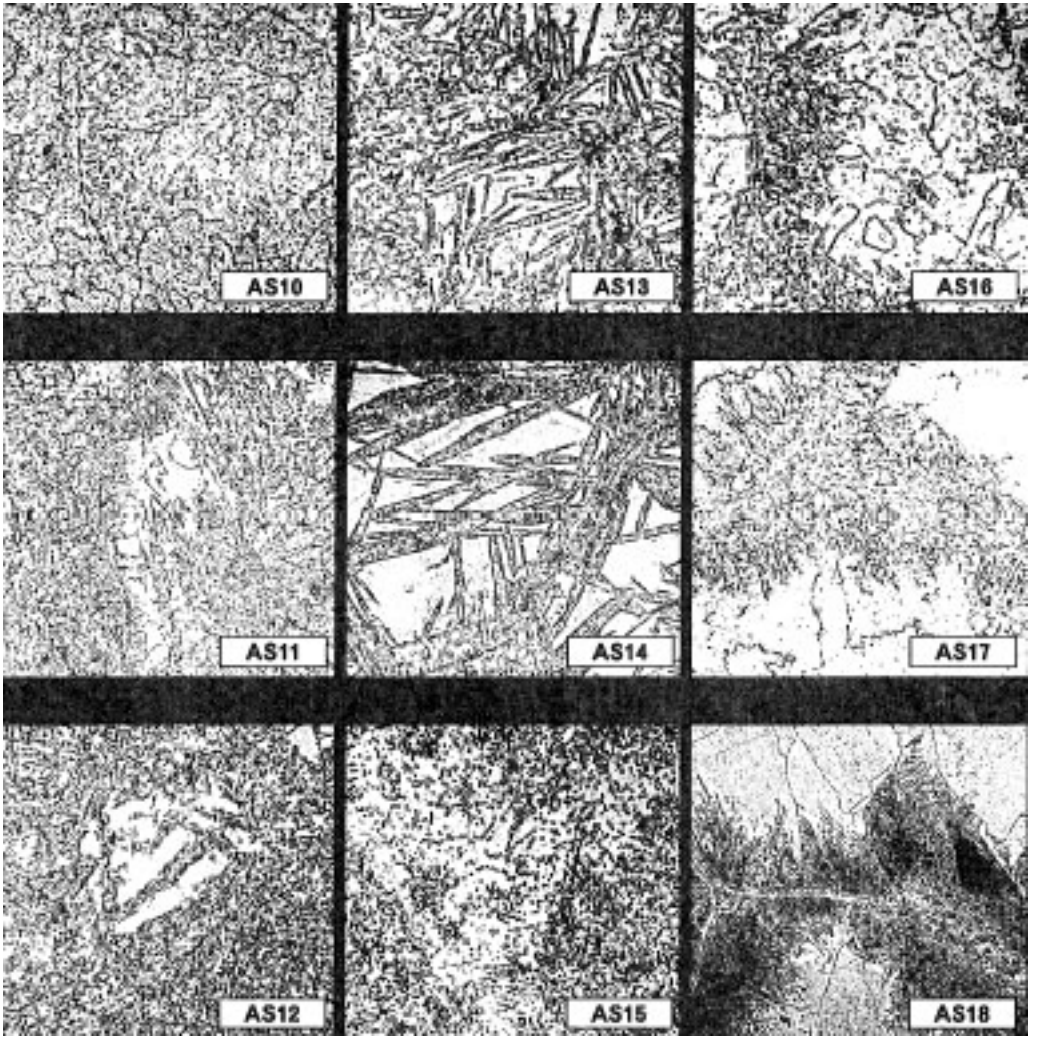

Figure 1.5.2.1 (continued) Annealed quality "AS" microstructure chart for annealed H-13 steel showing acceptable (AS1-AS9) and unacceptable (AS10-AS18) microstructures according to NADCA—all microstructures at 500x and etched with 5% Nital (Ref. 4)

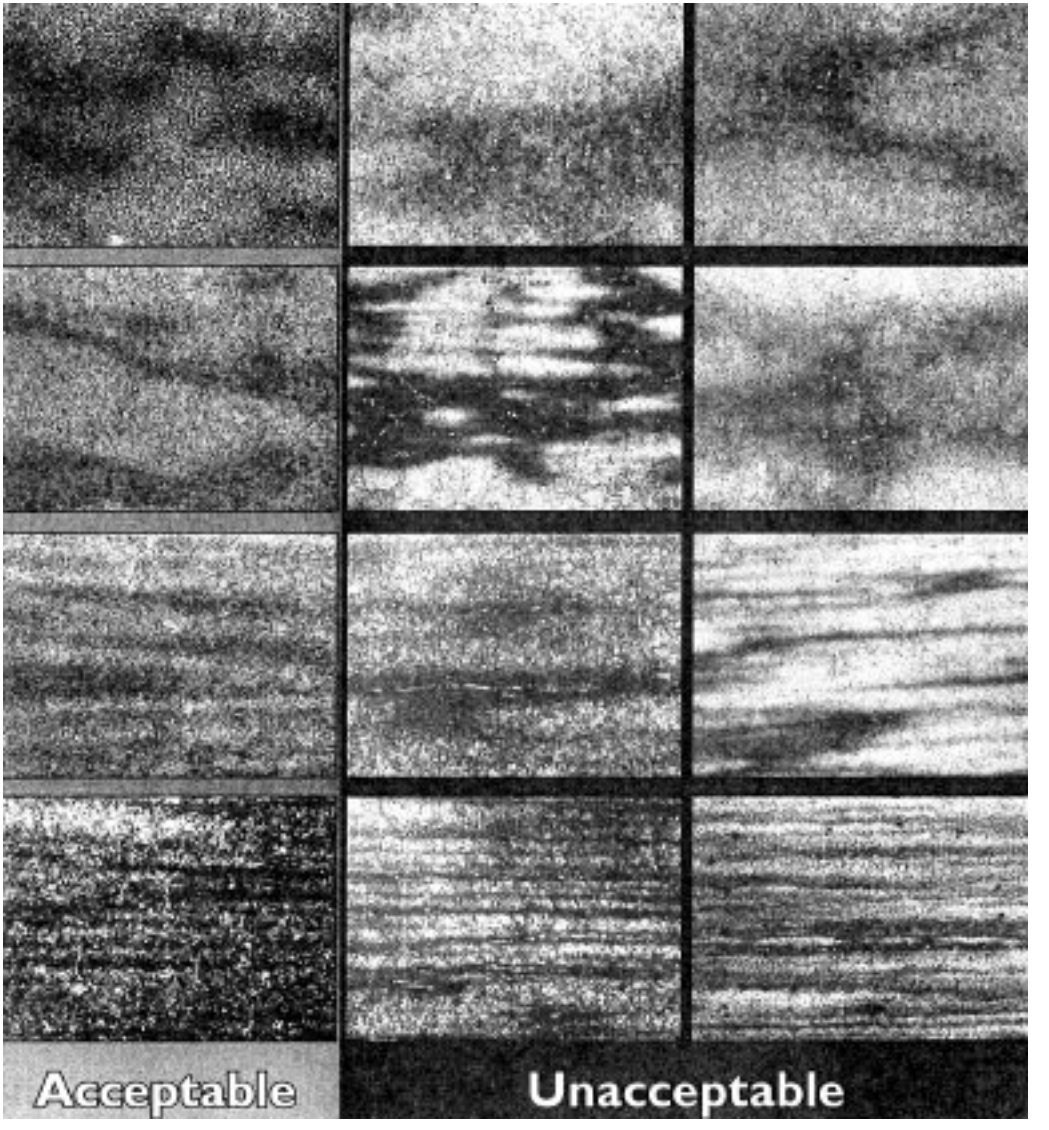

Figure 1.5.2.2 Banding microsegregation chart for annealed H-13 steel blocks showing acceptable and unacceptable microstructures according to NADCA—all microstructures at 50x and etched with Villella's reagent (Ref. 4)

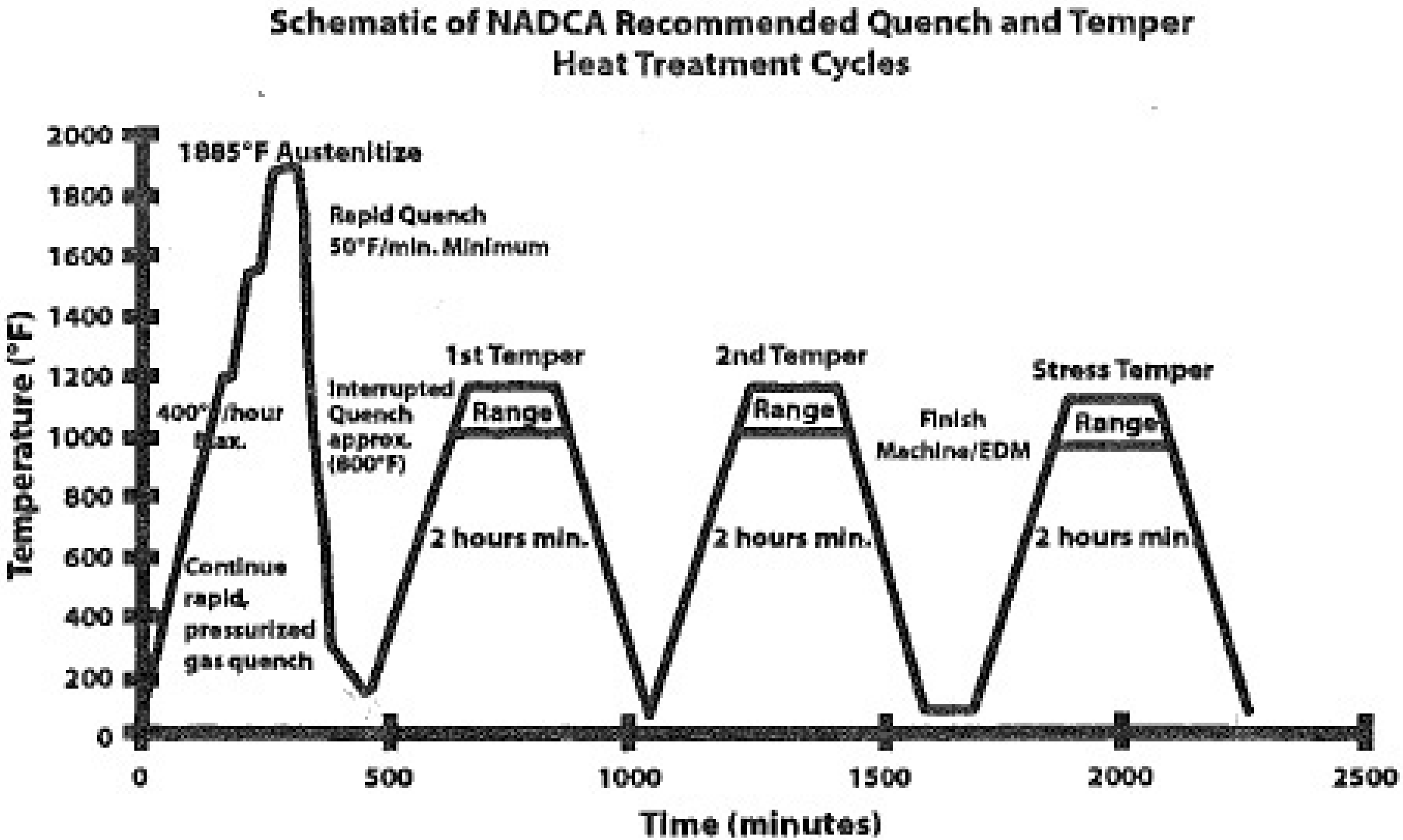

Figure 1.5.4.1 Schematic of NADCA-recommended austenitizing, quenching, and tempering heat treatment cycle for H-13 steel (Ref. 4)

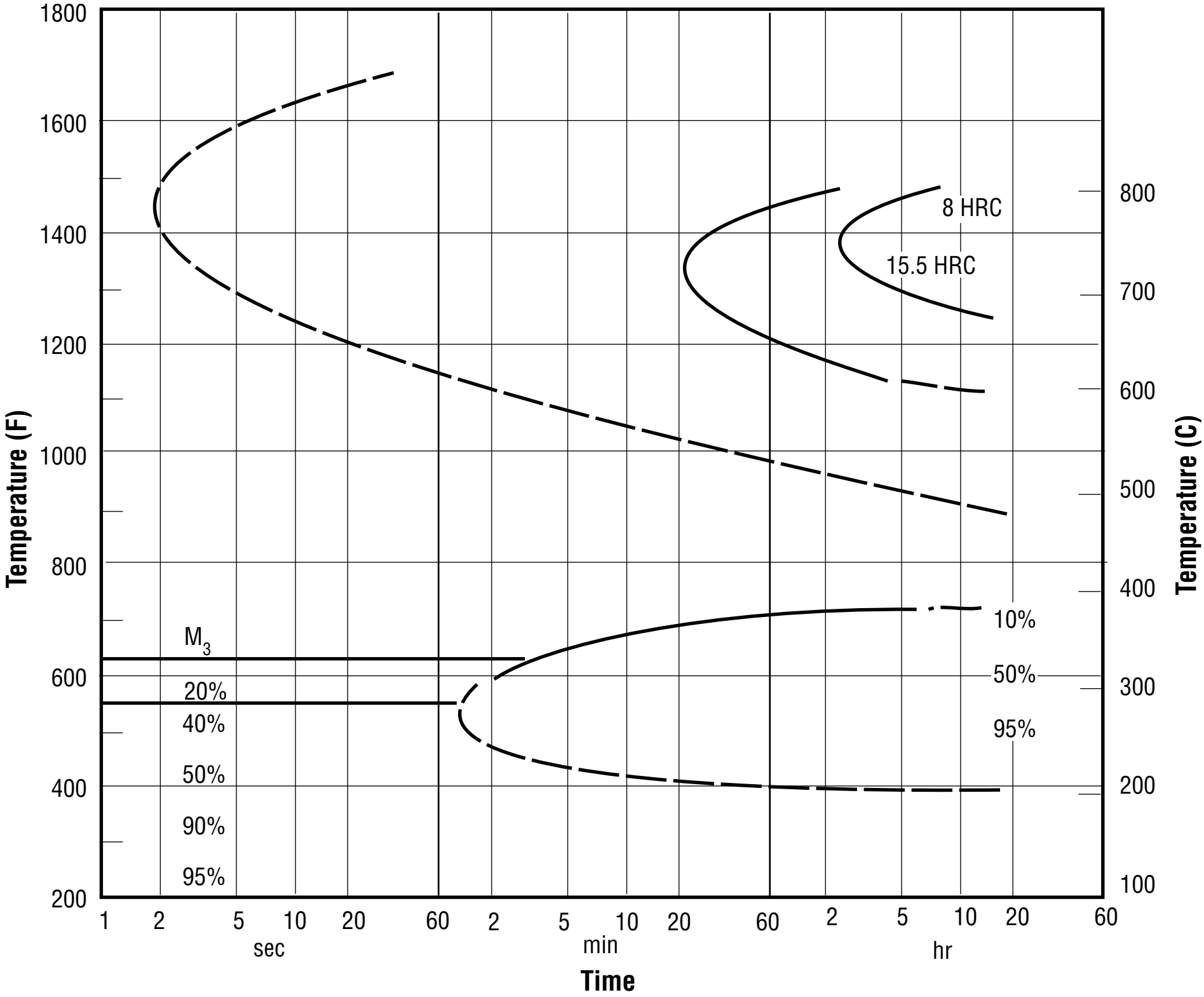

Figure 1.5.5.1 Isothermal phase transformation diagram for H-13 steel (0.40 C, 1.05 Si, 5.00 Cr, 1.35 Mo, 1.10V) austenitized at 1850F (Ref. 3)

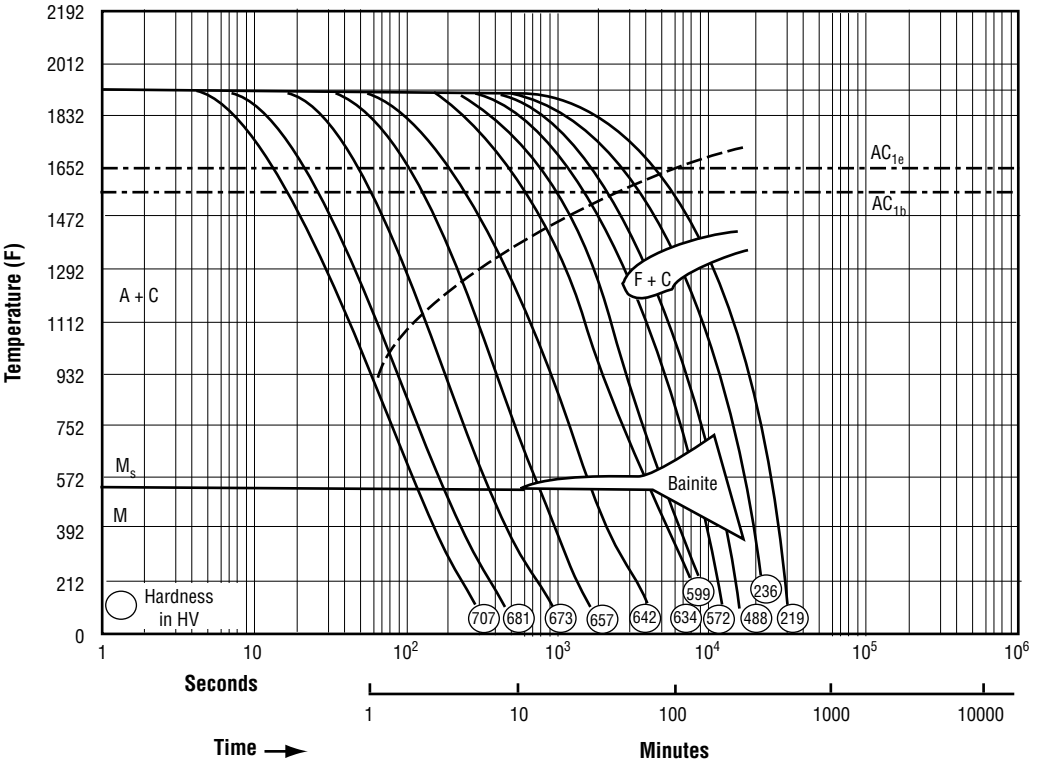

Figure 1.5.5.2 Time-temperature transformation diagram for premium grade H-13 steel (Thyrotherm 2344 ESR Magnum, ThyssenKrupp Specialty Steels, Inc.) austenitized at 1870–1920F (Refs. 17, 18)

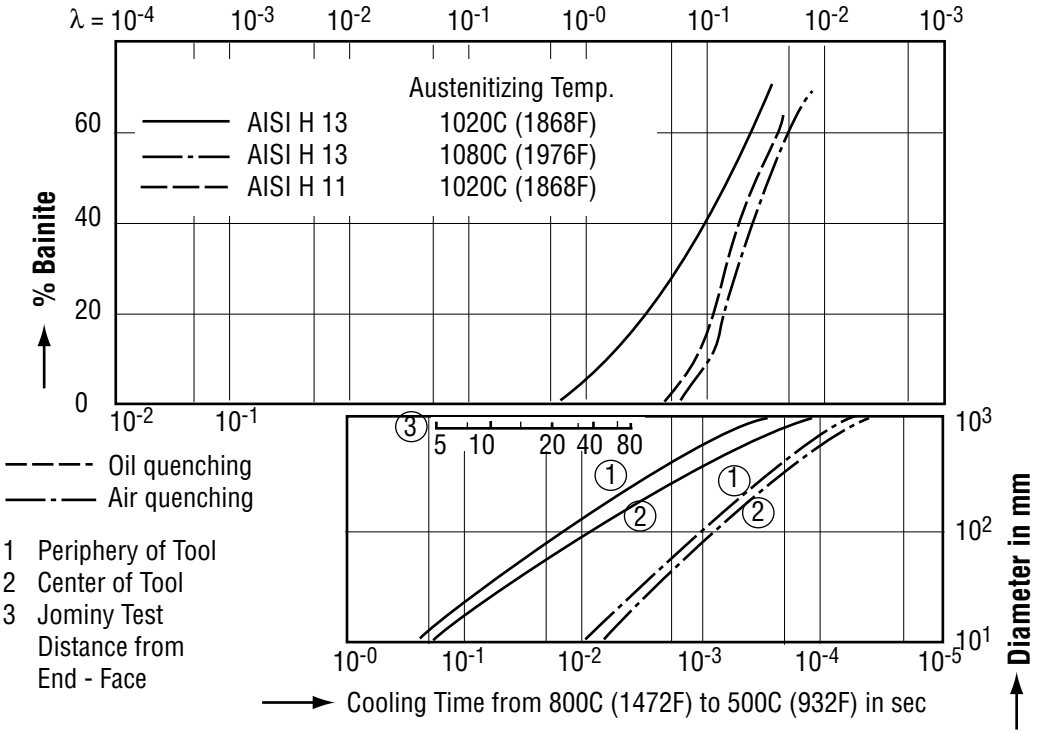

Figure 1.5.5.3 Kinetics of bainite transformation for H-13 and H-11 steels compared at given austenitizing temperatures (Ref. 29)

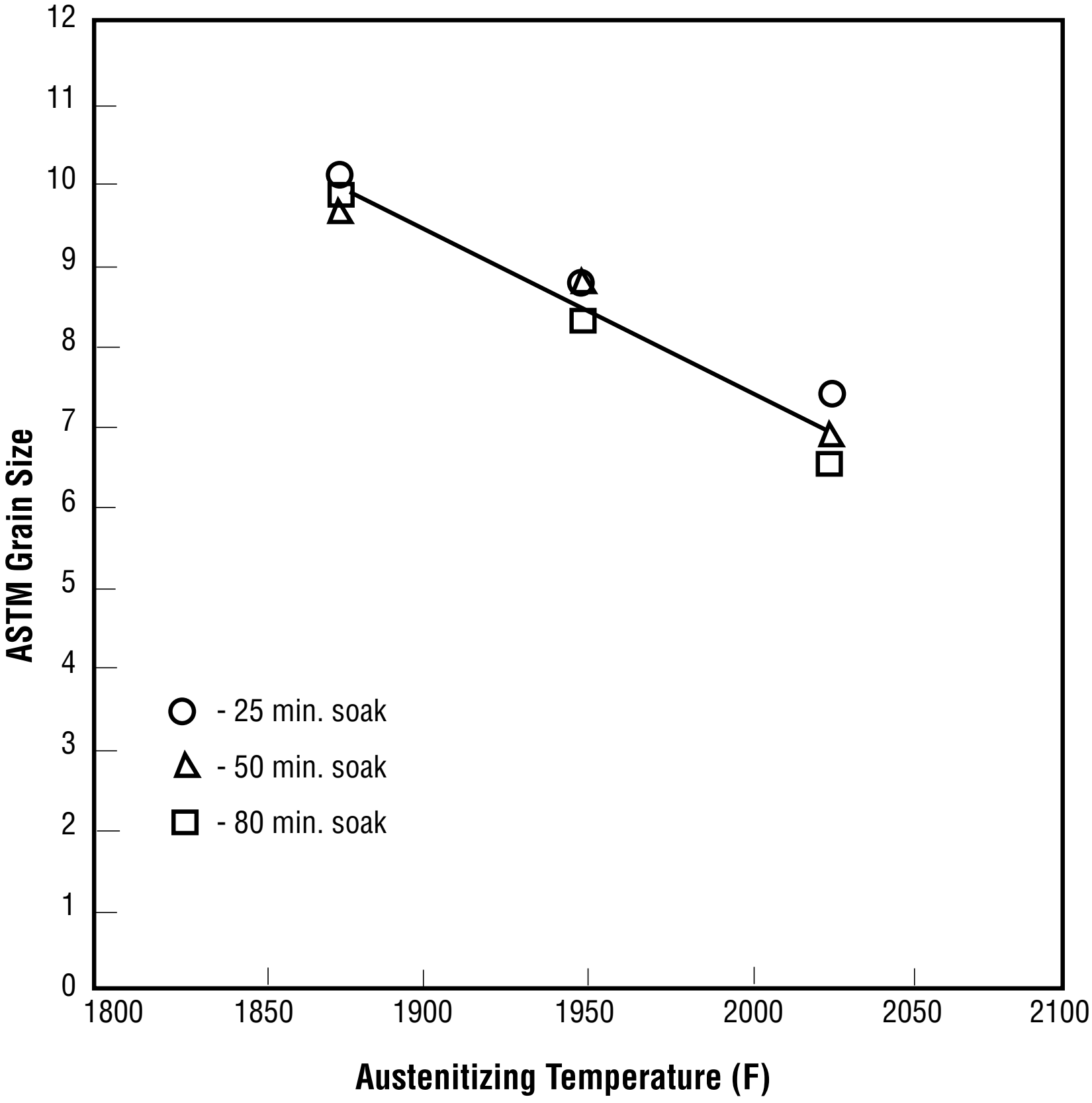

Figure 1.5.5.4 ASTM grain size versus austenitizing temperature for H-13 steel and air cooled for 0.5-in. cube samples soaked at temperature for 25–80 minutes (Ref. 28)

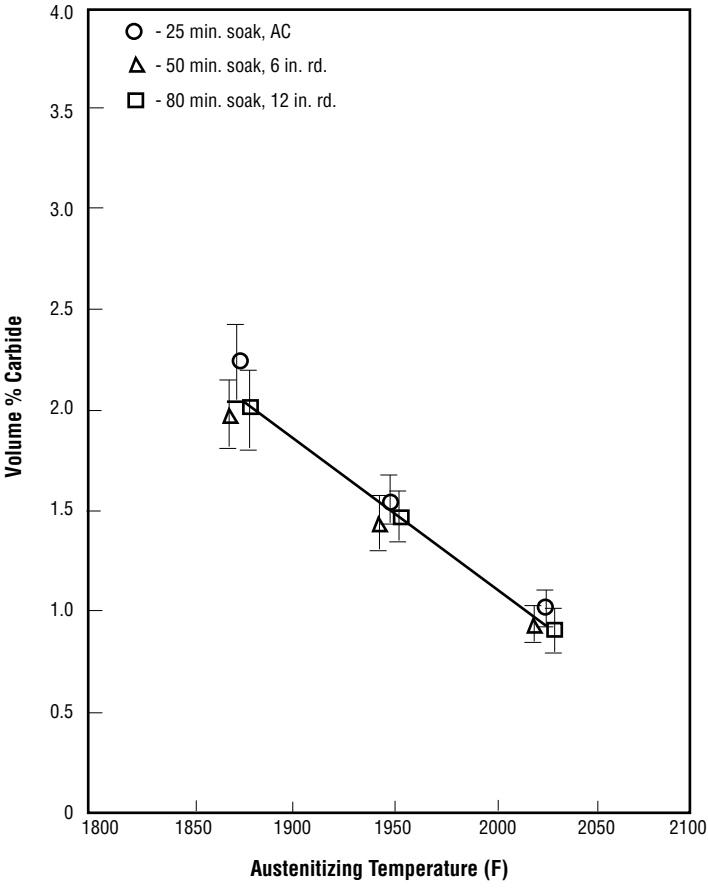

Figure 1.5.5.5 Volume % carbide (95% confidence interval) in the as-quenched condition of air cooled (AC) small sections and larger 6- and 12-in rounds of H-13 steel as a function of austenitizing temperature for given soak times (Ref. 28)

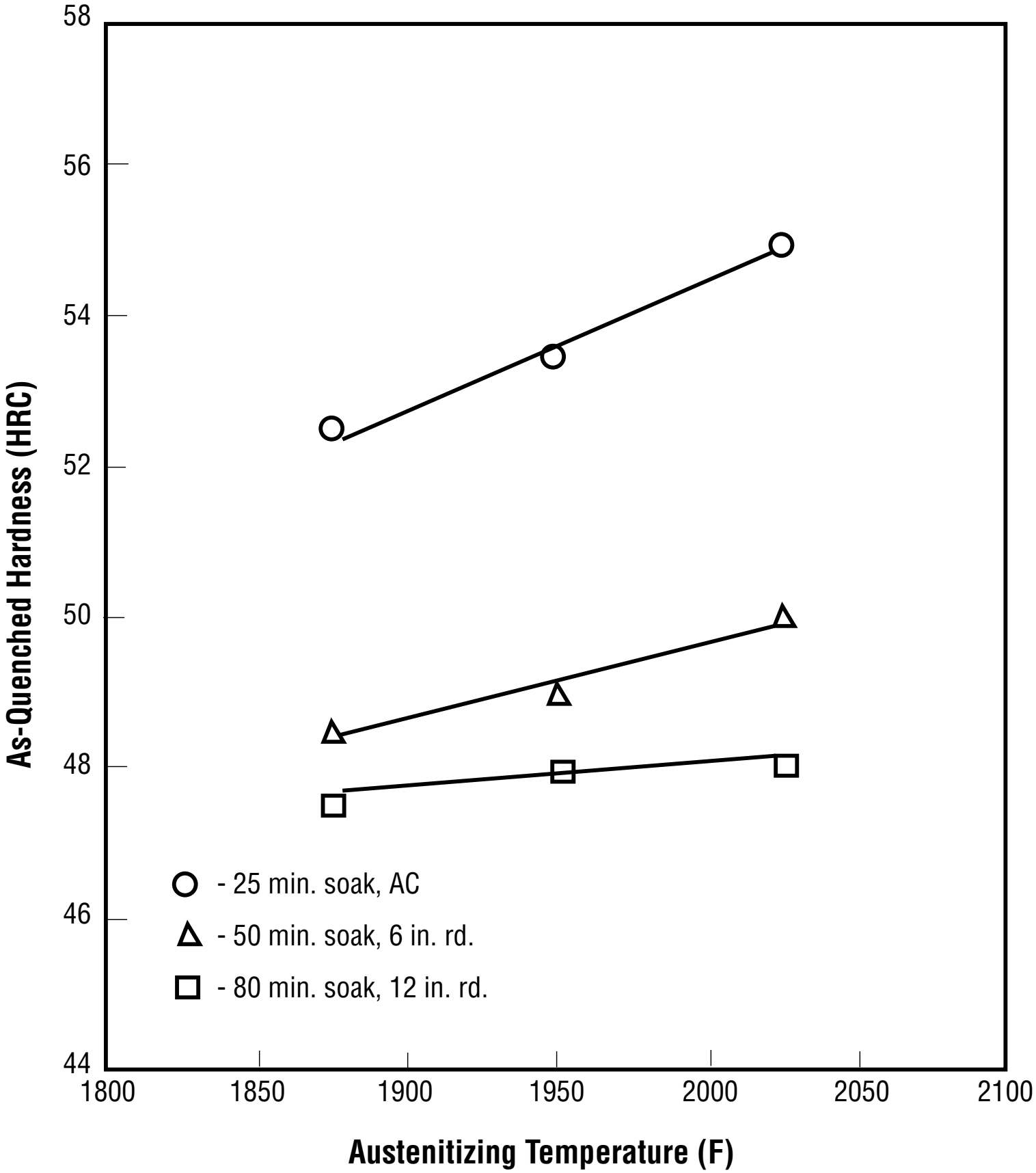

Figure 1.5.5.6 As-quenched hardness as a function of austenitizing temperature of air cooled (AC) small sections and larger 6- and 12-in rounds of H-13 steel for given soak times (Ref. 28)

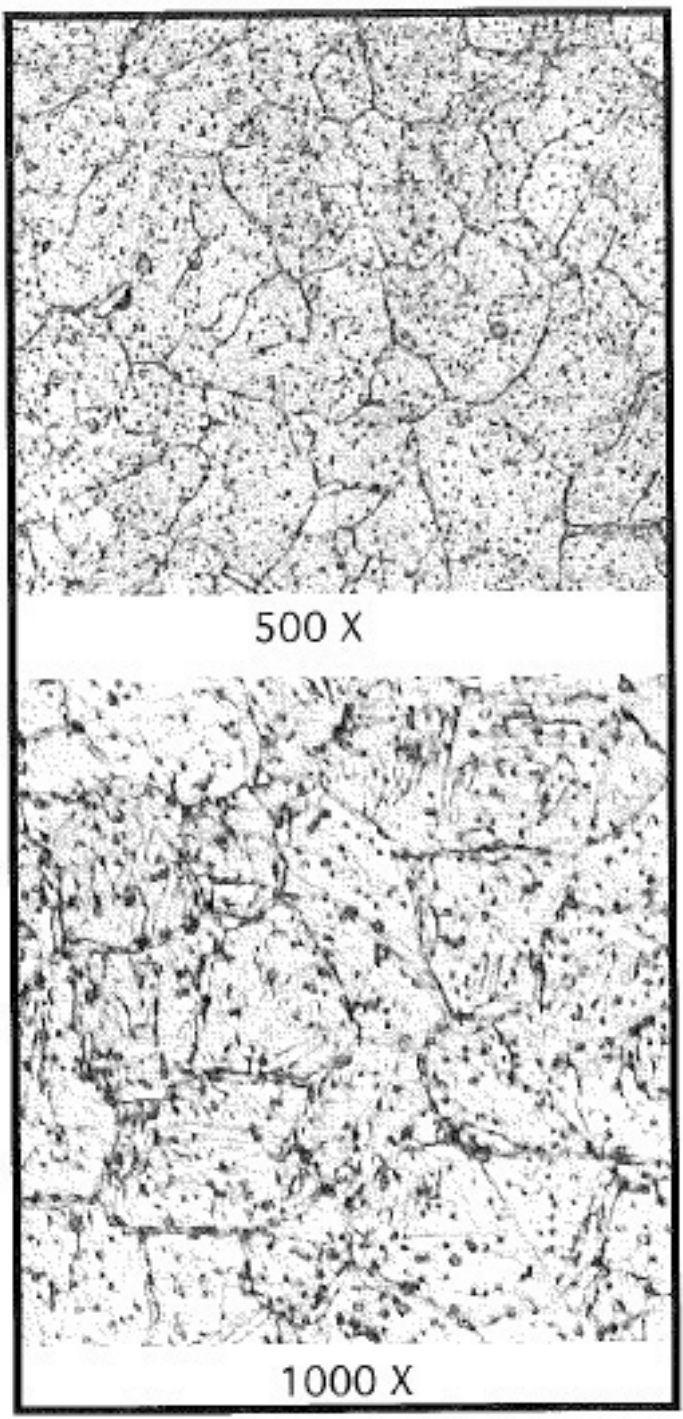

Figure 1.5.5.7 As-Quenched microstructure for H-13 steel showing moderate carbide precipitation at grain boundaries and finely dispersed carbides in matrix (Ref. 30)

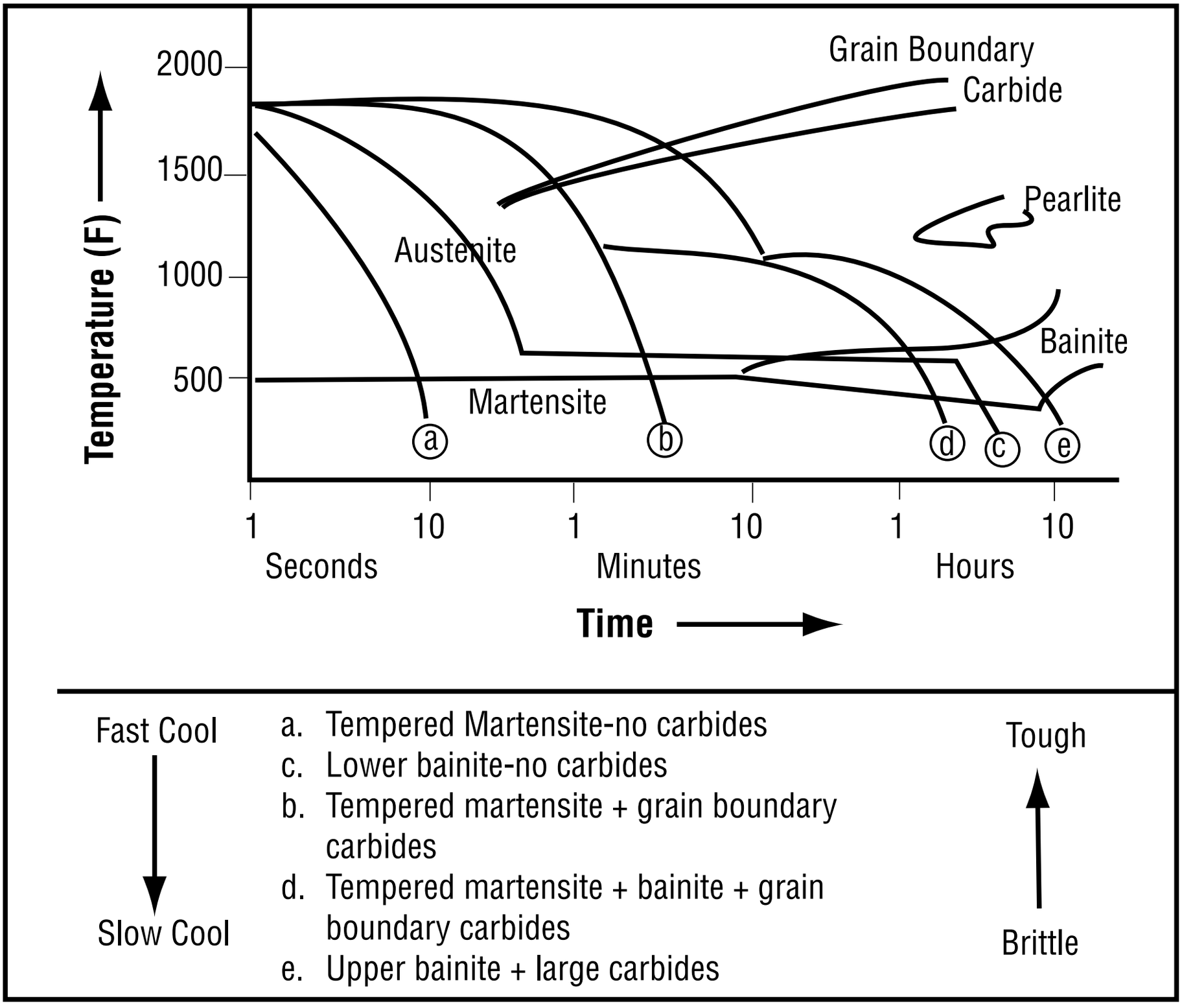

Figure 1.5.5.8 Continuous cooling transformation diagram for H-13 steel austenitized at 1970F showing cooling curves A through E (Ref. 30)

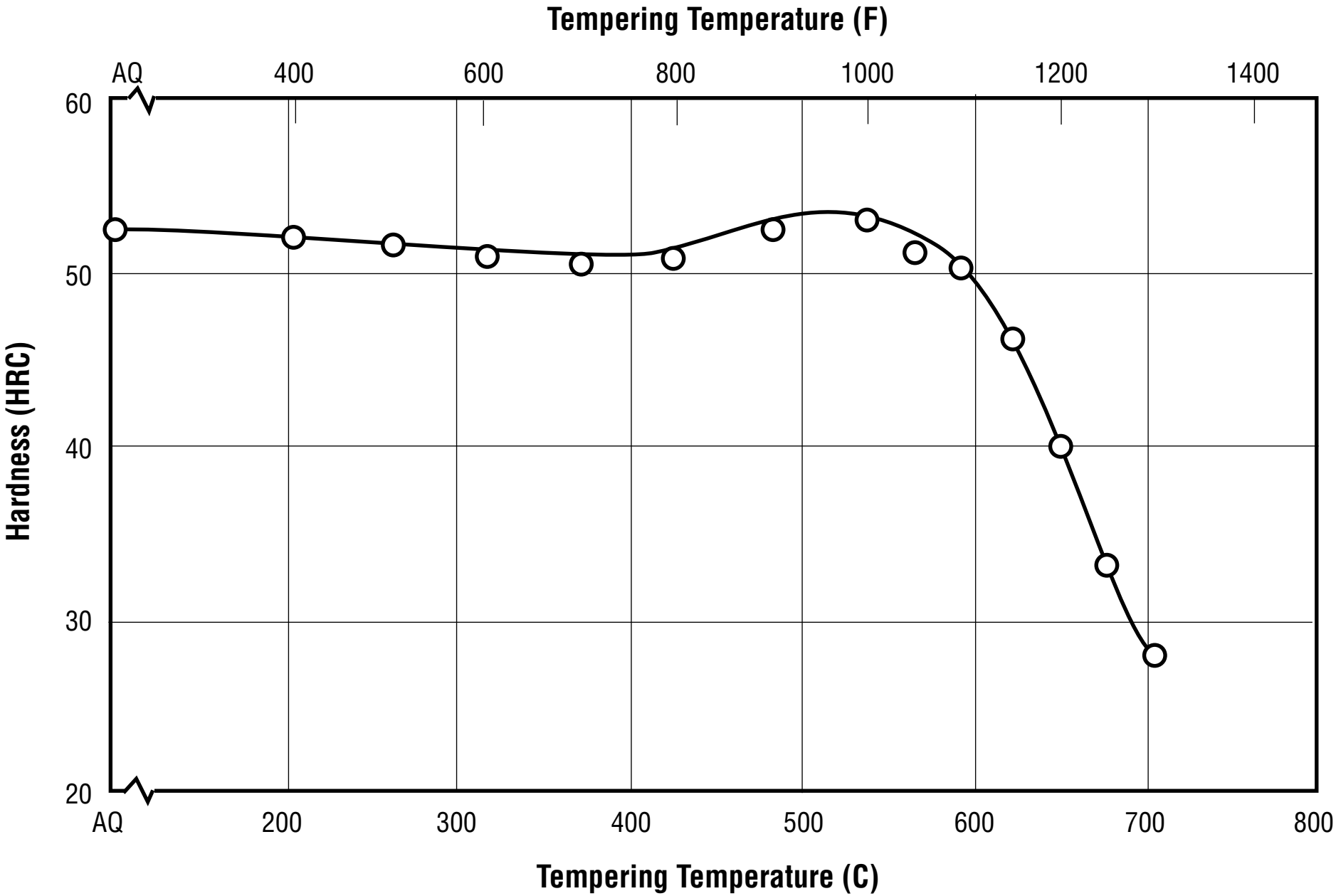

Figure 1.5.8.1 Hardness variation with tempering temperature for H-13 steel air cooled from 1875F and tempered 2 h at temperature (Ref. 1)

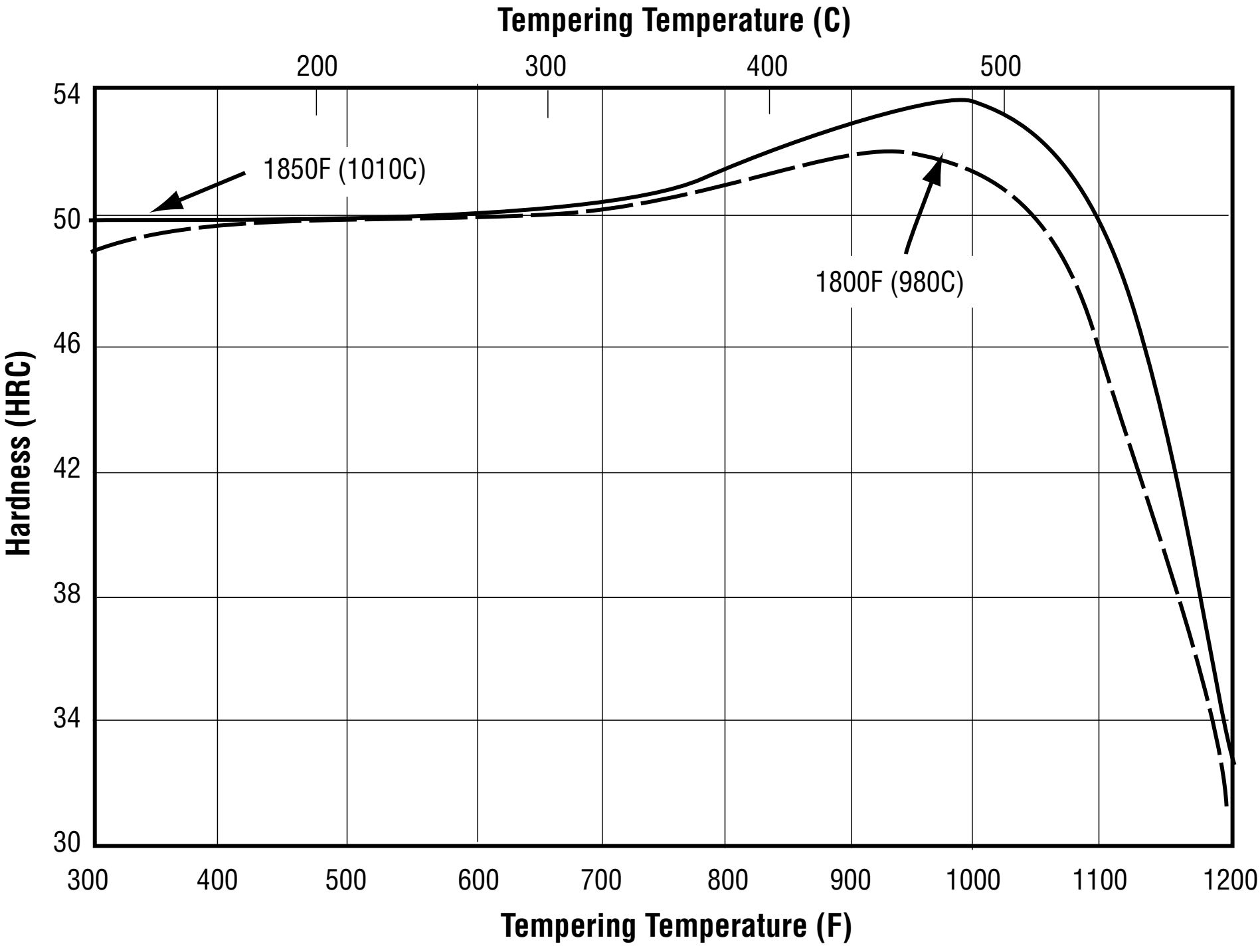

Figure 1.5.8.2 Hardness as a function of tempering temperature for H-13 steel austenitized at 1850F and 1800F, air cooled, and double tempered (Ref. 3)

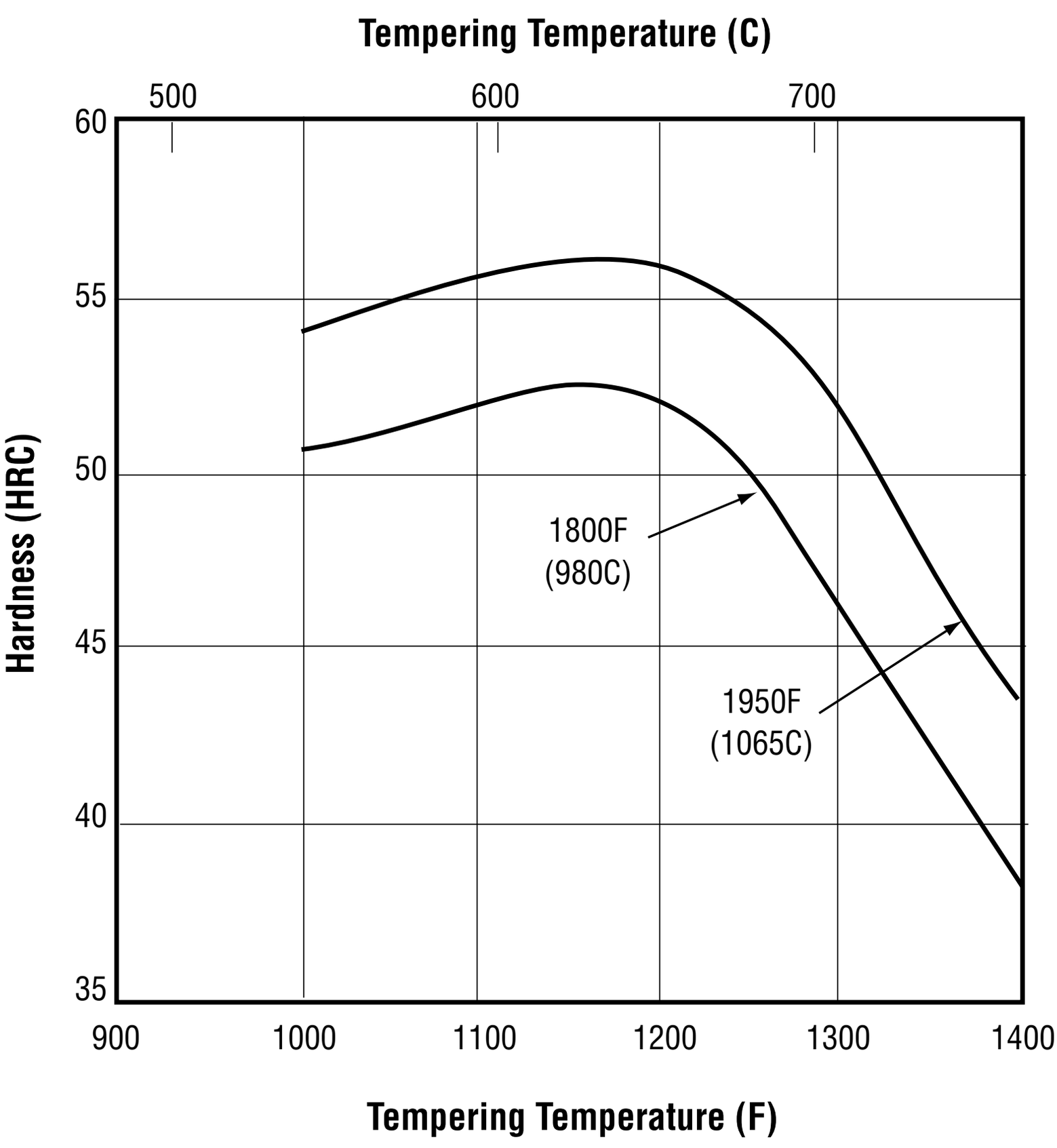

Figure 1.5.8.3 Hardness as a function of tempering temperature for H-13 steel austenitized at 1950F and 1800F, air cooled, and tempered for 2 h (Ref. 3)

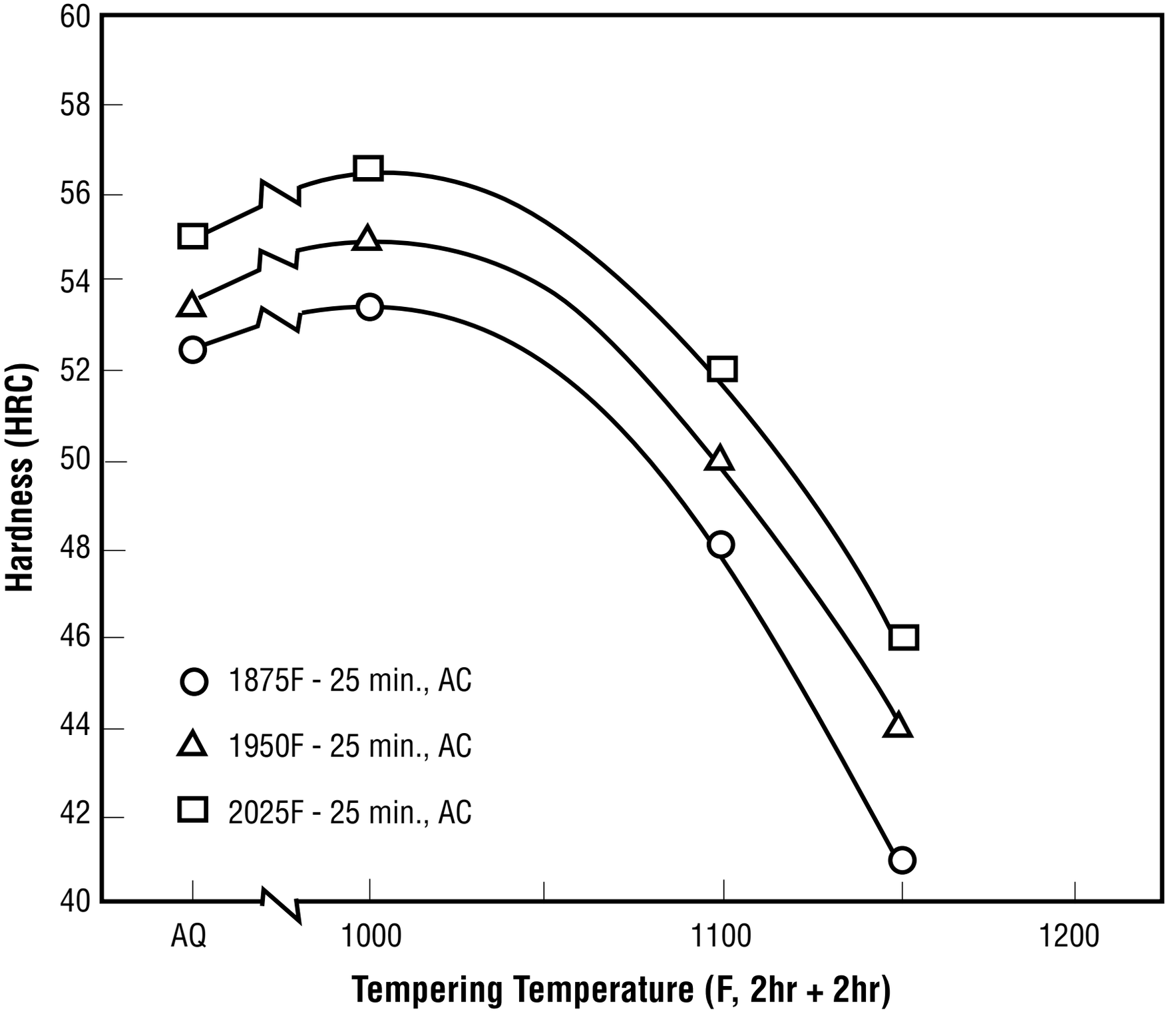

Figure 1.5.8.4 Tempering curve (double tempered 2 h + 2 h) for H-13 steel after air quenching (AC) 0.5-in. square samples from 1875, 1950, and 2050F (Ref. 28)

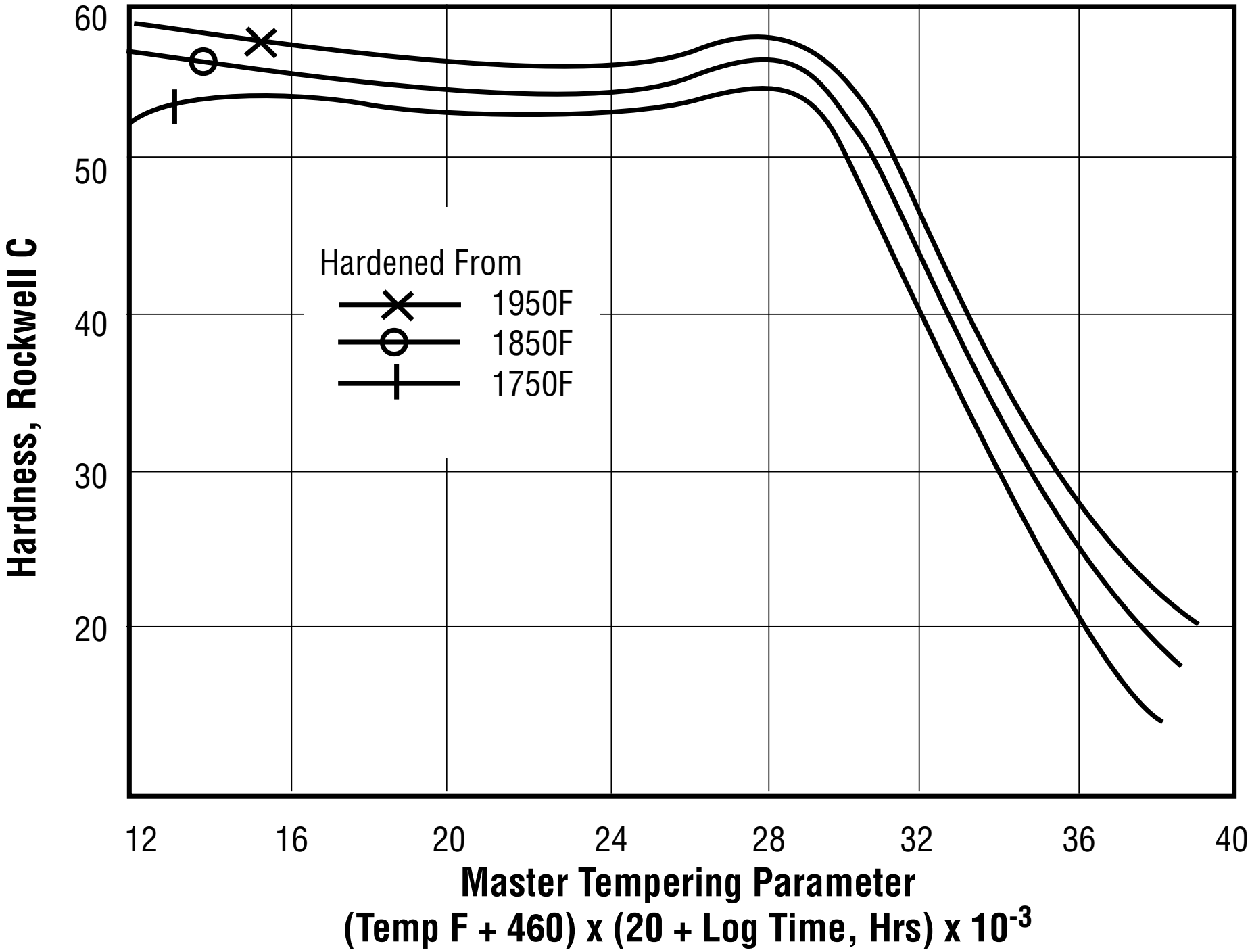

Figure 1.5.8.5 Master tempering parameter curve for H-13 steel hardened by austenitizing at 1750–1950F and quenching (Ref. 4)

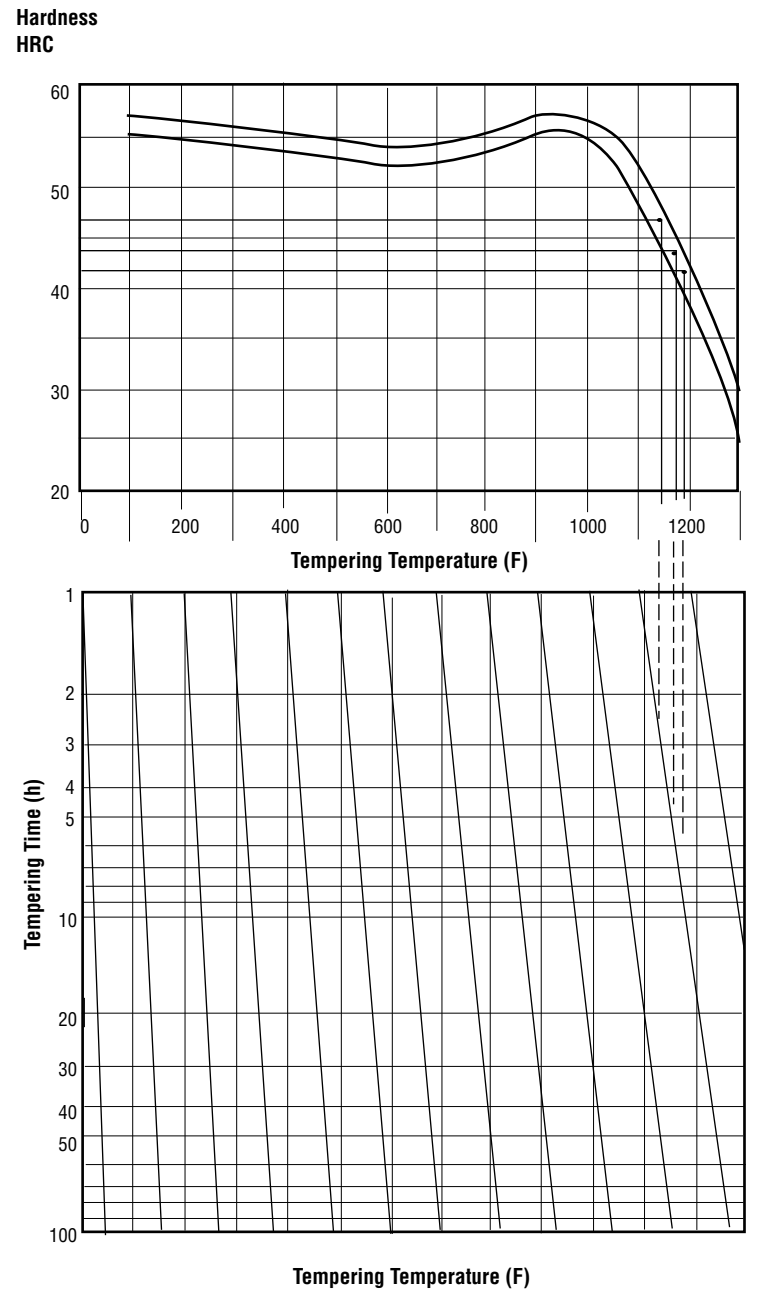

Figure 1.5.8.6 Time-temperature tempering diagram for H-13 steel hardened by austenitizing at 1875F (Ref. 32)

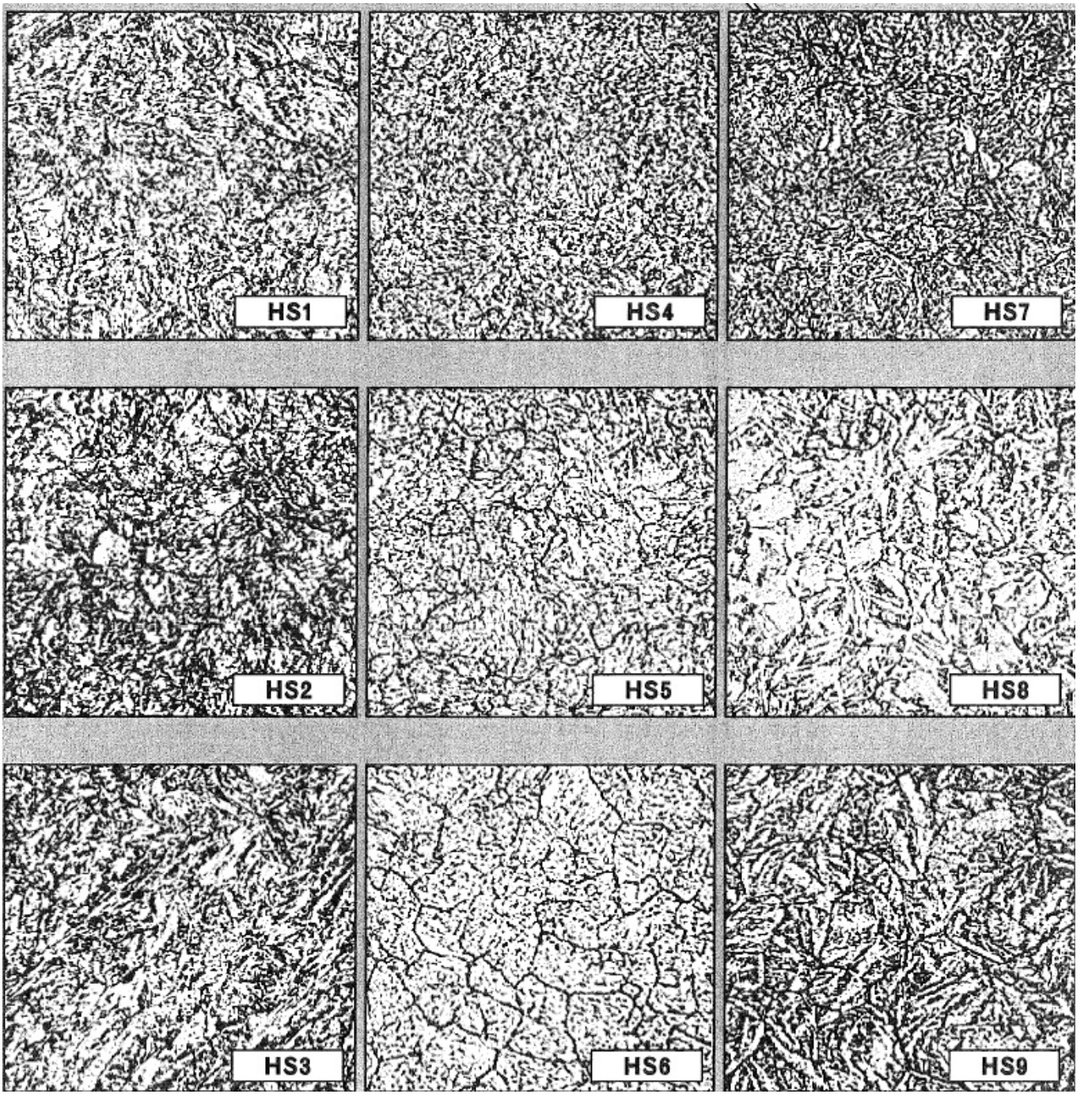

Figure 1.5.8.7 Acceptable microstructures (500x, 5% Nital etch) of H-13 steel properly heat treated by austenitizing, quenching, and tempering as per NADCA acceptance criteria (numbering HS1-HS9 does not denote a quality ranking as all are acceptable) (Ref. 4)

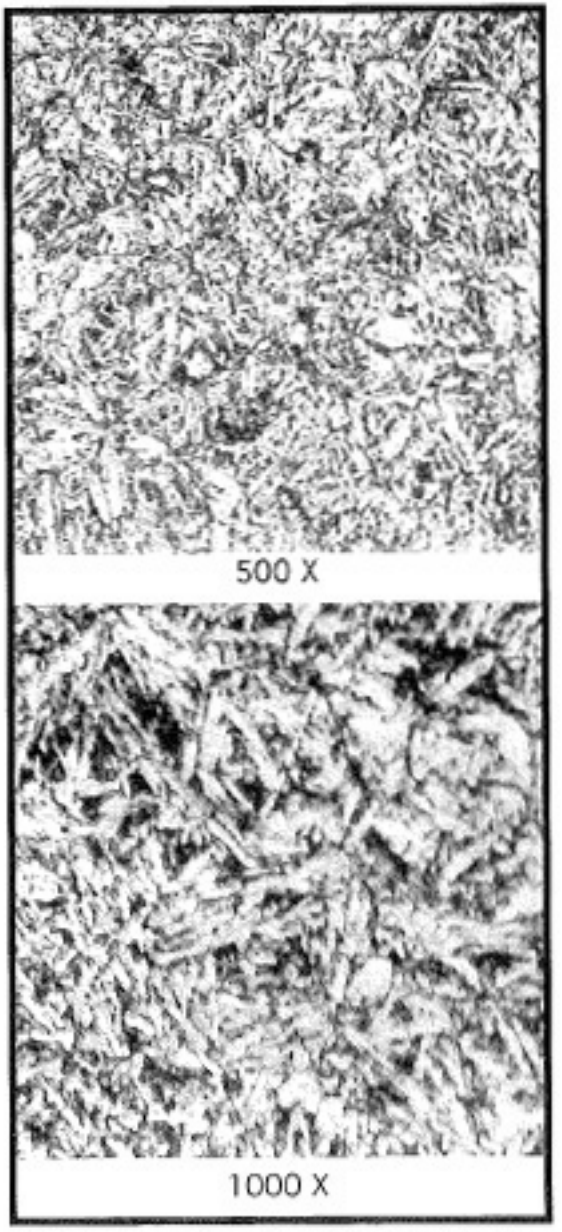

Figure 1.5.8.8 Typical microstructure from the center of a six-inch-thick H-13 steel die hardened commercially in a vacuum furnace at 1850F and double tempered (2 h at 1050F + 2 h at 1100F) (Ref. 30)

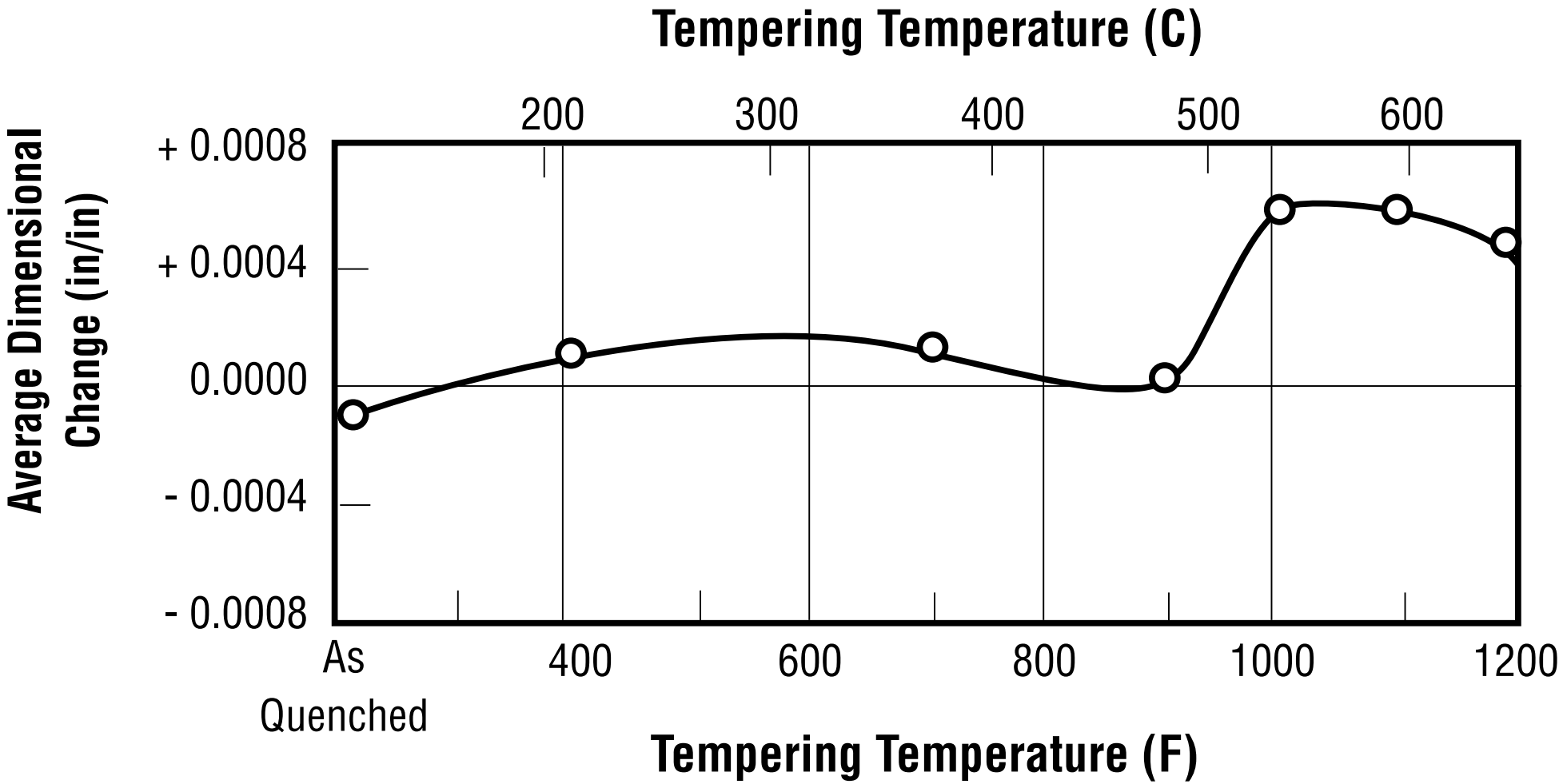

Figure 1.5.8.9 Dimensional change of H13 steel in a 1 x 2 x 6 in. block versus tempering temperature (Ref. 3)

Table 1.5.8.10 Typical dimensional changes in hardening and tempering H-11 and H-13 steels (Ref. 2)

Tool Steel	Hardening Treatment		Total Change in Linear Dimensions (%)		
	Austenitizing Temperature (F)	Quenching Medium	After Quenching	After Tempering at	
				900F	1000F
H-11	1850	Air	0.11	0.01	0.12
H-13	1850	Air	-0.01	0.00	0.06

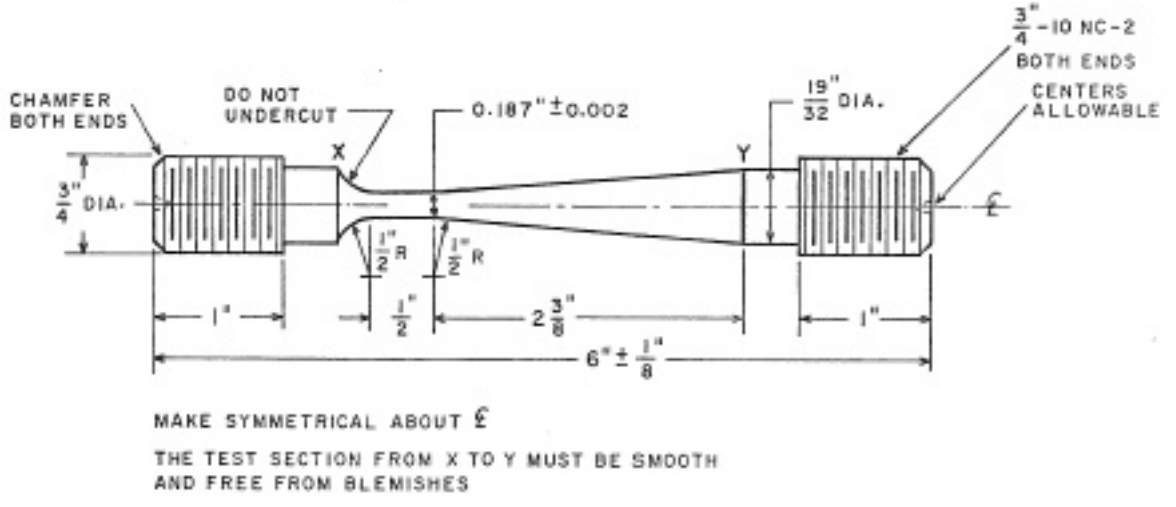

Figure 1.5.9.1 Variable section creep specimen used to study stress accelerated tempering of H-13 steel as reported in Figures 1.5.9.2–1.5.9.5 (Ref. 25)

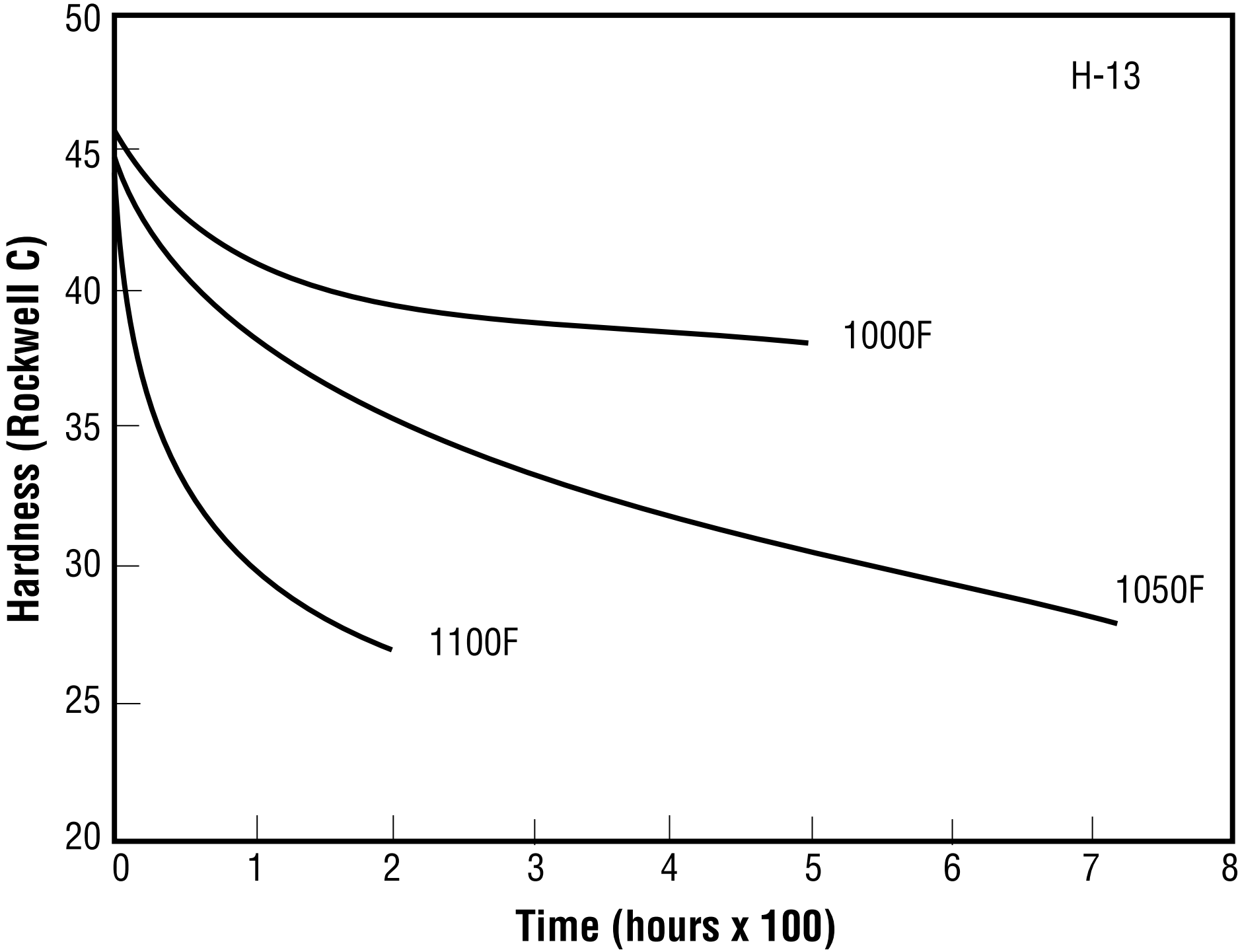

Figure 1.5.9.2 Tempering curves for H-13 steel constructed from unstressed section of test specimen shown in Figure 1.5.9.1 (Ref. 25)

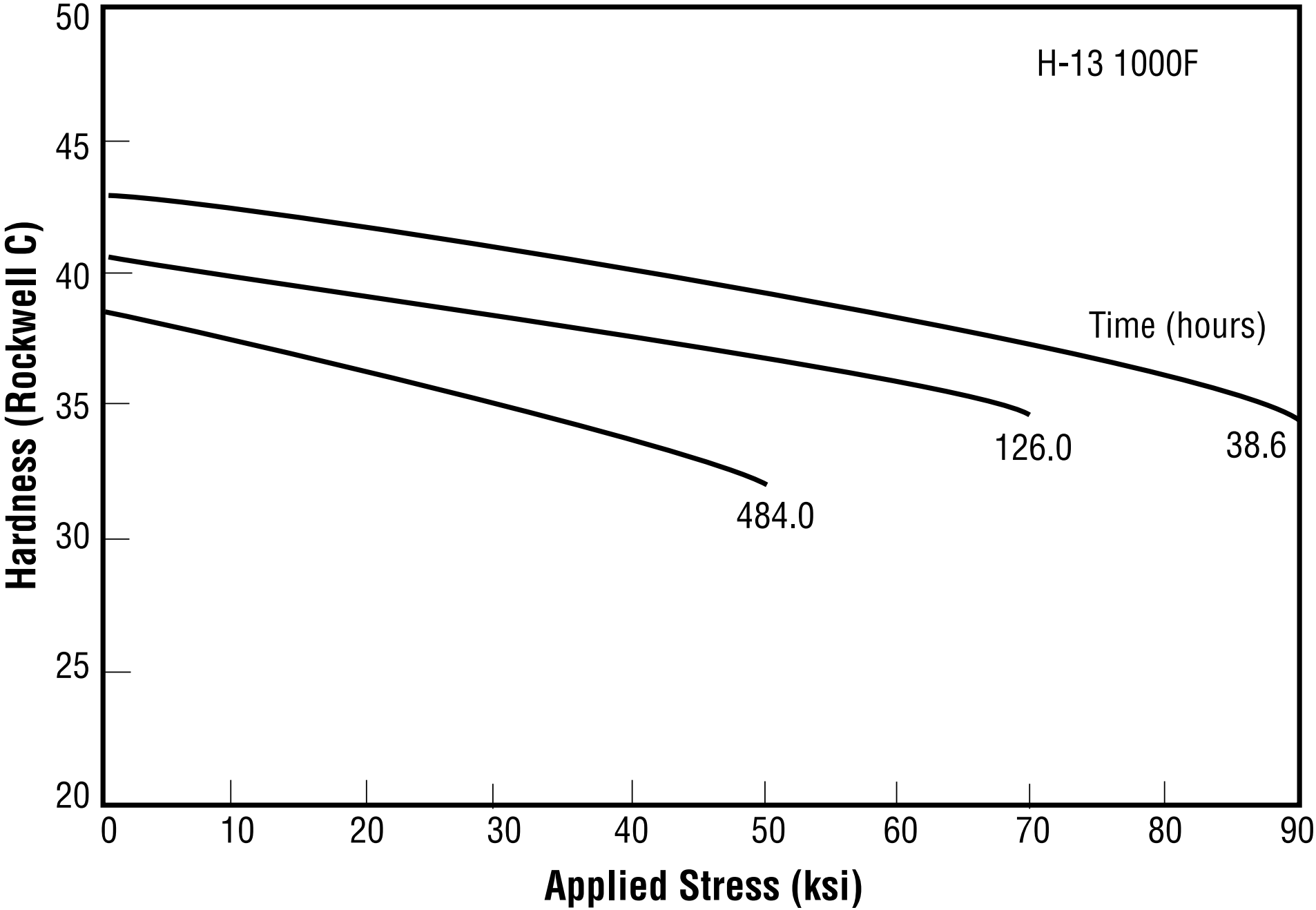

Figure 1.5.9.3 Hardness change (microhardness surveys converted to Rockwell C) in H-13 steel measured along variable section creep specimen shown in Figure 1.5.9.1 due to stress accelerated tempering at 1000F (Ref. 25)

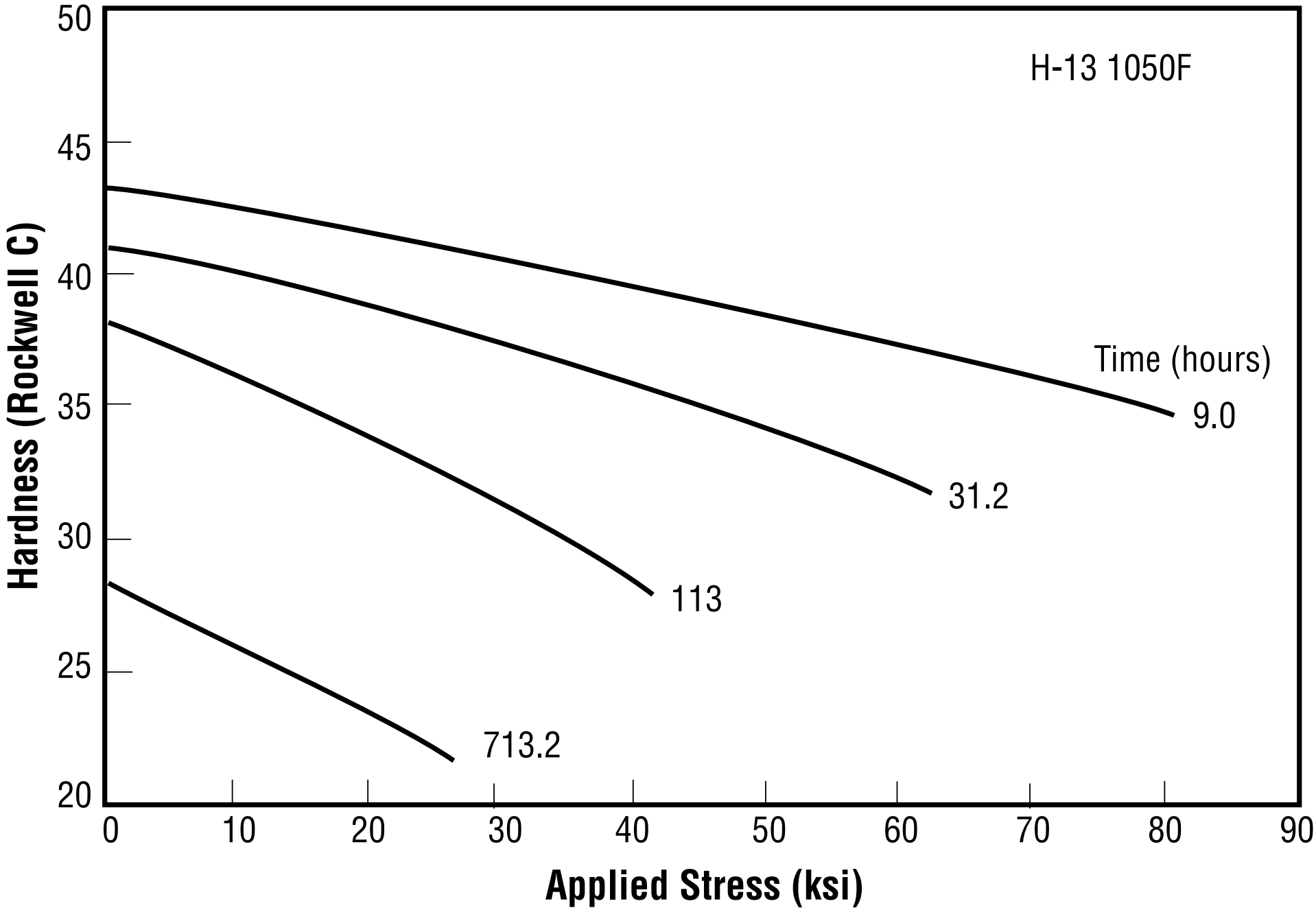

Figure 1.5.9.4 Hardness change (microhardness surveys converted to Rockwell C) in H-13 steel measured along variable section creep specimen shown in Figure 1.5.9.1 due to stress accelerated tempering at 1050F (Ref. 25)

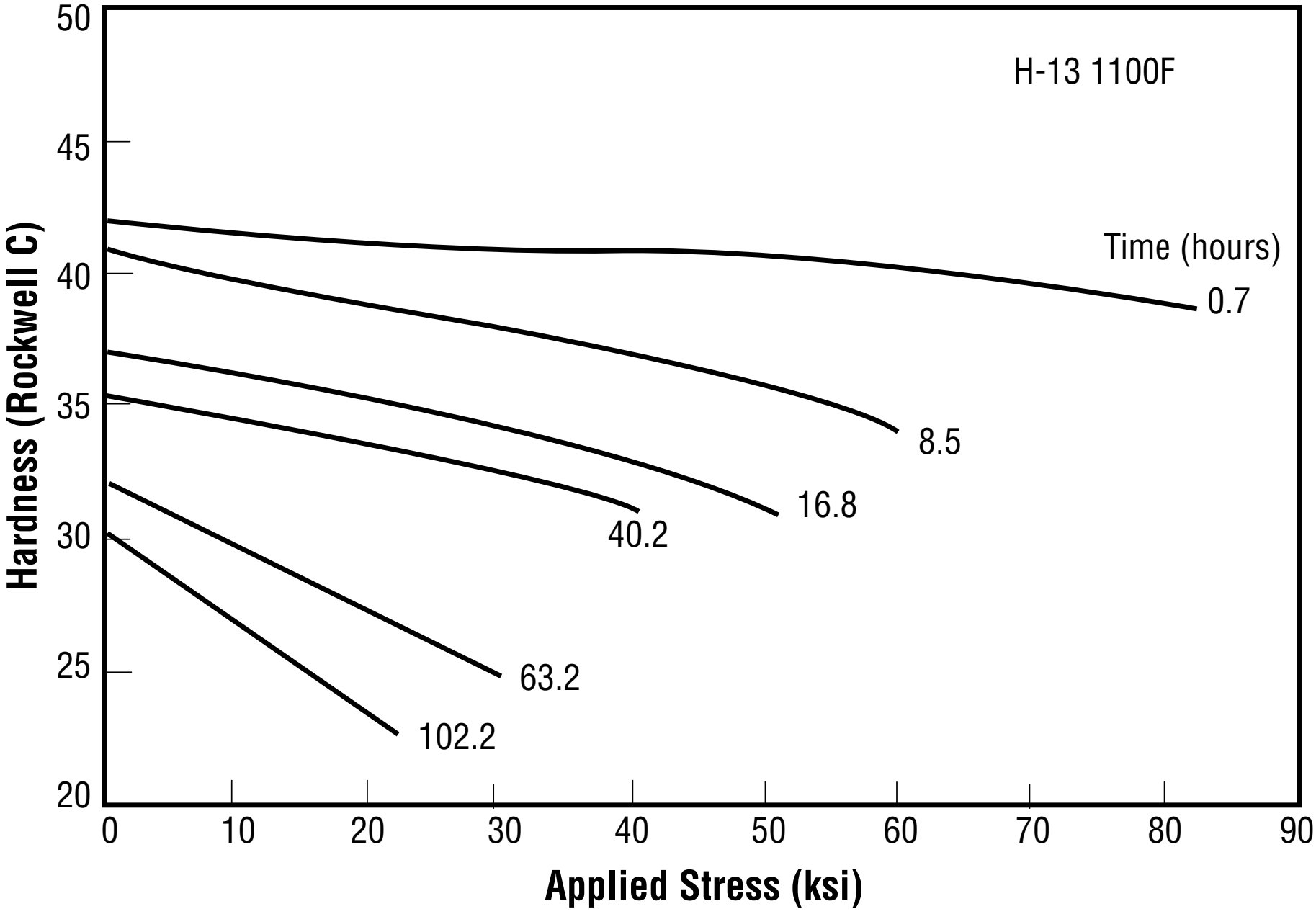

Figure 1.5.9.5 Hardness change (microhardness surveys converted to Rockwell C) in H-13 steel measured along variable section creep specimen shown in Figure 1.5.9.1 due to stress accelerated tempering at 1100F (Ref. 25)

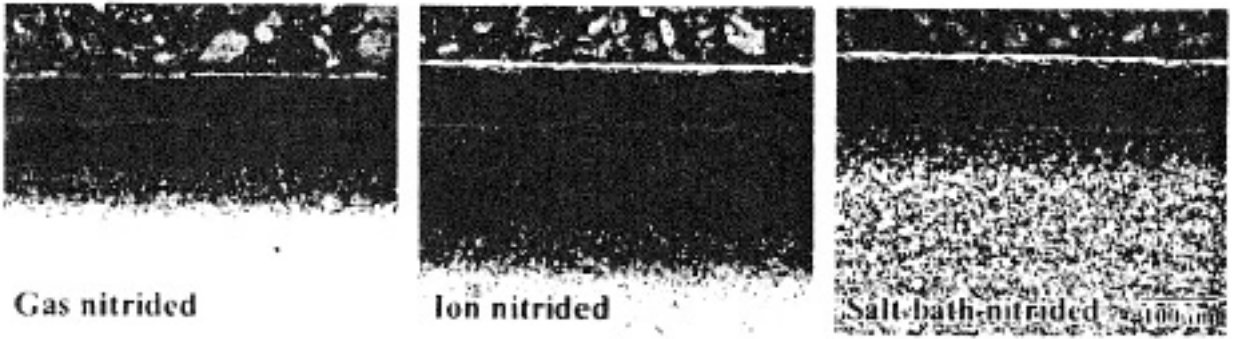

Figure 1.5.11.1 Cross-sectional optical micrographs of gas nitrided, ion nitrided, and salt bath nitrided H-13 steel after austenitization at 1890F and triple tempering (70X magnification) (Ref. 34)

Table 1.5.11.2 Thickness of surface layers of nitrided H-13 steel after austenitization at 1890F and triple tempering depending on nitriding treatment (Ref. 34)

Nitriding Treatment	**White Layer Thickness** (mils)	**Diffusion Layer Thickness** (mils)
Gas Nitrided at 1095F	0.35	6.42
Ion Nitrided at 985F	0.51	11.89
Salt Bath Nitrided	0.39	3.15

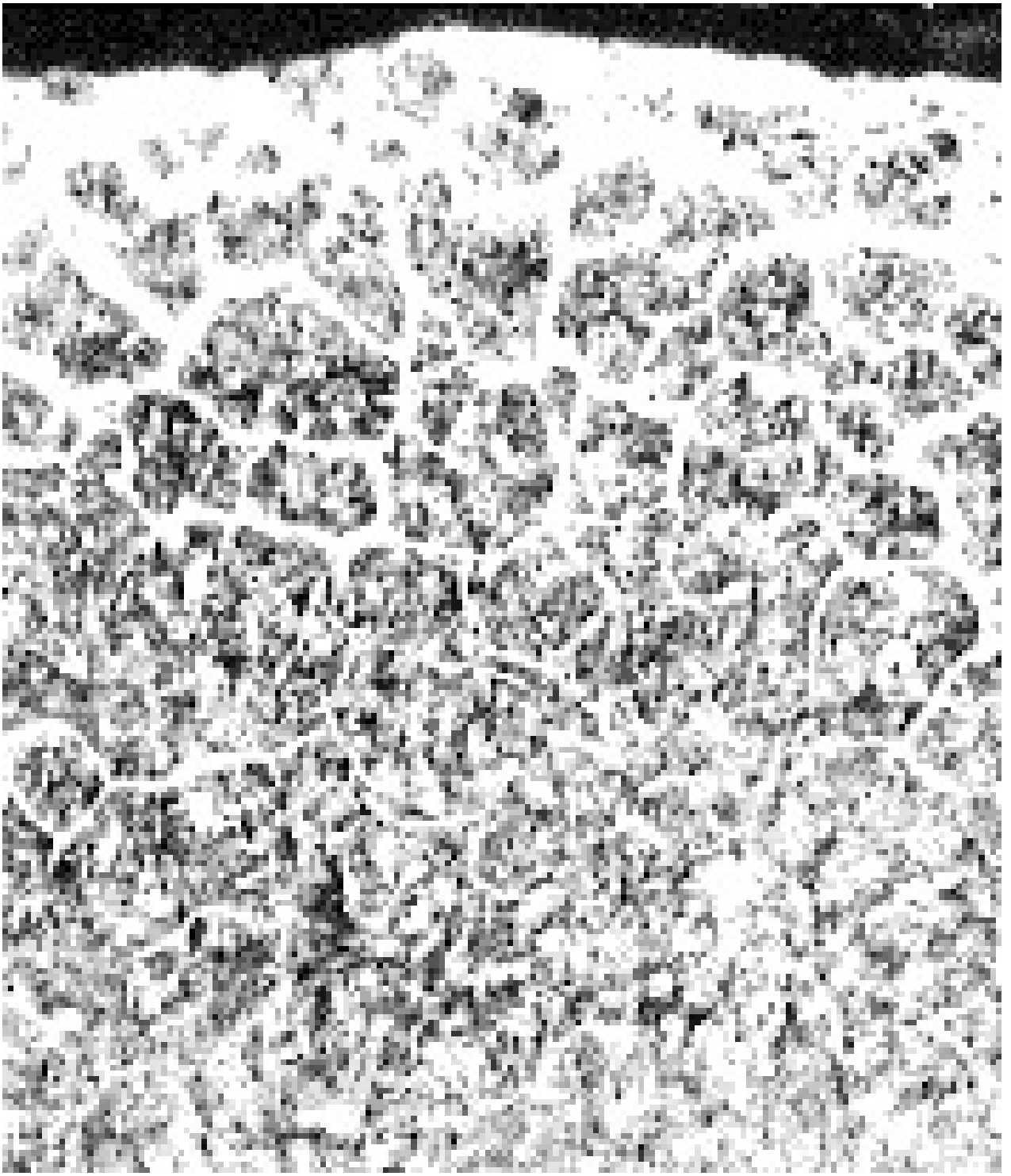

Figure 1.5.11.3 Gas nitrided case (24 h at 975F) produced on H-13 steel that was austenitized at 1890F, triple tempered at 950F, and surface activated in manganese phosphate (300X magnification) (Ref. 35)

Table 1.6.1.1 Effect of oil and air quenching on room temperature hardness of small H-13 steel test pieces (1 in. round x 2 in. long) cut from annealed bars austenitized for six minutes at indicated temperatures and quenched in oil or still air (Ref. 31)

Hardening Temperature (F)	Oil Quenched	Air Quenched
	Hardness (HRC)	Hardness (HRC)
1750	49.0	48.5
1800	51.0	50.5
1850	53.0	52.5
1900	54.5	54.0
1950	56.0	54.5
2000	57.0	55.0
2050	57.0	56.0
2100	59.0	57.0

Table 1.6.1.2 Effect of tempering on room temperature hardness of small H-13 test pieces (1 in. round x 1 in. long) austenitized at 1800, 1850, 1900, and 1950F, quenched in still air, and tempered for two hours at indicated temperatures (Ref. 31)

Tempering Temperature (F)	Austenitized 1800F	Austenitized 1850F	Austenitized 1900F	Austenitized 1950F
	Hardness (HRC)	Hardness (HRC)	Hardness (HRC)	Hardness (HRC)
None	50.5	52.5	54.0	54.5
600	50.0	52.0	52.5	53.5
700	50.0	52.0	53.0	53.5
800	50.5	52.0	54.0	54.0
900	51.5	53.5	54.5	55.5
1000	53.5	54.5	55.0	56.5
1100	51.0	53.0	53.0	53.5
1200	40.5	42.5	42.5	45.5

Table 1.6.1.3 Effect of tempering on room temperature hardness of large H-13 test pieces (4 x 4 x 4 in.) ground on two saw-cut ends, preheated at 1500F for one hour, austenitized at 1850F for one hour in a controlled atmosphere, quenched in oil or still air, and tempered for three hours at indicated temperatures (Ref. 31)

Tempering Temperature (F)	Hardness (HRC)	
	Air Cooled	Oil Quenched
None	53.5	53.5
1000	55.0	55.0
1100	47.5	48.5
1125	43.0	44.0
1150	39.5	40.5
1175	37.5	38.5
1200	36.5	38.5
1300	26.5	26.5

Table 1.6.1.4 Resistance to tempering for H-13 steel austenitized at either 1800 or 1850F and double tempered (3 + 3 h) at indicated temperatures (Ref. 36)

Double Tempered (3 + 3 h) (F)	Air Cooled from	
	1800F (HRC)	1850F (HRC)
300	49.0	50.0
400	49.5	50.0
500	50.0	50.0
600	50.0	50.0
700	50.5	50.5
800	51.0	51.5
900	52.5	53.0
1000	51.5	53.5
1050	50.0	52.0
1100	46.0	49.5
1150	39.5	43.0
1200	31.0	32.0

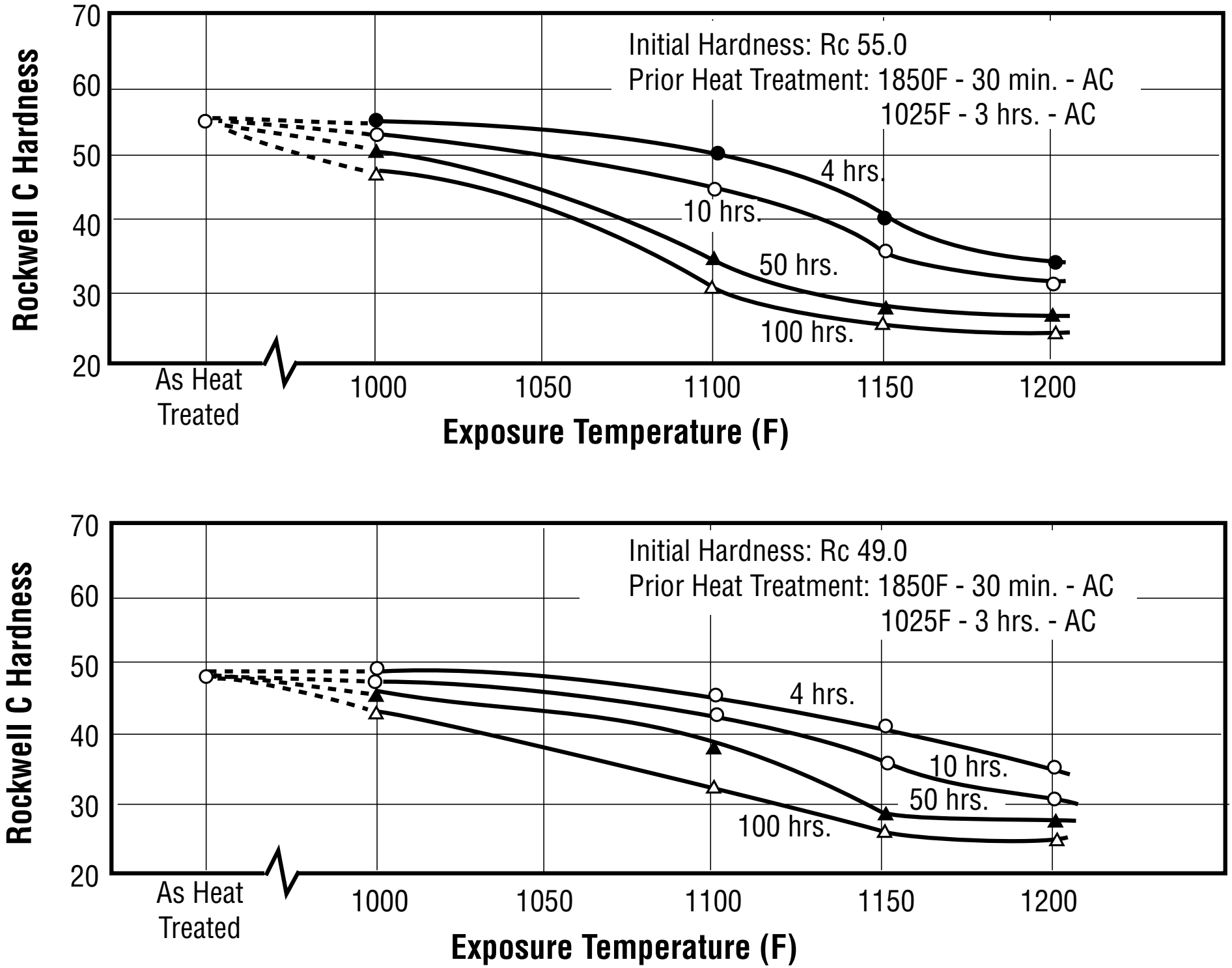

Figure 1.6.1.5 Room temperature hardness or "red hardness" of H-13 steel hardened and tempered as indicated after exposure to elevated temperatures for 4–100 h (Ref. 36)

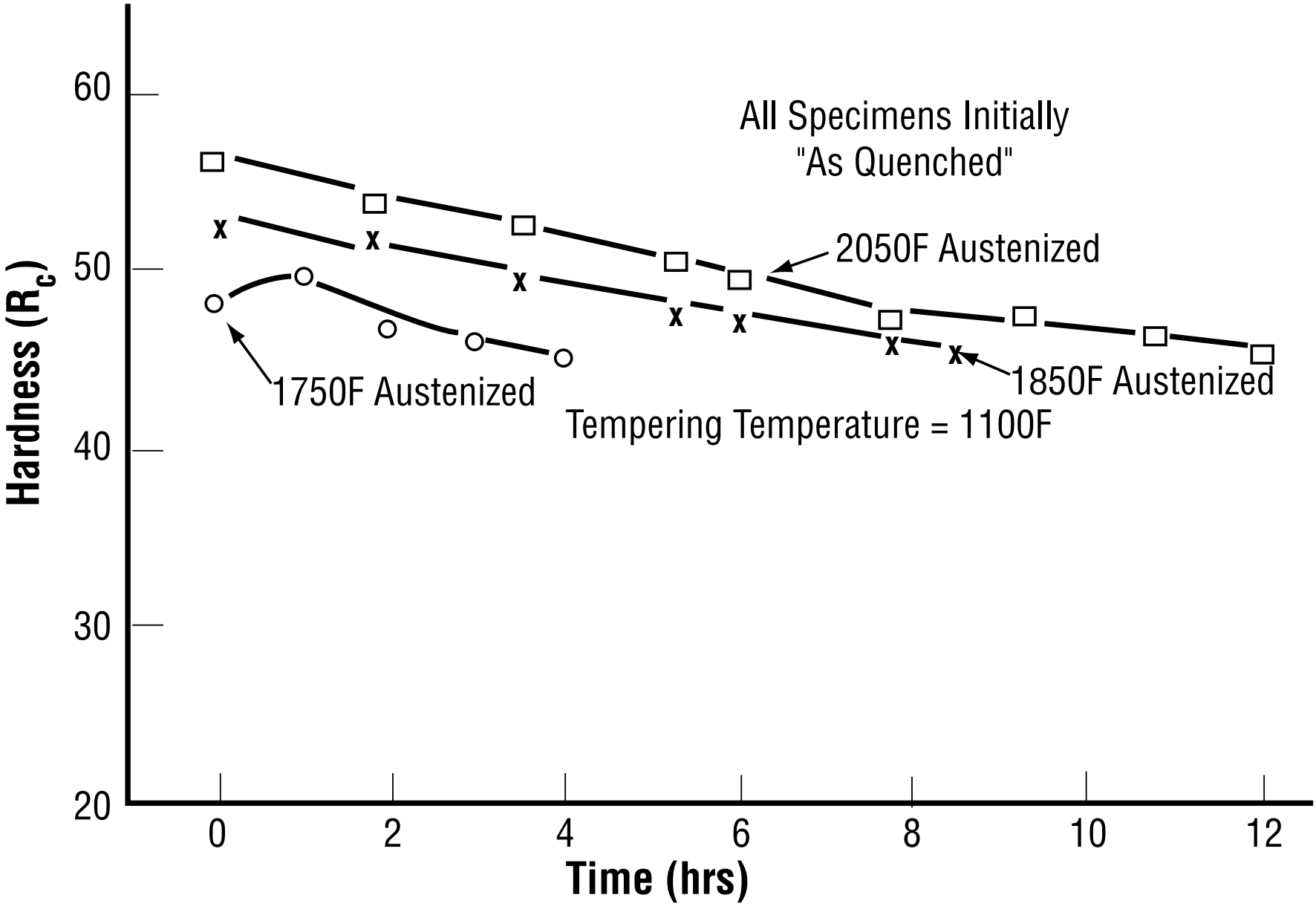

Figure 1.6.1.6 Tempering curves of H-13 steel air quenched after austenitizing at 1750, 1850, and 2050F showing hardness (R_c or HRC) as a function of time at a tempering temperature of 1100F (Ref. 22)

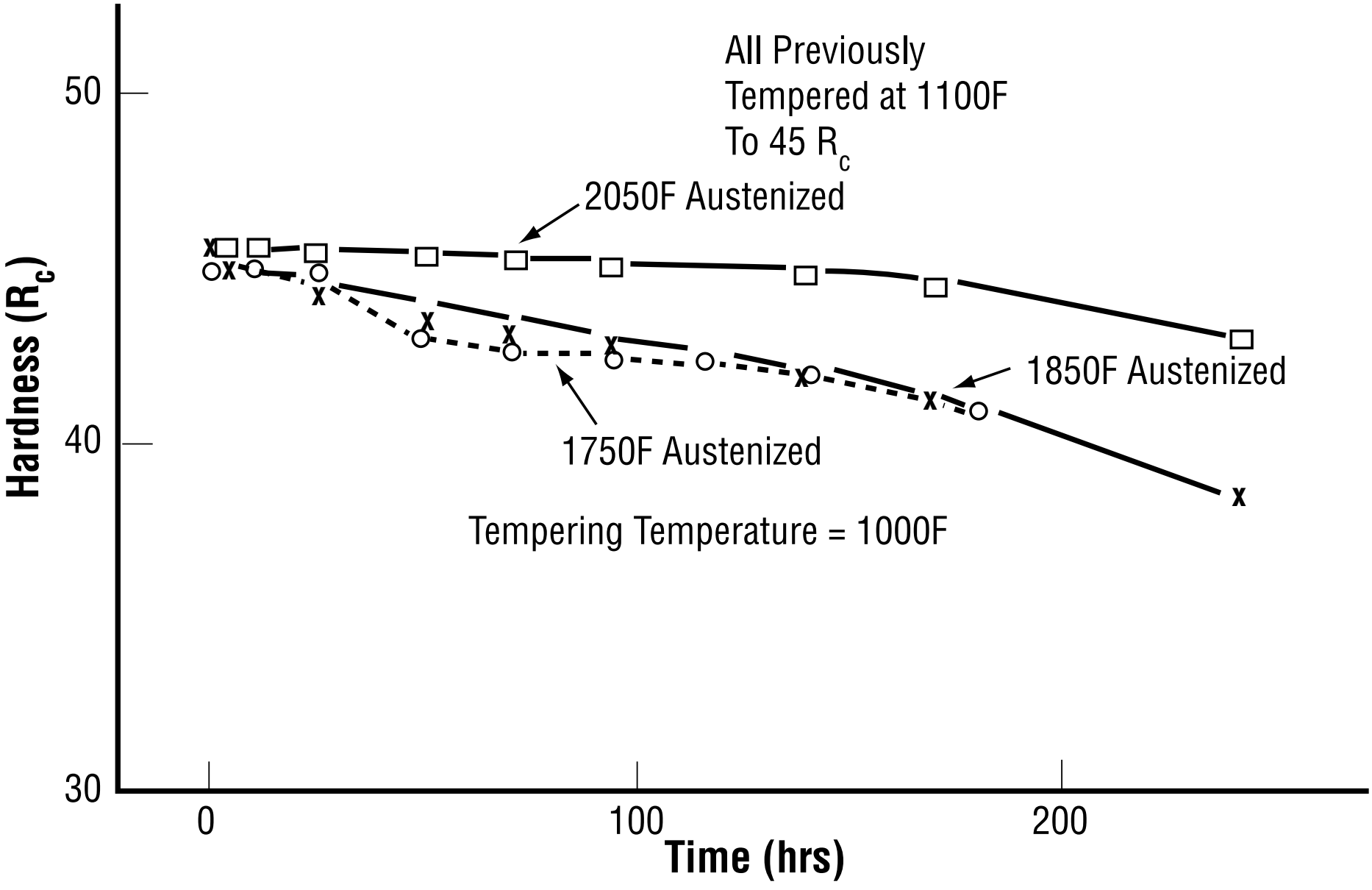

Figure 1.6.1.7 Tempering curves for H-13 steel air quenched after austenitizing at 1750, 1850, and 2050F, tempering to 45 HRC, and showing hardness (R_c or HRC) as a function of time at a tempering temperature of 1000F (Ref. 22)

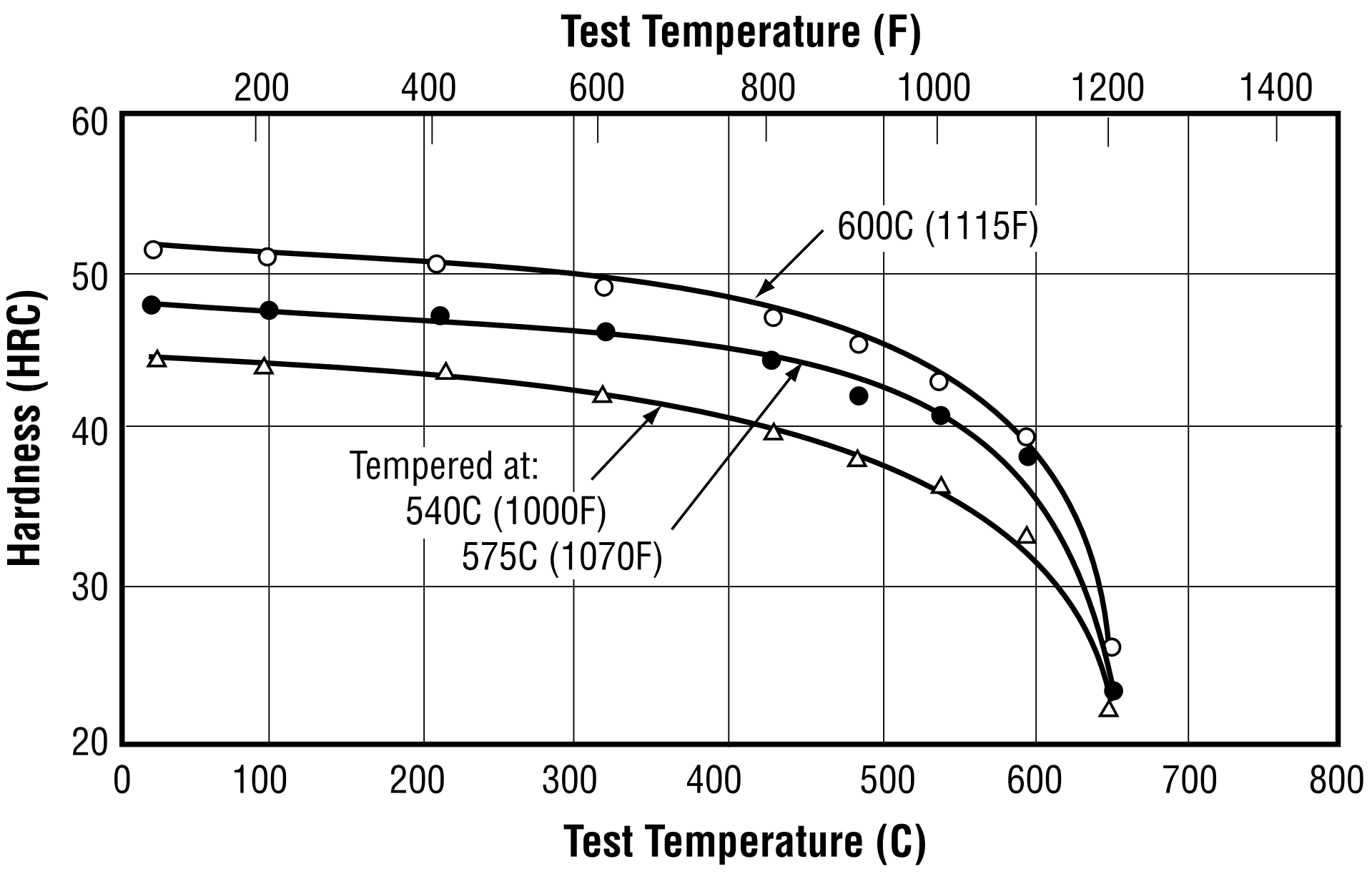

Figure 1.6.2.1 Typical hot hardness of H-13 steel for specimens oil quenched from 1850F and double tempered 2 + 2 h at indicated tempering temperature (Ref. 37)

Table 1.6.2.2 Brinell hot hardness of H-13 steel samples (1 in round x 7/8 in. long) hardened by oil quenching from 1850F and tempering for two hours at 1050F or test temperature if higher (Ref. 31)

Tempering Temperature (F)	RT Hardness after Tempering (HRC)	Test Temperature (F)	Hot Hardness* (BHN)
1050	53.5	800	495
1050	53.5	900	477
1050	53.5	1000	418
1100	51.5	1100	351
1200	38.0	1200	140
1300	39.5	1300	68

*Samples held for 30 min at hot hardness test temperature before testing.

Table 1.6.2.3 Rockwell C hot hardness of H-13 steel heat treated to indicated room temperature hardness levels (Ref. 36)

RT Hardness after Tempering (HRC)	Rockwell C Hot Hardness* at Temperature (HRC)				
	600F	800F	1000F	1100F	1200F
55.5	51.0	48.0	39.0	33.5	23.5
46.5	41.0	39.0	33.0	21.5	17.0

*Samples held for 30 min at hot hardness test temperature before testing.

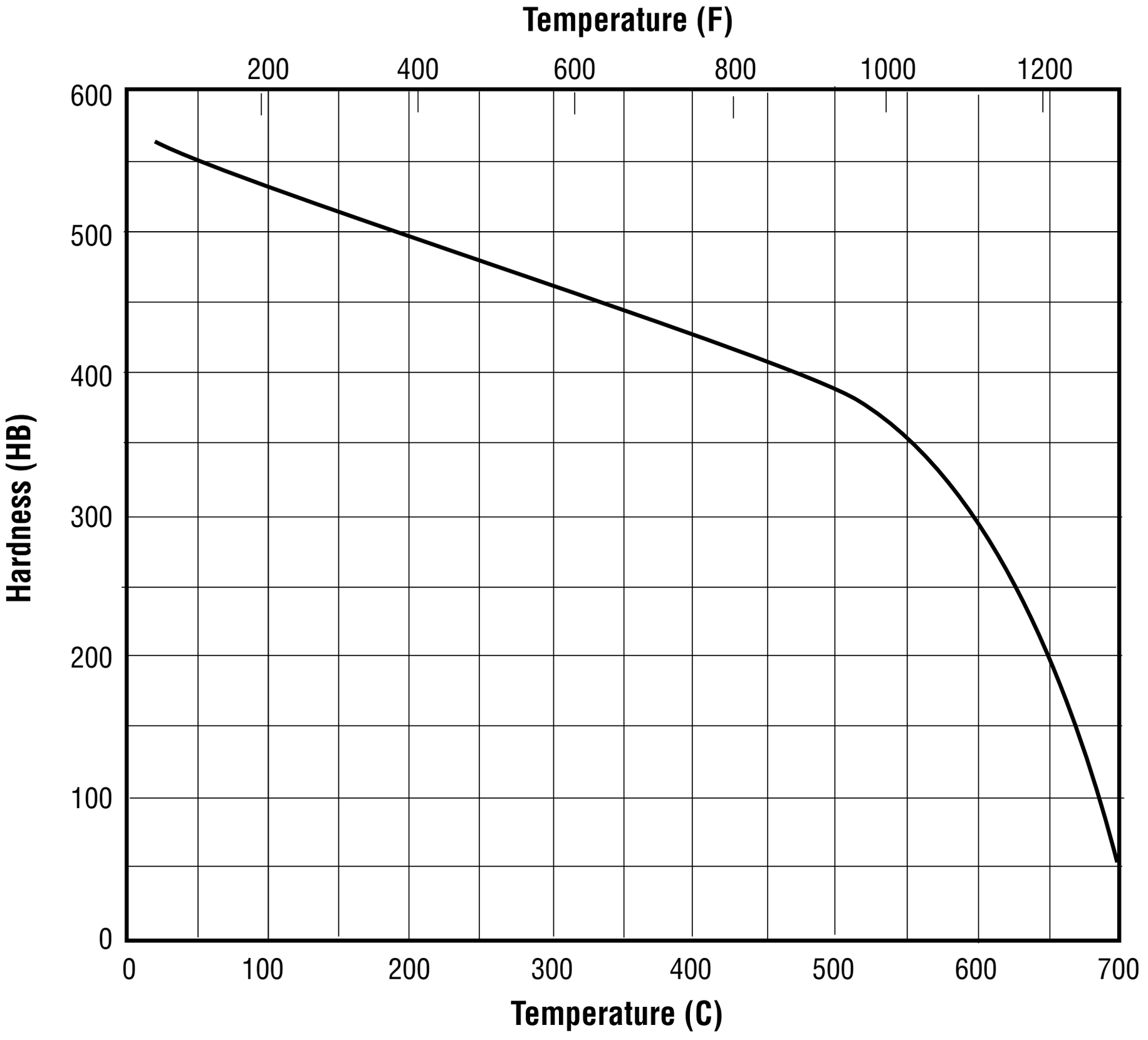

Figure 1.6.2.4 Effect of temperature on hot Brinell hardness (HB) of hardened (austenitized and quenched, untempered) H-13 steel (Ref. 44)

Table 1.6.3.1 Case and core hardness on ½-in.-square test pieces of nitrided H-13 steel hardened at 1850F and tempered at 1050F, ground, and nitrided as indicated (Ref. 31)

Nitriding Cycle (h)	Nitrided Case Depth (in.)	Case Hardness* (HRC)	Core Hardness (HRC)
24	0.007	72	49
48	0.012	73	47
72	0.019	74	45

*HRC conversion from 15 N Rockwell superficial hardness tests.

Table 2.1.3.1 Thermal conductivity of H-13 steel as a function of temperature (Ref. 2)

Temperature (F)	Thermal Conductivity (Btu/ft-hr-F)
420	16.5
660	16.4
890	16.4
1120	16.6

Table 2.1.3.2 Thermal conductivity of Thyrotherm 2344 ESR Magnum premium grade AISI H-13 steel at indicated temperatures (Ref. 18)

Temperature (F)	Thermal Conductivity (Btu/ft-hr-F)
70	14.7
400	15.6
800	17.5
1200	19.1

Table 2.1.4.1 Average linear thermal expansion coefficient of H-13 steel over indicated temperature range (Ref. 44)

Temperature Range (F)	Average Linear Thermal Expansion Coefficient (in/in/F x 10^{-6})
80-200	6.1
80-400	6.4
80-800	6.8
80-1000	6.9
80-1200	7.3
80-1450	7.5
500-1200	7.8
500-1450	8.0
800-1200	8.1
800-1450	8.2

Table 2.1.4.2 Average thermal expansion coefficient of Nu-Die V (Crucible Steel) and VDC (Timken Latrobe Steel) H-13 steel from room temperature (RT) to indicated temperature (Refs. 12, 16)

Temperature Range (F)	Average Thermal Expansion Coefficient (in/in/F x 10^{-6})	
	Nu-Die V H-13	VDC H-13
RT-200	6.1	5.8
RT-400	6.4	6.3
RT-800	6.8	6.9
RT-1000	7.0	--
RT-1200	7.3	7.3
RT-1500	--	7.5

Table 2.1.4.3 Average thermal expansion coefficient of Thyrotherm 2344 ESR Magnum premium grade AISI H-13 steel over indicated temperature range (Ref. 18)

Temperature Range (F)	Average Thermal Expansion Coefficient (in/in/F x 10^{-6})
70-200	6.00
70-400	6.66
70-800	6.80
70-1200	7.51

Table 2.1.4.4 Average thermal expansion coefficient of Crucible CPM® Nu-Die® EZ patented H-13 particle metallurgy sulfurized steel from room temperature (RT) to indicated temperature (Ref. 43)

Temperature Range (F)	Average Thermal Expansion Coefficient (in/in/F x 10^{-6})
RT-200	6.1
RT-400	6.4
RT-800	6.8
RT-1000	7.0
RT-1200	7.3

Table 2.2.1.1 Density of Thyrotherm 2344 ESR Magnum premium grade AISI H-13 steel over the temperature range 70–1200F (Ref. 18)

Temperature (F)	Density (lb/cu in)
70	0.281
400	0.280
800	0.276
1200	0.275

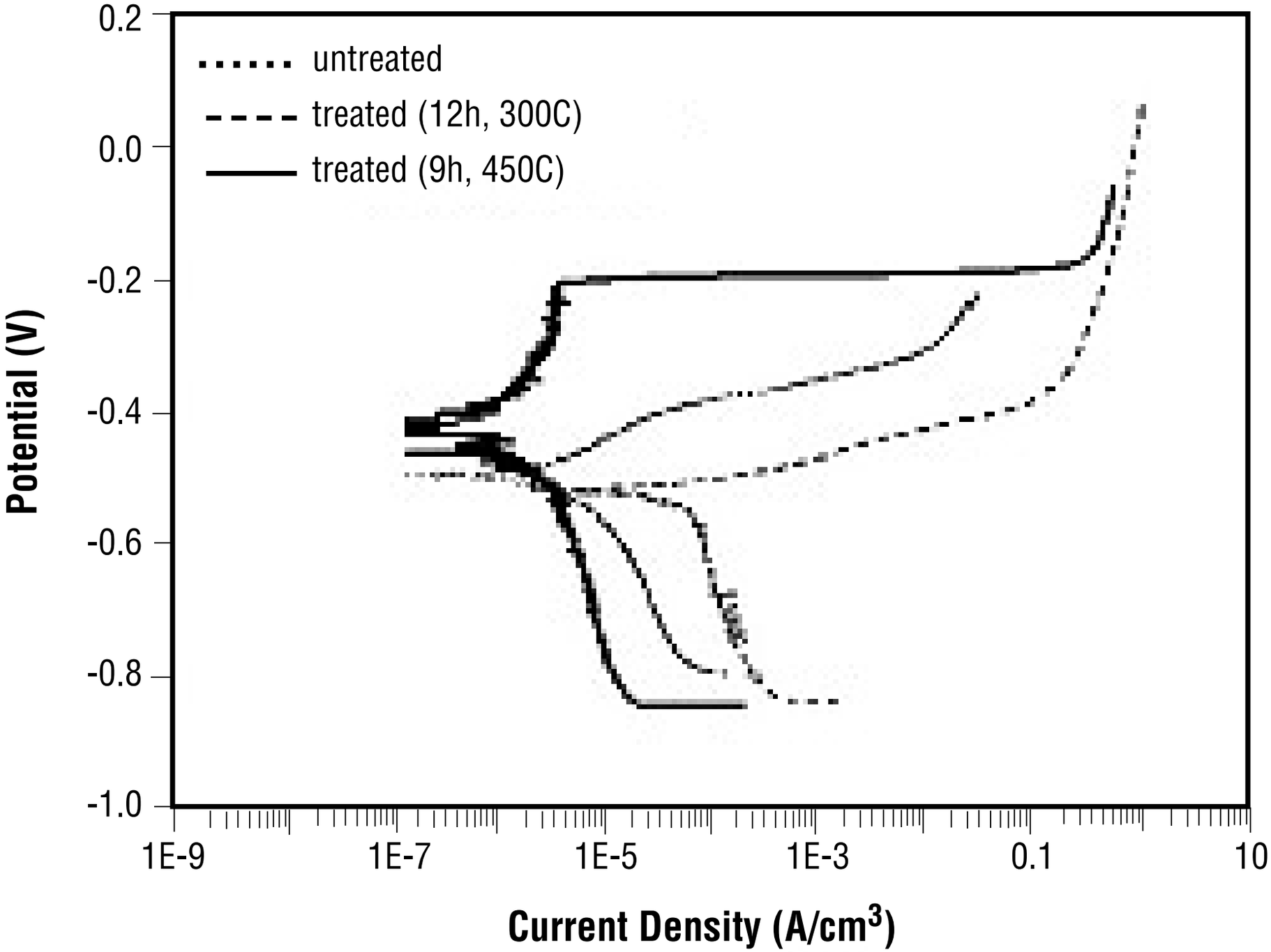

Figure 2.3.1.1 Potentiodynamic polarization curves of AISI H-13 steel measured in a 3.5% NaCl solution at pH = 6 on an (…) untreated sample, (----) nitrogen plasma immersion ion implantation (PIII) processed sample (T=300C, t=12 h), and (—) nitrogen PIII processed sample (T=450C, t=9 h) (Ref. 45)

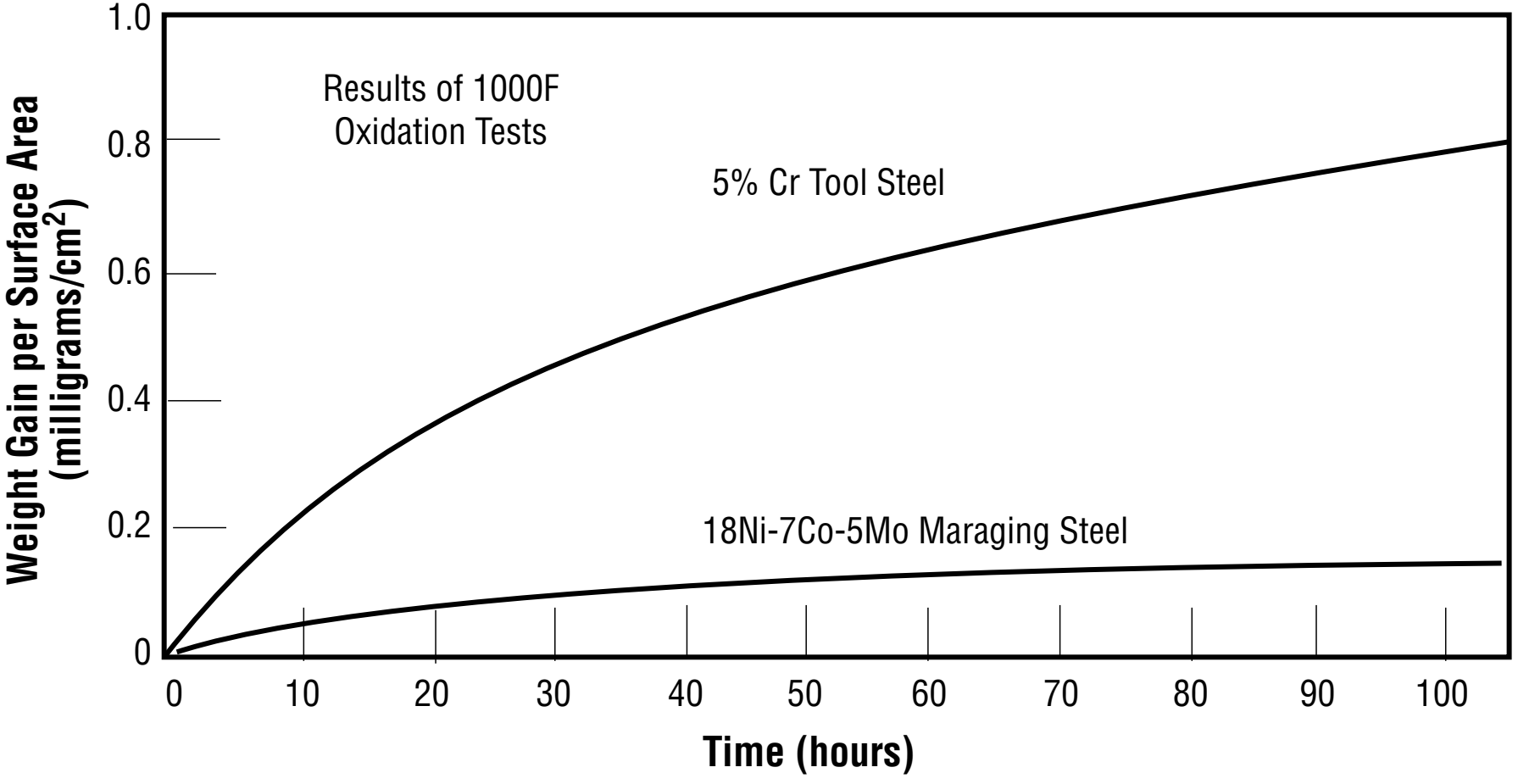

Figure 2.3.3.1 Comparative oxidation resistance of H-13 and maraging steels at 1000F (Ref. 46)

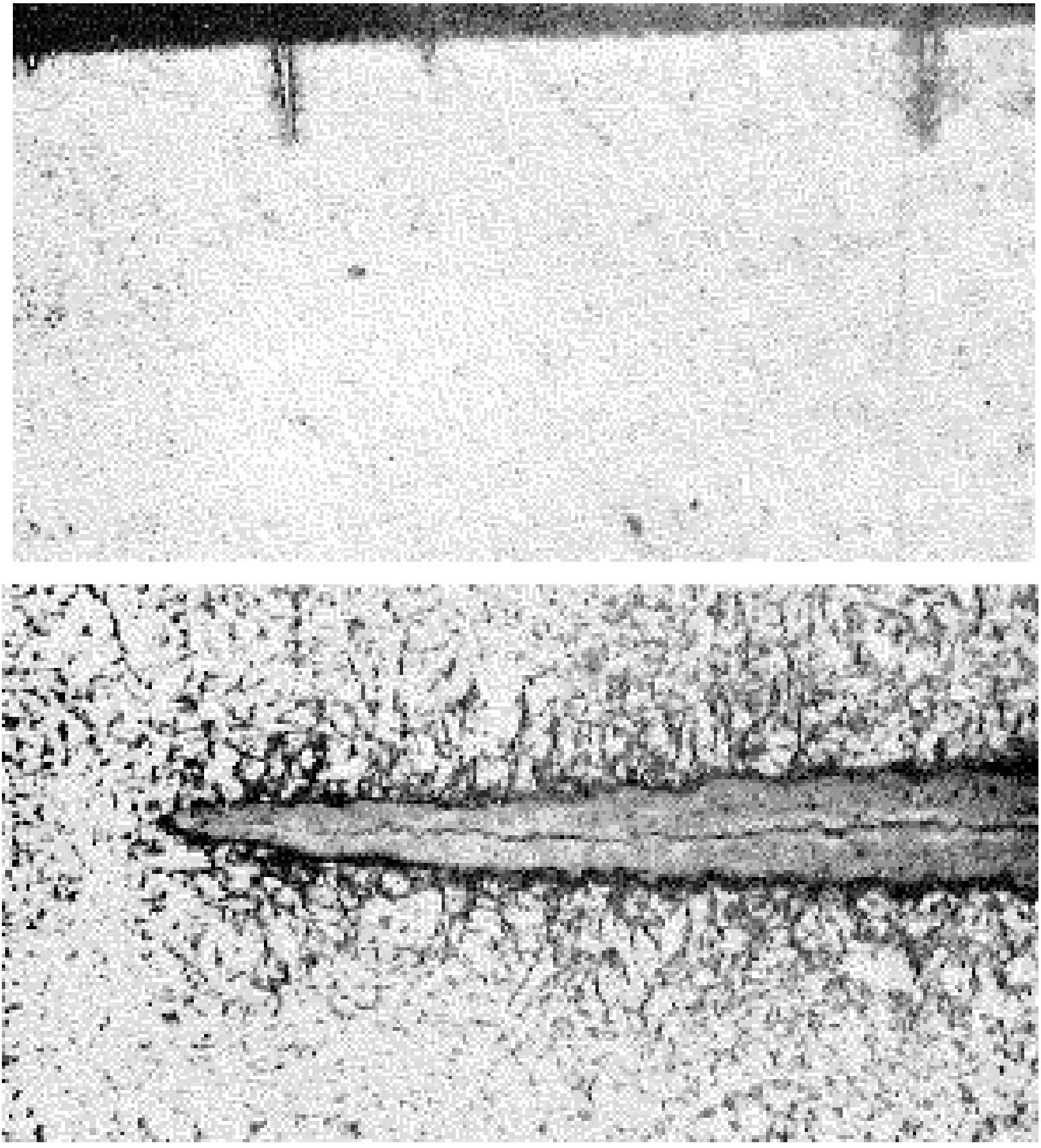

Figure 2.3.3.2 Cross sectional view of oxide buildup in thermal fatigue crack in hardened H-13 steel specimen: (a) 50x, nital etch and (b) 500x, nital etch (Ref. 22)

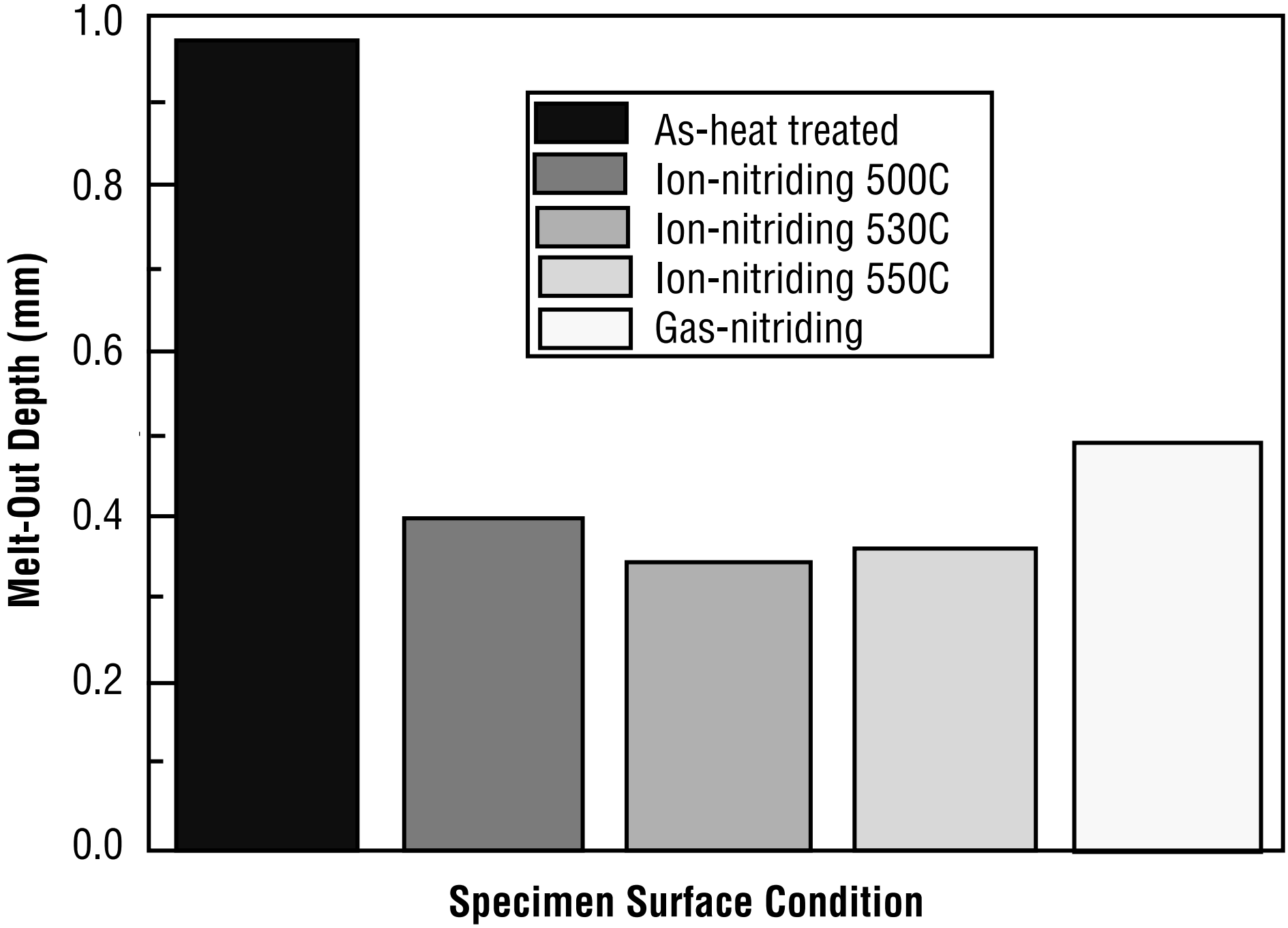

Figure 2.3.5.1 Variations in corroded/eroded depth of immersion test specimens of hardened and tempered H-13 steel as heat treated and machined and separately nitrided by gas or ion nitriding maintained in a molten Al-Si-Cu (KS ALDC) aluminum alloy at 1300F for 43 h (Ref. 47)

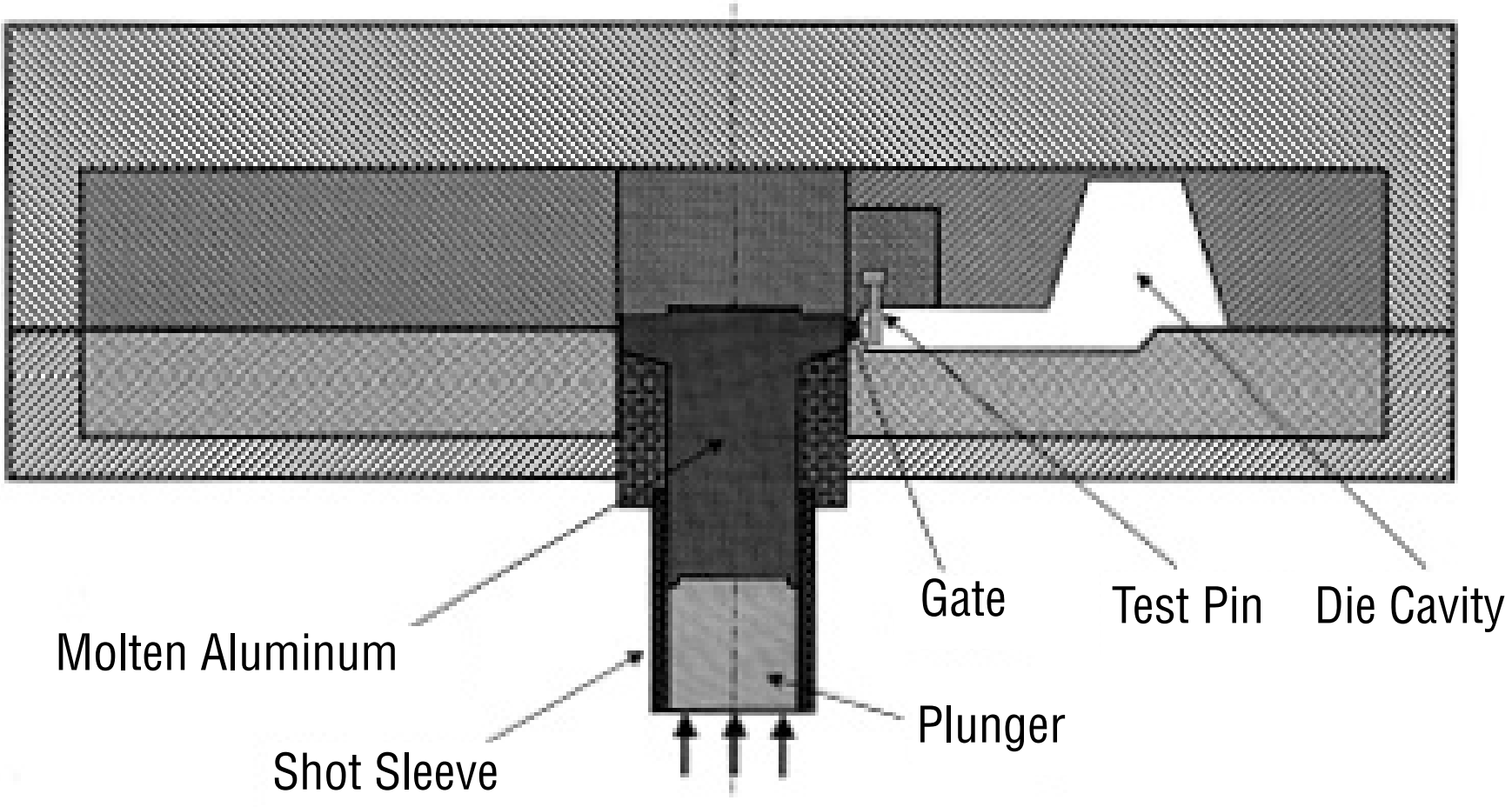

Figure 2.3.5.2 Schematic diagram of accelerated washout testing arrangement at Case Western Reserve University (CWRU) with molten aluminum alloy injected into die cavity at ~70 in/s (Ref. 48)

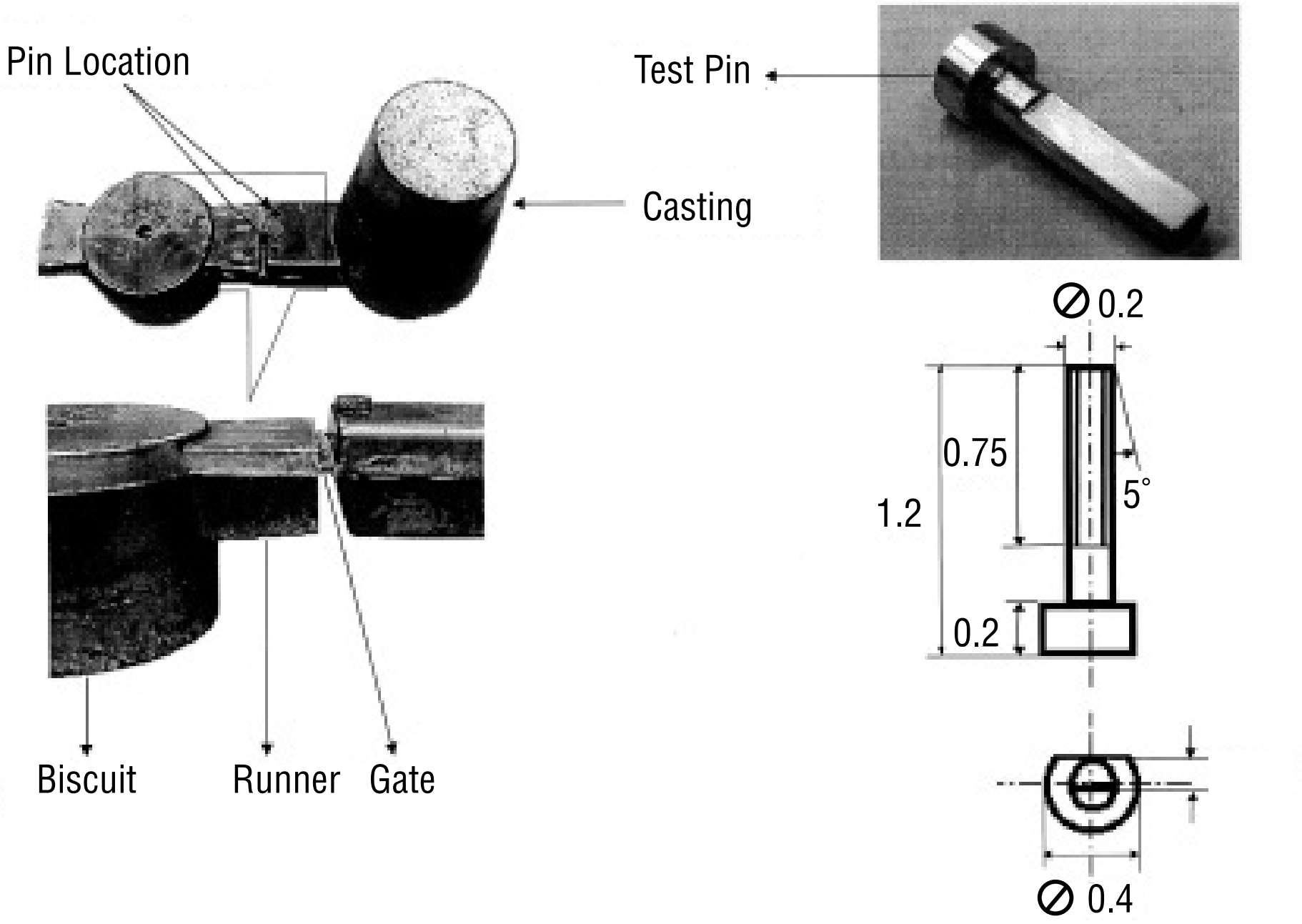

Figure 2.3.5.3 Test pin design and position within die cavity of CWRU accelerated washout test arrangement shown in Figure 2.3.5.2 (Ref. 48)

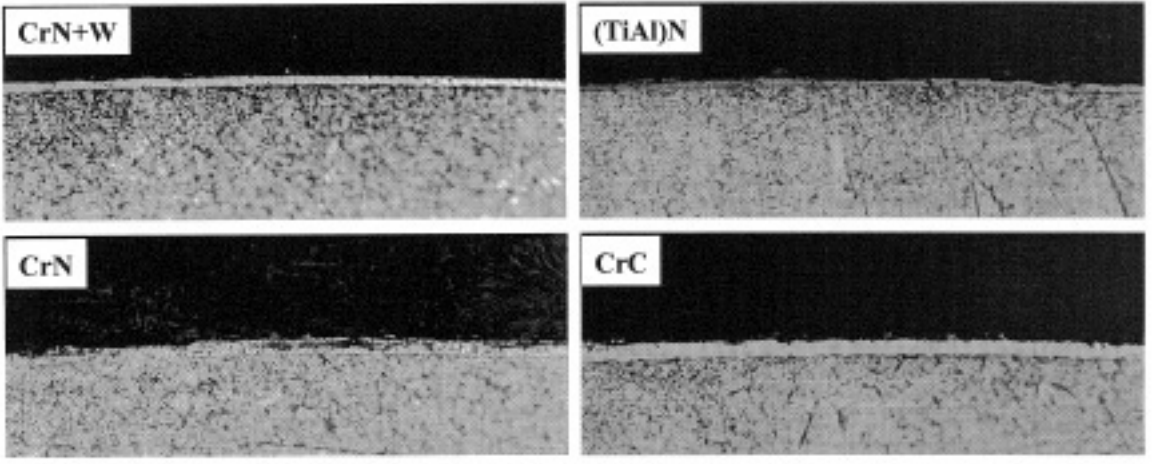

Figure 2.3.5.4 Microstructural cross sections (500x) PVD coated pin specimens tested in CWRU accelerated washout arrangement shown in Figure 2.3.5.2 (Ref. 48)

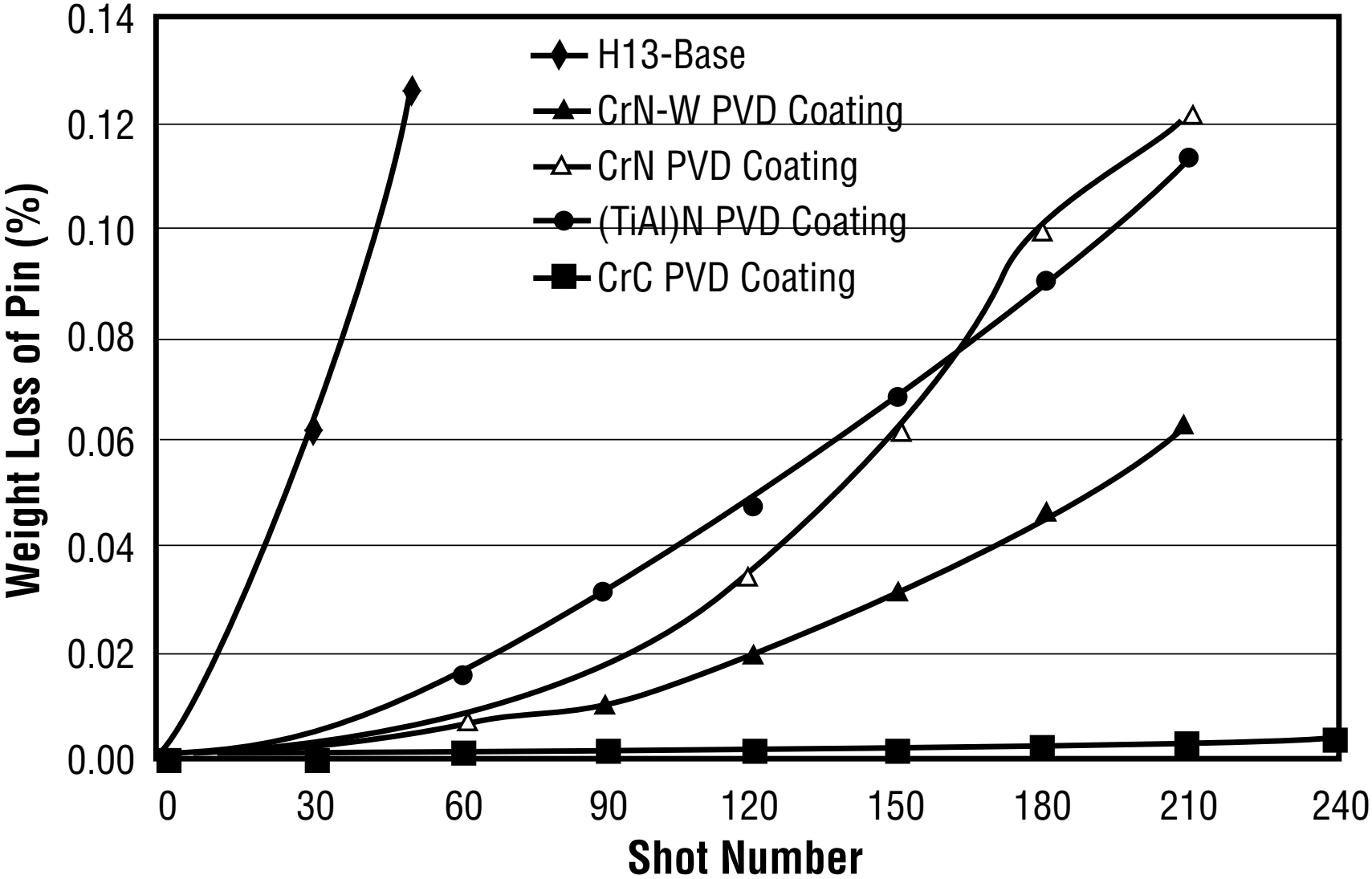

Figure 2.3.5.5 Effect of various types of PVD coatings shown in Figure 2.3.5.4 on washout resistance of H-13 steel die casting core pins in CWRU accelerated washout test shown in Figures 2.3.5.2 and 2.3.5.3 (Ref. 48)

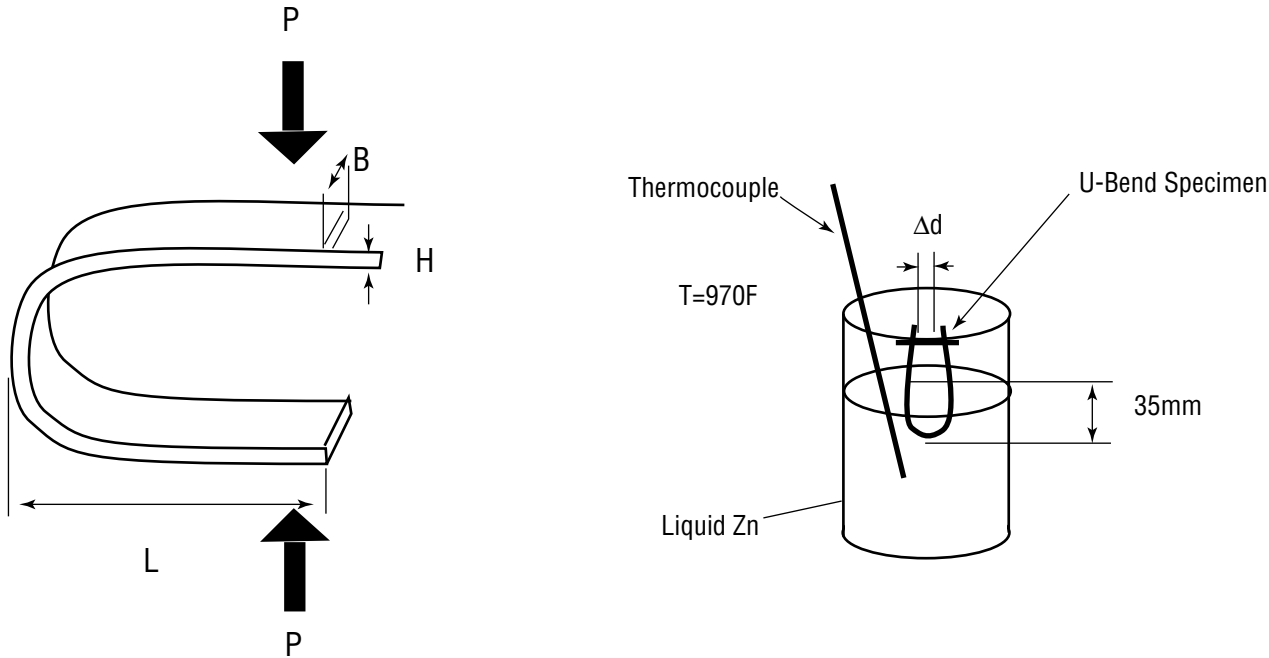

Figure 2.3.6.1 Schematic drawing of TPTC U-bend liquid zinc embrittlement test procedure conducted on H-13 steel plate specimens: original annealed specimen bent into U-shape, heat treated, bent to an incipient plastic flow condition at a displacement of Dd (left), displacement held by fastener, and immersed in a molten zinc bath (right) (Ref. 50)

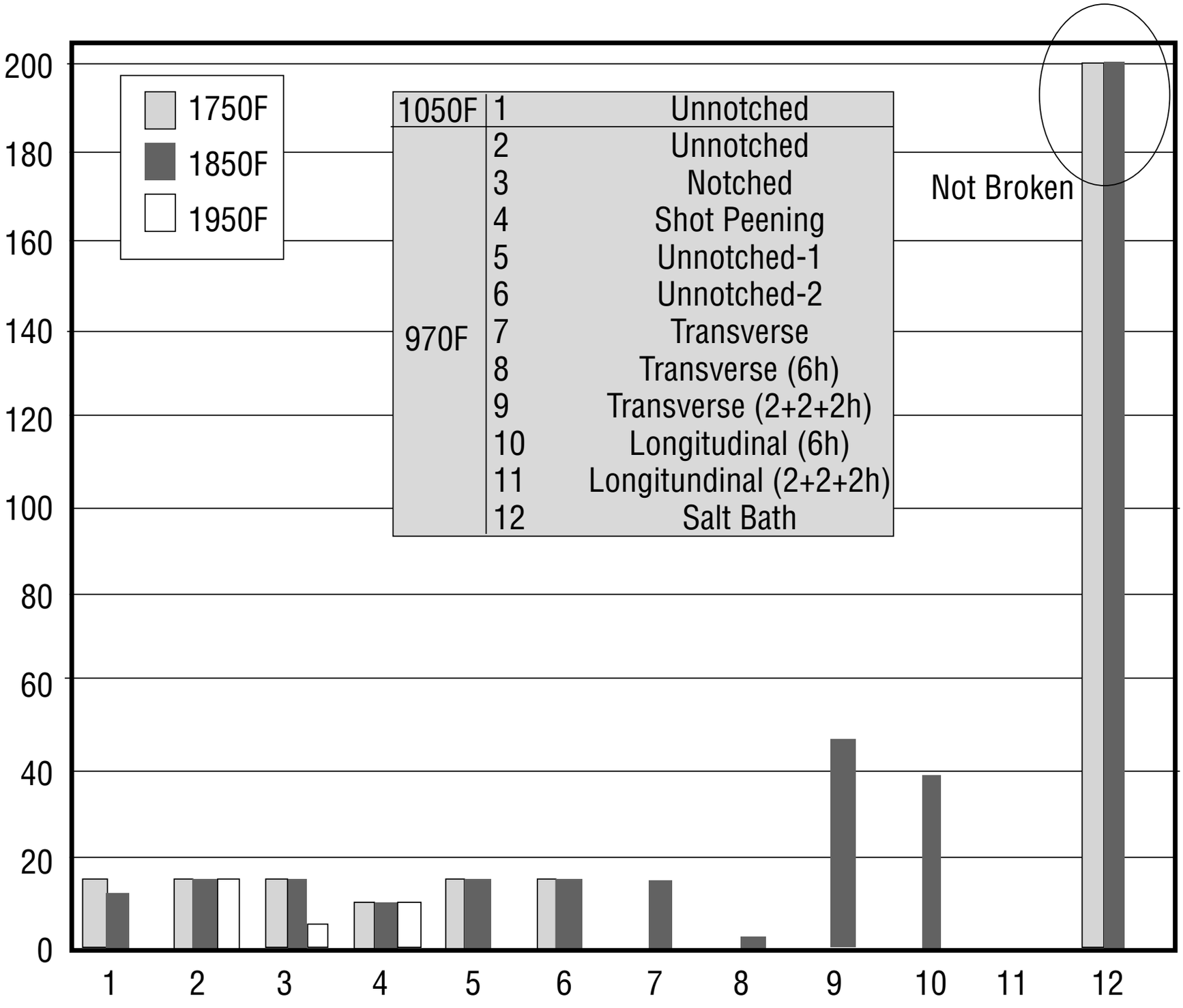

Figure 2.3.6.2 Liquid zinc embrittlement TPTC U-bend test data (Y-axis: time to fracture in hours; X-axis: test conditions as shown in Figure 2.3.6.1) conducted on H-13 steel plate specimens (Ref. 50)

Table 3.2.1.1 Typical longitudinal room temperature mechanical properties of H-13 steel bar oil quenched from an 1850F austenitizing temperature and tempered at different temperatures (Ref. 1)

Tempering Temperature* (F)	Tensile strength (ksi)	Yield strength (ksi)	Elongation In 4 D (%)	Reduction in area (%)	Charpy V-notch impact energy		Hardness (HRC)
					(ft-lb)	(J)	
980	284	228	13.0	46.2	12	16	52
1030	266	222	13.1	50.1	18	24	50
1065	251	213	13.5	52.4	20	27	48
1100	229	198	14.4	53.7	21	28.5	46
1120	217	187	15.4	54.0	22	30	44

*Double tempered, 2 + 2 hours, at given tempering temperature.

Table 3.2.1.2 Transverse mechanical properties at room temperature of air melted and electroslag remelted (ESR) H-13 steel large section bars oil quenched from 1850F and double tempered, 2 + 2 hours, at 1090F to a final hardness of 48 HRC (Ref. 1)

Property*	Air melted**	Electroslag Remelted***
Tensile strength	234 ksi	239 ksi
Yield strength	202 ksi	207 ksi
Elongation in 4D	2.9%	5.6%
Reduction in area	5.7%	12.8%
Charpy V-notch Impact energy	4 ft-lb	5 ft-lb

* Specimens taken from mid-radius of round bar.

** Round section, 14-in. in diameter.

*** Round section, 18-in. in diameter.

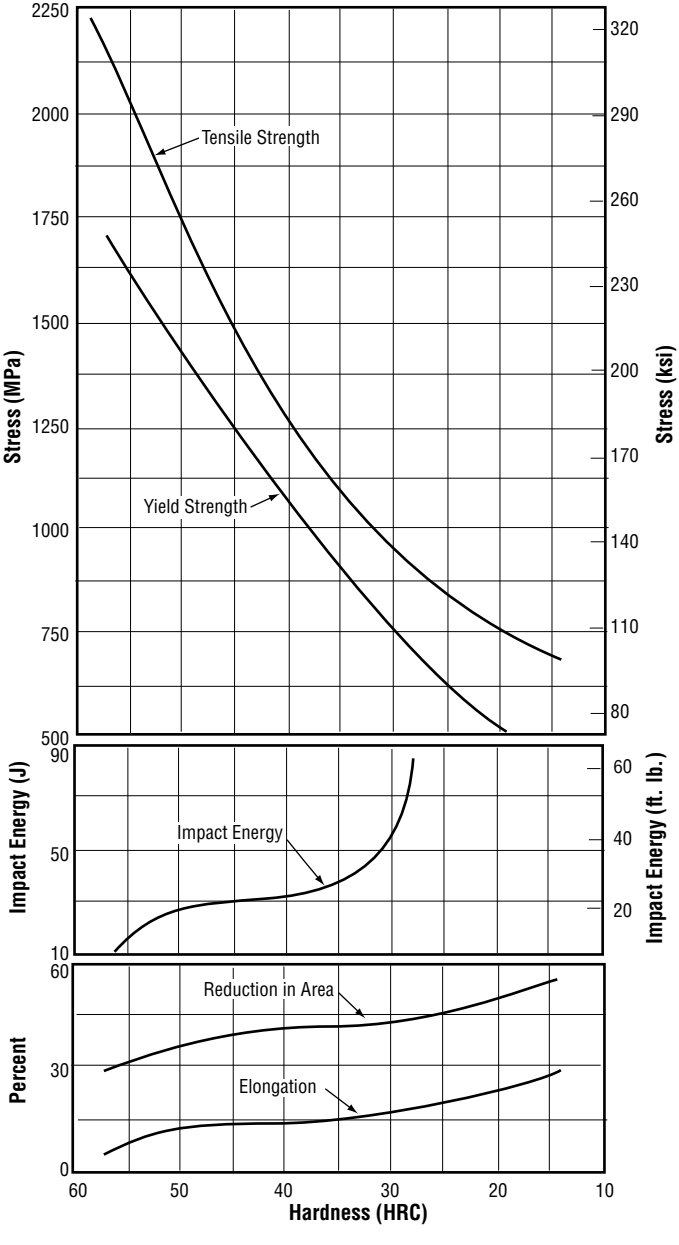

Figure 3.2.1.3 Room temperature tensile properties of H-13 steel in relation to hardness and Charpy V-notch impact energy (Ref. 44)

Table 3.2.1.4 Room temperature tensile properties of annealed and heat treated H-13 steel (Ref. 16)

Condition	Hardness (HRC)	Yield Strength* (ksi)	Ultimate Strength* (ksi)	Elongation* (%)	Reduction of Area* (%)
Annealed	15	54	97	32.0	66.0
Heat treated**	46	204	218	13.0	47.0
Heat Treated**	51	250	281	5.0	10.0

*Standard ASTM 0.505 in. round tensile specimens cut from 1.125 in. bar stock , average of two tests.
**Austenitized at 1825F, air cooled, and double tempered to hardness shown.

Table 3.2.3.1 Longitudinal Charpy V-notch impact properties at room temperature of H-13 bar air cooled from an 1850F austenitizing temperature and tempered at different temperatures (Ref. 1)

Tempering temperature (F)	Hardness (HRC)	Charpy V-notch Impact Energy	
		(ft-lb)	(J)
975	54	10	14
1050	52	10	14
1125	47	18	24
1140	43	18	24

Table 3.2.3.2 Transverse Charpy V-notch impact toughness at room temperature of various grades of H-13 steel at 45–46 HRC (Ref. 43)

Grade	Hardness (HRC)	Transverse Charpy-V Notch Impact Toughness (ft-lb)
Premium Quality H-13	46	10
Conventional Sulfurized H-13	45	2
CPM Nu-Die EZ (Crucible)	45	7-9

Table 3.2.3.3 Izod impact properties at room temperature of H-13 steel specimens machined from ½-in. square bar stock to 0.394 in. square, preheated to 1500F, austenitized at 1850F, oil quenched, and tempered at indicated temperatures for 2 h (Ref. 31)

Tempering Temperature (F)	Hardness (HRC)	Izod Impact Energy Absorbed* (ft-lb)
None	55.0	8.0
600	53.5	12.0
700	54.0	12.5
800	54.0	11.0
900	55.0	9.0
1000	54.5	10.0
1100	51.0	14.0
1200	41.0	26.0
1300	28.5	52.0
1400	25.5	64.0

*Results given are an average of four samples.

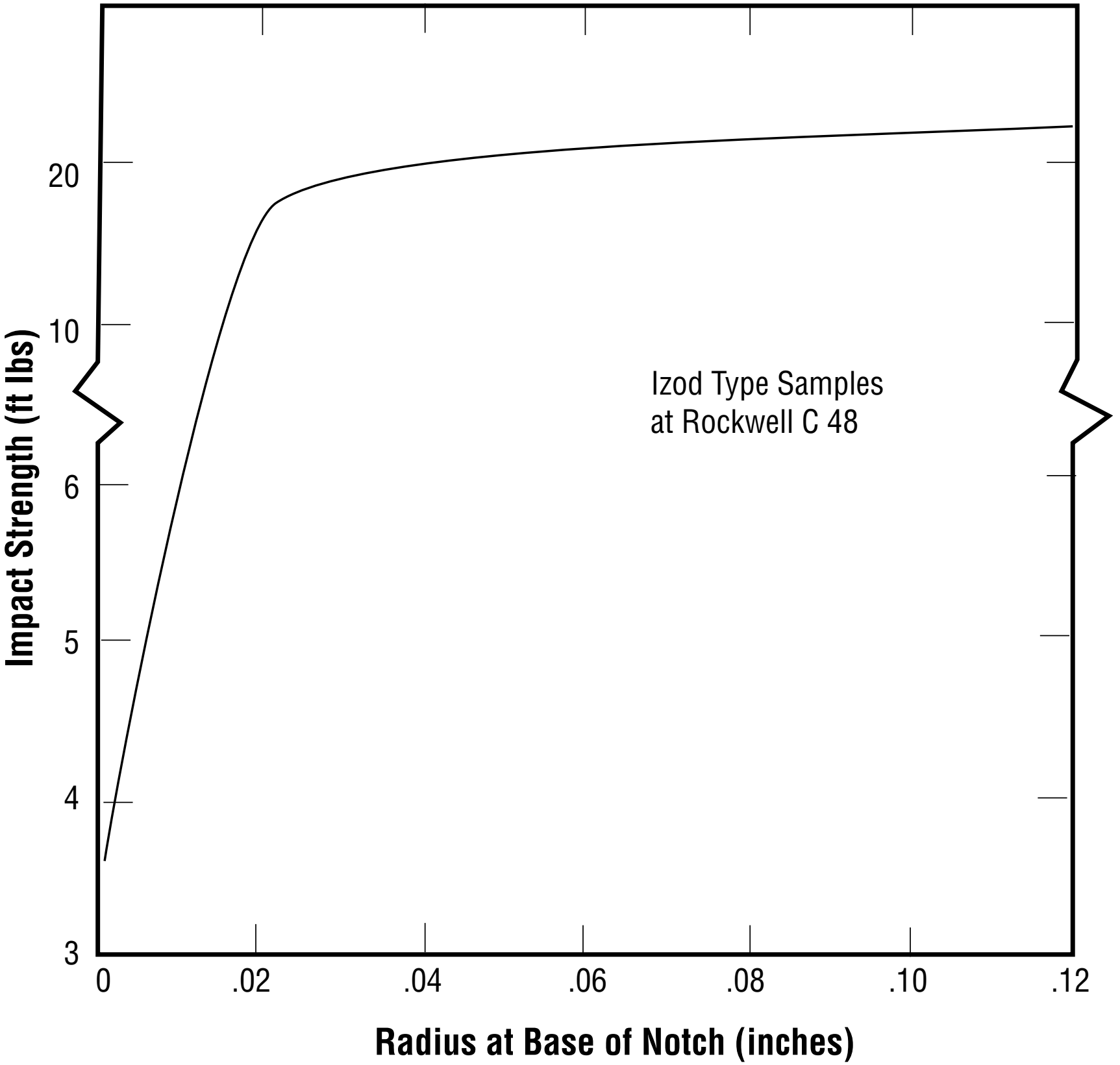

Figure 3.2.7.1.1 Effect of notch radius on the impact strength of Izod type specimens of H-13 steel heat treated to 48 Rockwell C and tested at room temperature (Ref. 61)

Table 3.2.7.2.1 Longitudinal plane strain fracture toughness of H-13 steel air cooled from 1920F and tempered two hours at temperature (Ref. 58)

Tempering Temperature (F)	Plane Strain Fracture Toughness (K_{Ic}) (ksi-in$^{1/2}$)
750	43.4
885	30.0
930	24.9
985	22.1
1020	21.0
1110	30.2
1155	47.7
1200	70.7

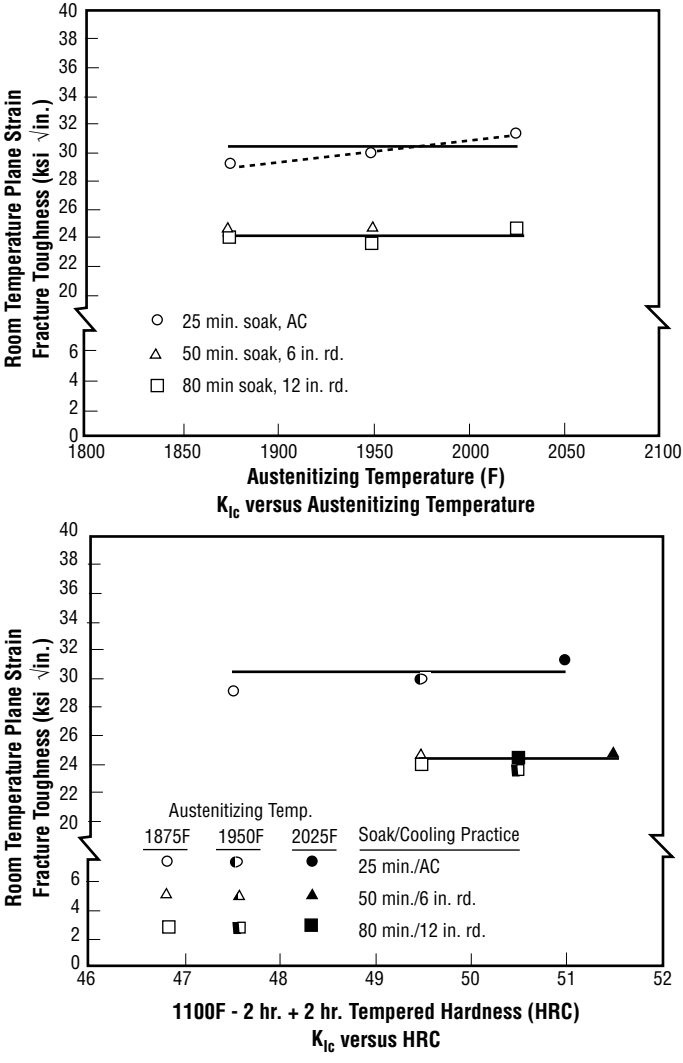

Figure 3.2.7.2.2 Room temperature plane strain fracture toughness (K_{Ic}) of small and large size specimens of H-13 steel versus austenitizing temperature (a) and tempered hardness (b) after all specimens were double tempered at 1100F (2 + 2 h) for austenitizing soak times and cooling conditions given (25 min soak and air quench for small specimens and 50 and 60 min soak and simulated laboratory quench for 6- and 12-in. rounds) (Ref. 28)

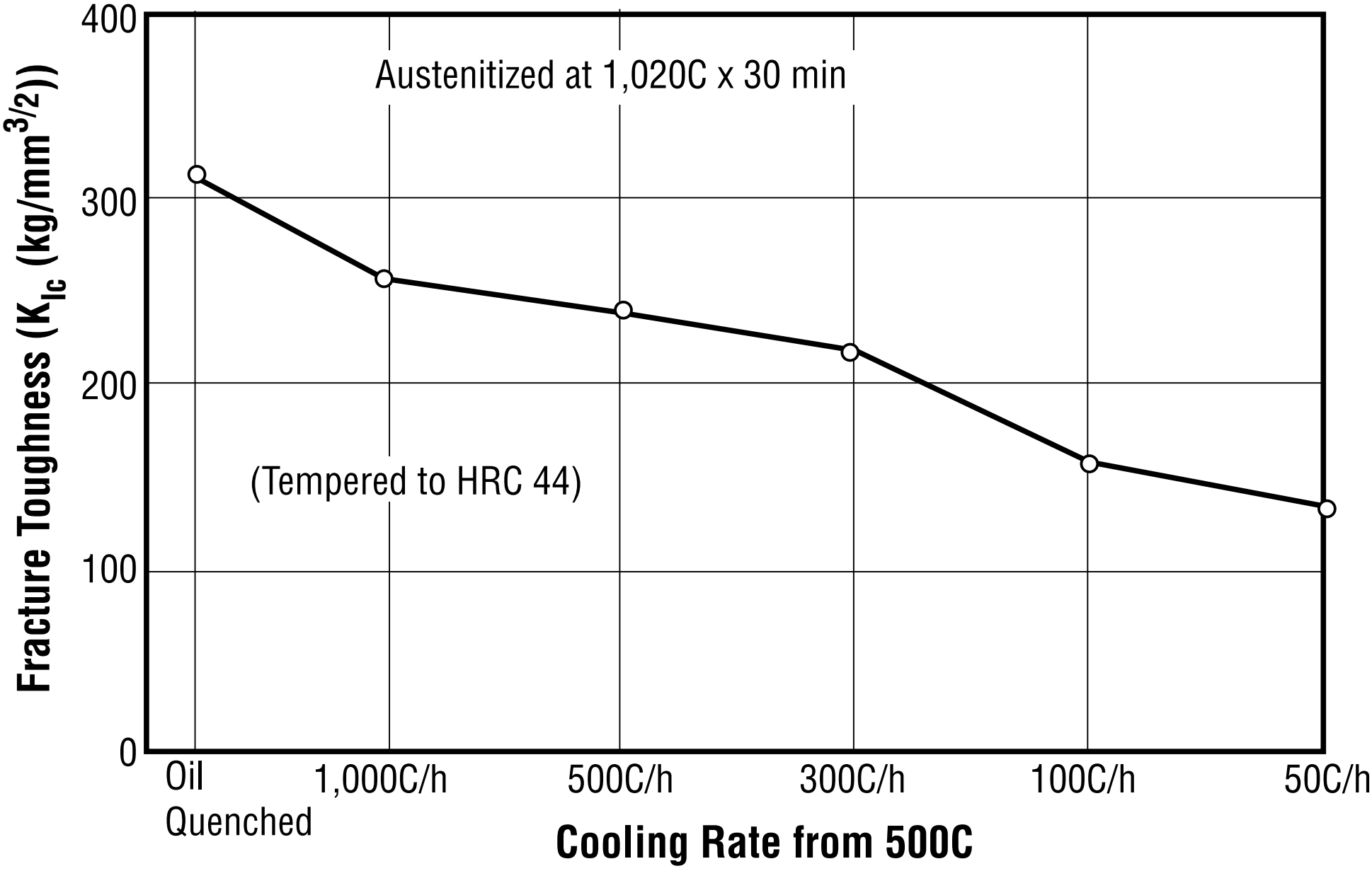

3.2.7.2.3 *[Figure]* Variation of room temperature plane strain fracture toughness K_{Ic} of heat treated H13 steel, austenitized at 1870F fro 30 min, quenched at various rates, and tempered to 44 HRC, as a function of quench rate (Ref. 76)

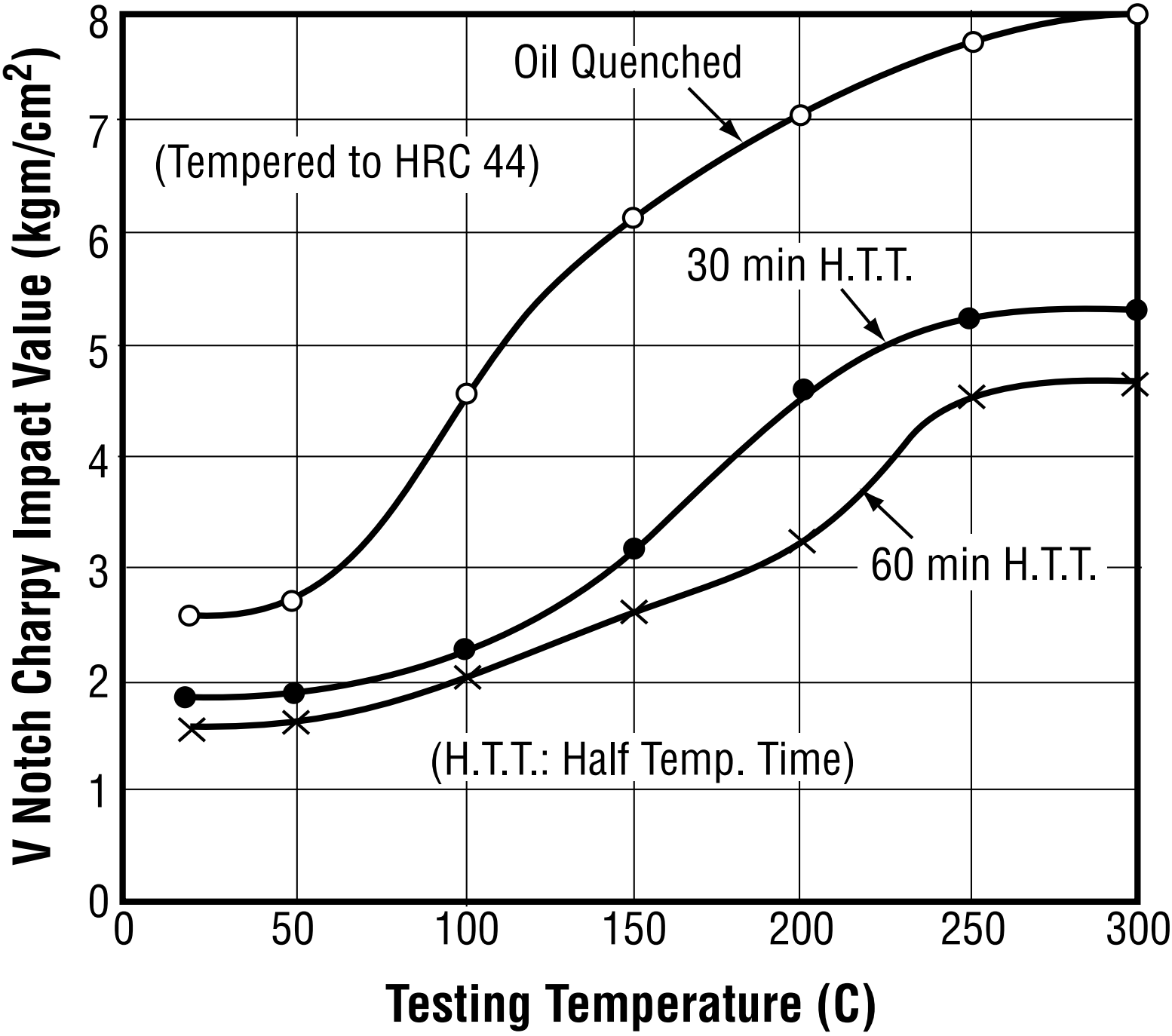

3.2.7.2.4 *[Figure]* Charpy V-notch (CVN) impact values of H13 steel quenched at various rates after austenitizing at 1870F for 30 min and tempered to 44 HRC (Ref. 76)

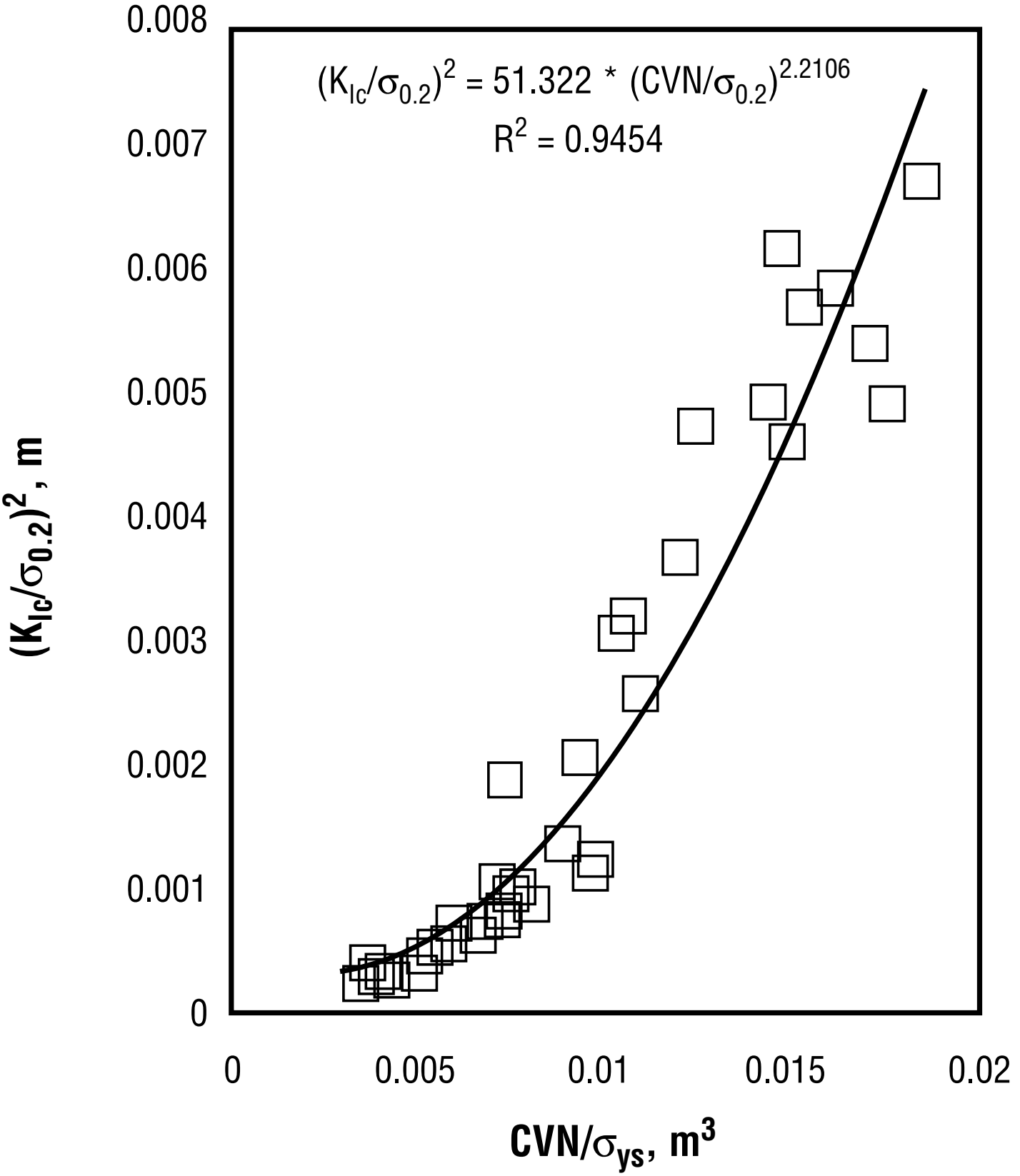

3.2.7.2.5 *[Figure]* Correlation between $(K_{Ic}/\sigma_{ys})^2$ and CVN/σ_{ys} at room temperature for H13/H11 steels (Ref. 77)

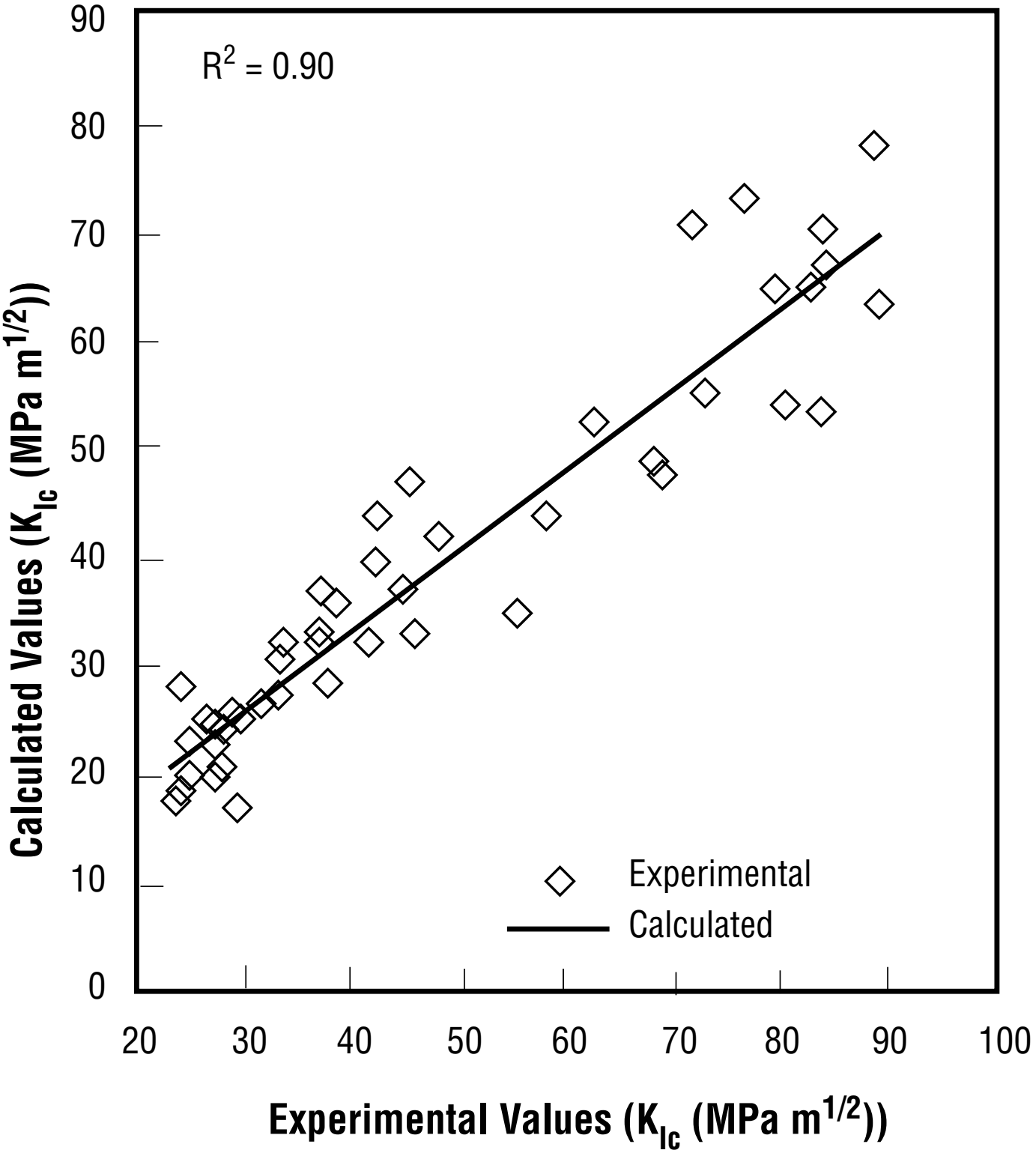

3.2.7.2.6 *[Figure]* Experimental values of K_{Ic} at room temperature compared with values of K_{Ic} calculated from CVN and HRC data at room temperature (see linear regression relationship in 3.2.7.2) for H13 and H11 steels (Ref. 77)

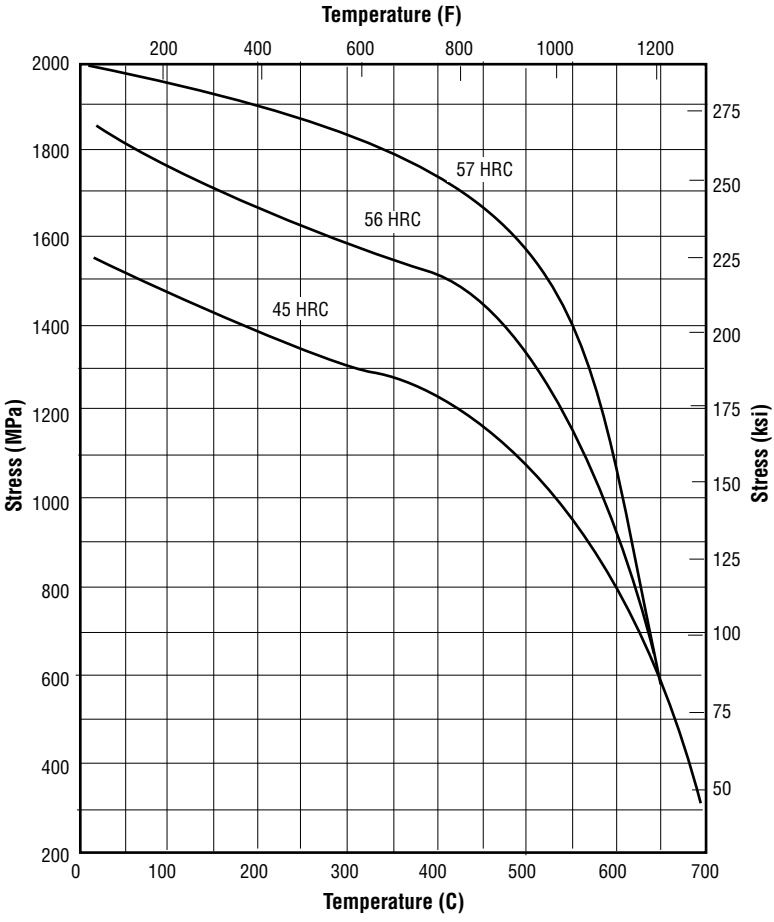

Figure 3.3.1.1 Effect of elevated temperature on tensile strength of H-13 steel heat treated to room temperature Rockwell C (HRC) hardness values given (Ref. 44)

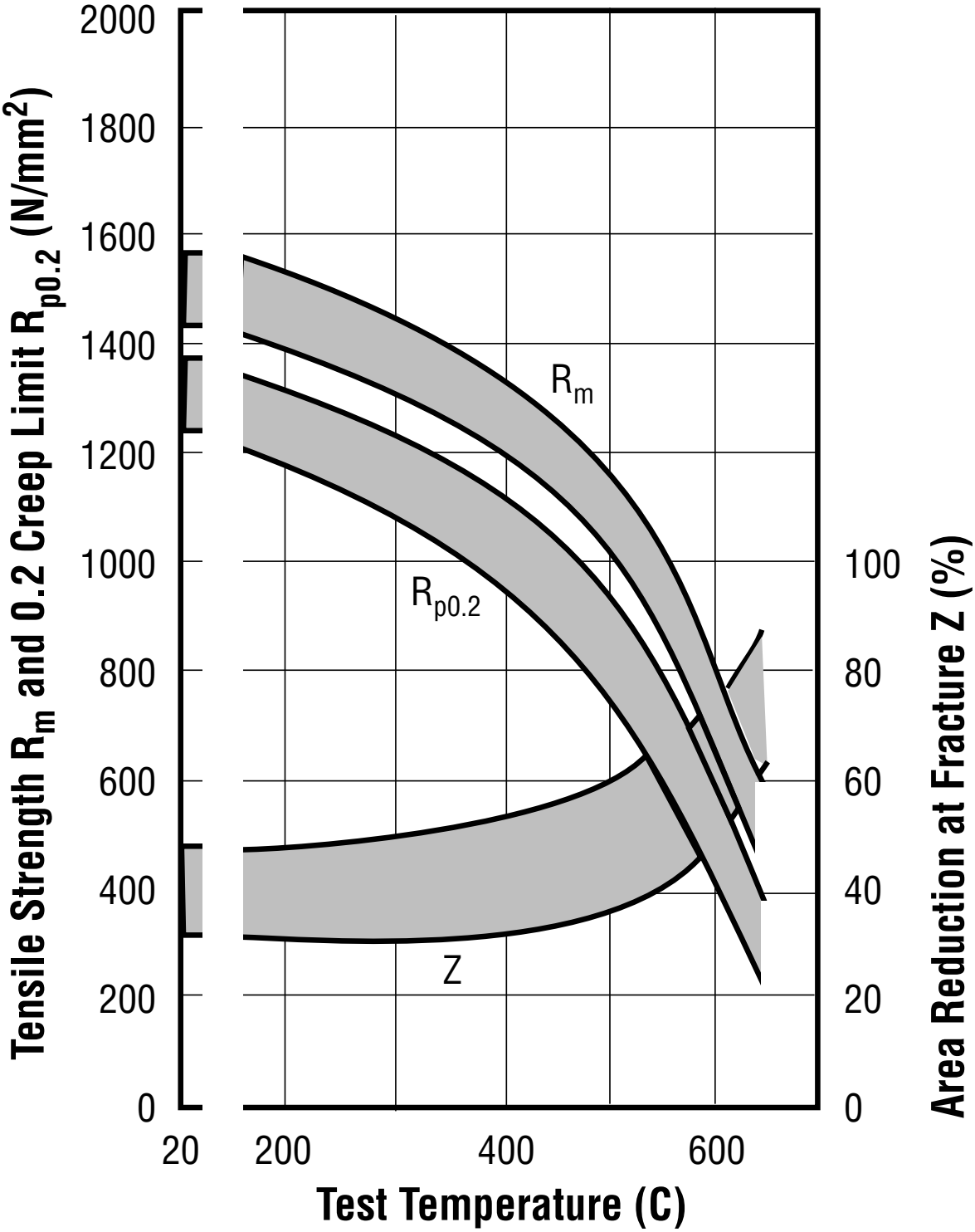

Figure 3.3.1.2 Effect of elevated temperature (C x 1.8 + 32 = F) on tensile and 0.2 yield (creep limit) strength (N/mm^2 x 0.145 = ksi) and reduction in area of H-13 steel heat treated to room temperature strength level given (Ref. 17)

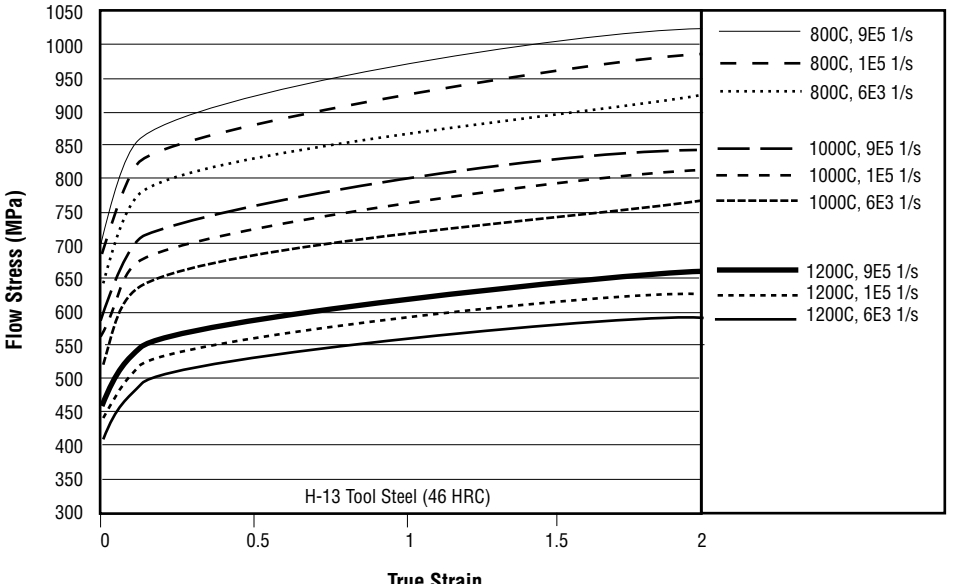

Figure 3.3.1.3 Flow stress (determined from modified Johnson-Cook model of flow stress and tuned by OXCUT computer program and experimental data from lathe machining experiments) of H-13 steel at temperatures of 800–1200C (1472-2192F) and strain rates of $6 \times 10^3 - 9 \times 10^5$ 1/s for H-13 steel originally at 46 Rockwell C (HRC) hardness (MPa x 0.145 = ksi) (Ref. 57)

Table 3.3.1.4 Elevated temperature tensile properties of heat treated H-13 steel (Ref. 16)

Test Temperature (F)	Room Temperature Hardness (HRC)	Yield Strength (ksi)	Ultimate Strength (ksi)	Elongation In 2 in. (%)	Reduction of Area (%)
700	51	229	264	12.5	23.0
500	48	--	210	11.0	35.0
750	48	--	197	13.0	46.0
1000	48	--	158	17.0	62.0
1250	48	--	73	24.0	80.0
800	44	138	171	17.0	56.0
900	44	128	156	20.0	65.0
1000	44	105	145	19.0	65.0
1100	44	88	110	22.0	69.0

Table 3.3.3.1 Charpy V-Notch properties of Nu-Die V (AISI H13) steel air cooled to room temperature from 1825/1875F, and double tempered (two hours minimum) to original room temperature (RT) hardness (Rockwell C or HRC) indicated and tested at elevated temperatures (Ref. 58)

Original RT Hardness (HRC)	Charpy V-Notch at Temperature F (ft-lb)				
	RT	500	1000	1050	1100
52	10	22	25	25	--
47	18	30	33	--	32
43	18	38	44	--	42

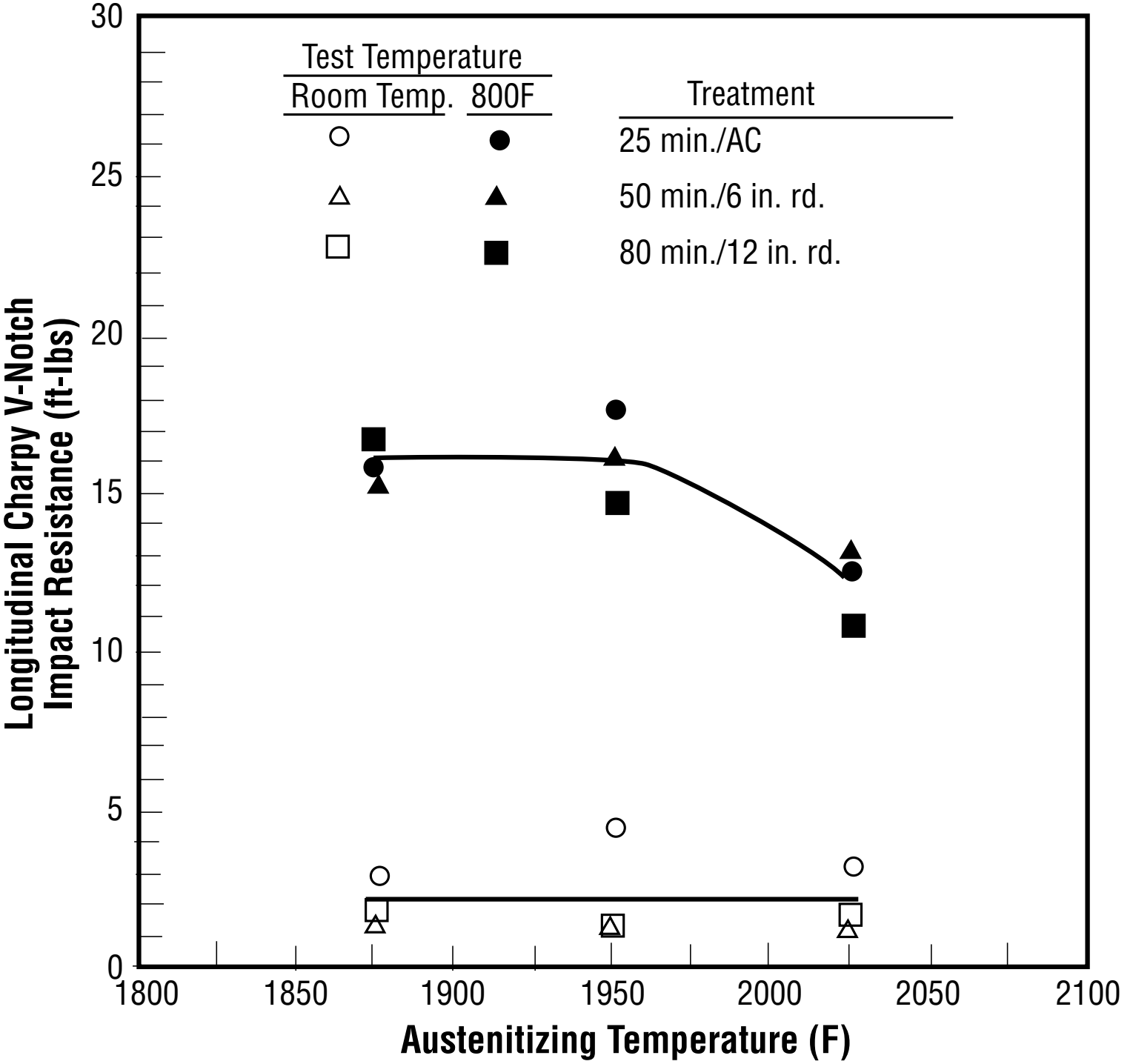

Figure 3.3.3.2 Longitudinal Charpy V-notch impact resistance versus austenitizing temperature for H-13 steel specimens austenitized for treatment times given, air quenched (small size specimens) or cooled to simulated quenching of 6- and 12-in. rounds, double tempered at 1000F (2 + 2 h), and subsequently tested at room temperature and 800F (Ref. 28)

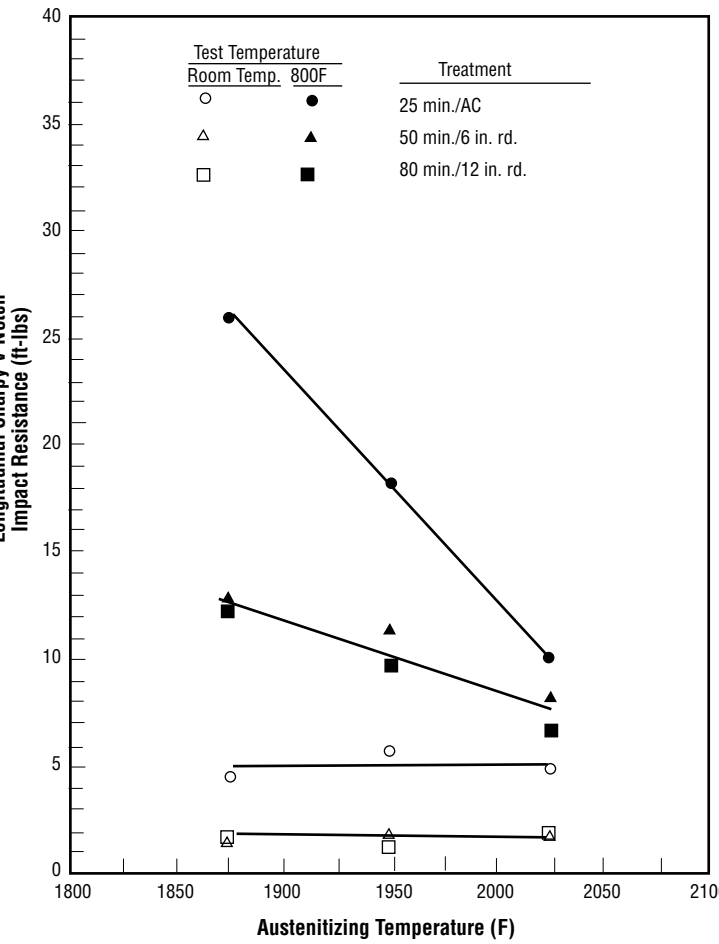

Figure 3.3.3.3 Longitudinal Charpy V-notch impact resistance versus austenitizing temperature for H-13 steel specimens austenitized for treatment times given, air quenched (small size specimens) or cooled to simulated quenching of 6- and 12-in. rounds, double tempered at 1100F (2 + 2 h), and subsequently tested at room temperature and 800F (Ref. 28)

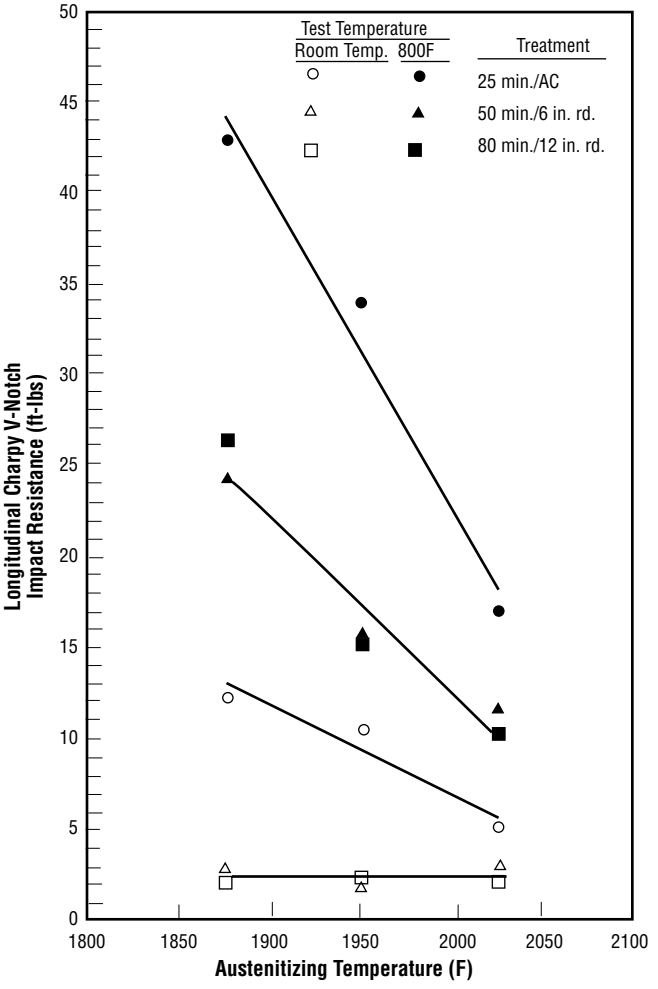

Figure 3.3.3.4 Longitudinal Charpy V-notch impact resistance versus austenitizing temperature for H-13 steel specimens austenitized for treatment times given, air quenched (small size specimens) or cooled to simulated quenching of 6- and 12-in. rounds, double tempered at 1150F (2 + 2 h), and subsequently tested at room temperature and 800F (Ref. 28)

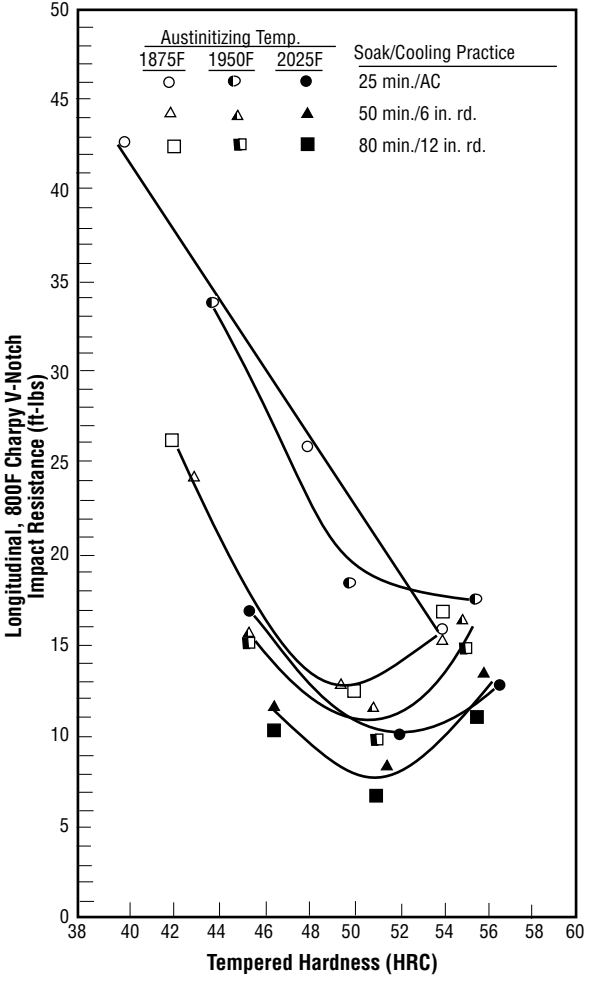

Figure 3.3.3.5 Longitudinal Charpy V-notch impact resistance versus tempered hardness for H-13 steel specimens austenitized at 1875, 1950, and 2025F for soak times given, air quenched (small size specimens) or cooled to simulated quenching of 6- and 12-in. rounds, tempered, and subsequently tested at 800F (Ref. 28)

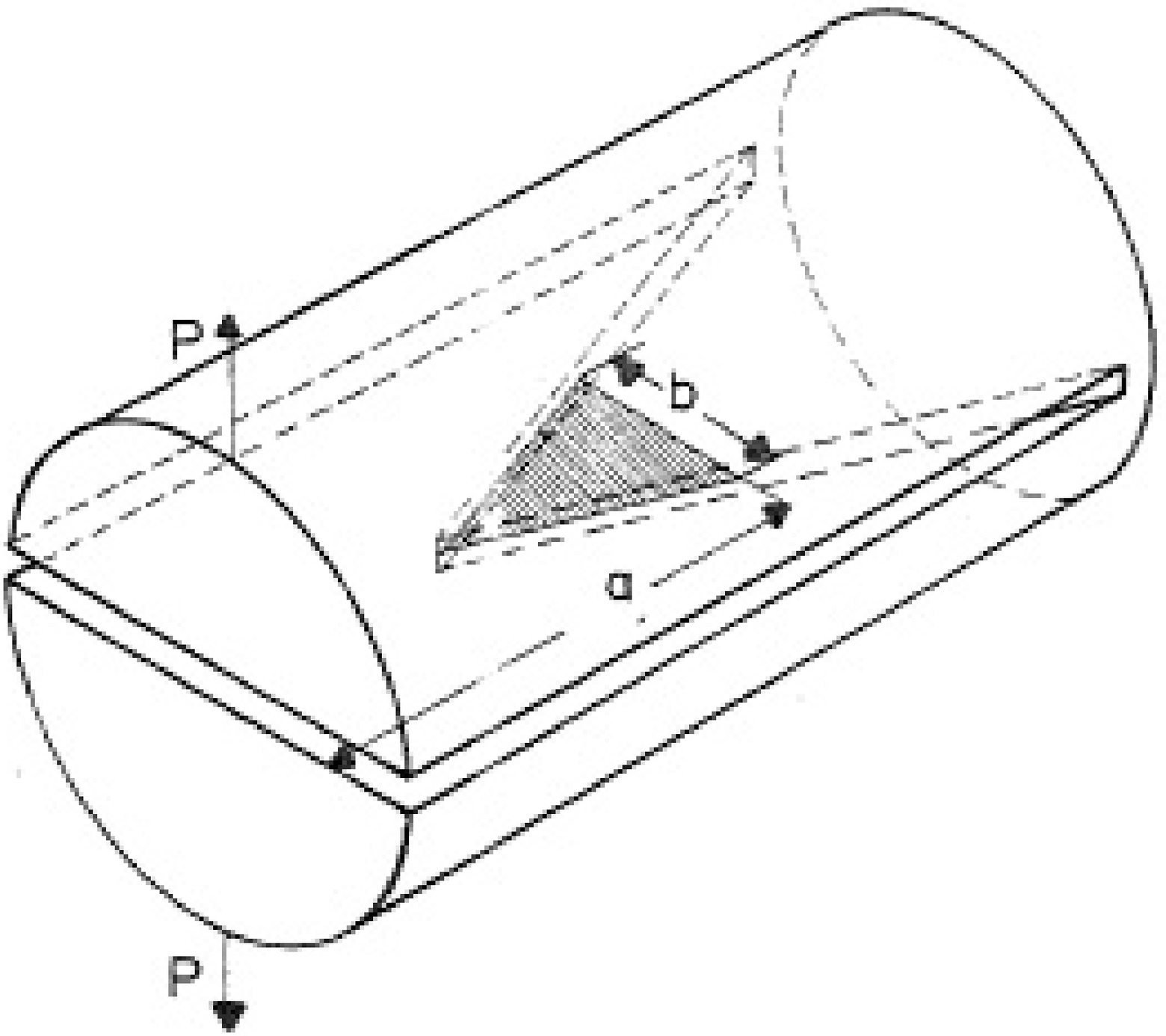

3.3.7.2.1 *Figure]* Short rod (chevron-notch) fracture toughness specimen used to obtain data shown in Figure 3.3.7.2.2 with shaded area denoting crack advance increment (Ref. 78, 79)

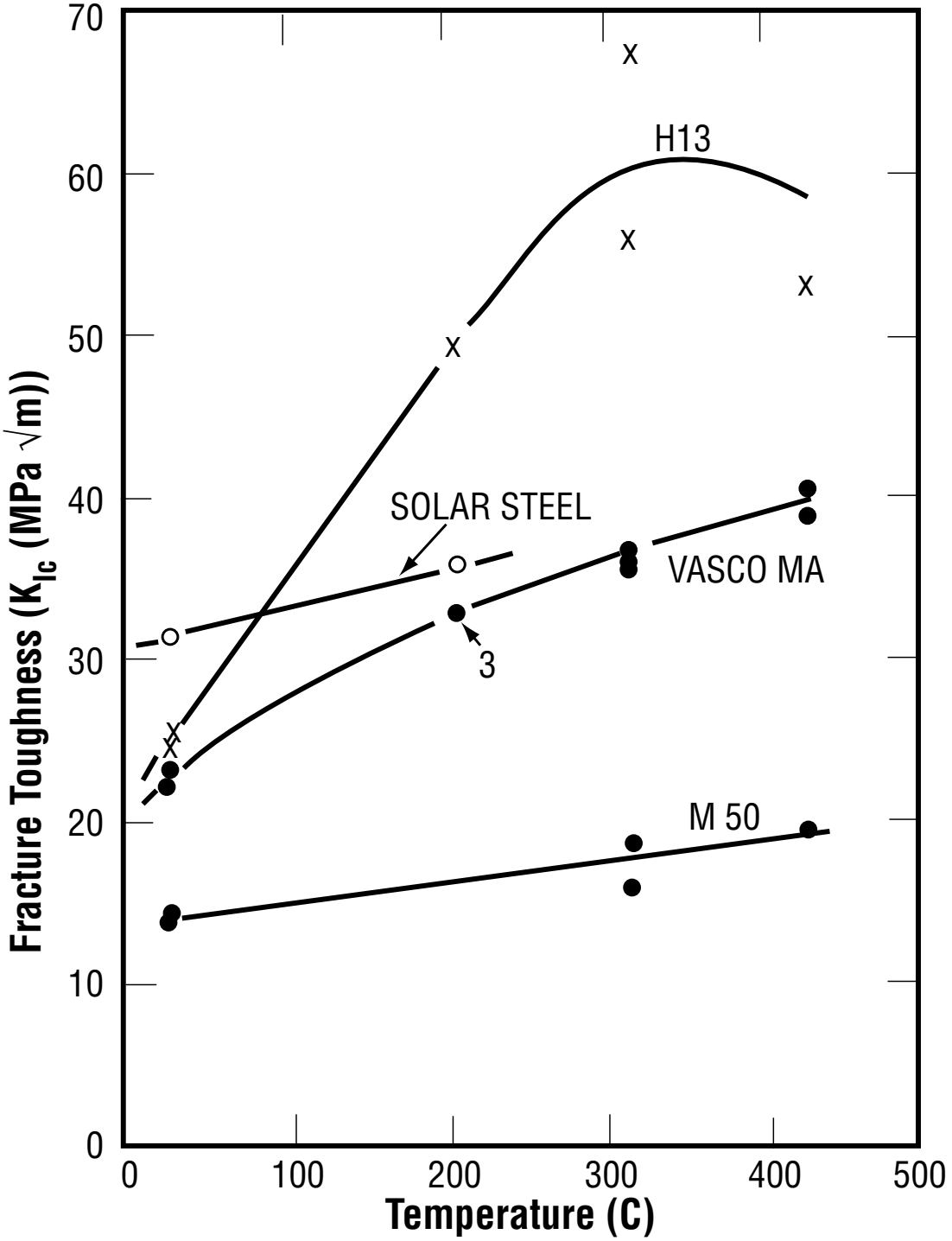

3.3.7.2.2 *[Figure]* Temperature dependence of K_{Ic} ($K\text{-}_{Iv} \sim K_{Ic}$) of H13 steel, VASCO MA ultrahigh strength steel, M 50 high temperature bearing steel, and S 2 tool steel used for drill bit bearings (SOLAR STEEL) (heat treatment and room temperature property data on these steels presented in Table 3.3.7.2.3) (Ref. 78)

Table 3.3.7.2.3 Heat treatments and room temperature properties of H13 and other steels tested for temperature dependence of plane strain fracture toughness with data as shown in Figure 3.3.7.2.2 (Ref. 63)

Steel	Austenitizing Temperature F	Quench	Temper	Austenitic Grain Size ASTM No.	Hardness HRC	Yield Strength ksi	Elongation %
H13	1825	Air	1000F, 2+2 h	8-9	54	238	9
VASCO MA	2040	Salt	975F, 2+2+2 h	8-9	59	292	6
M 50	2050	Salt	975F, 2+2 h	6-7	64	338	1.6
S 2	1580	Oil	375, 1 h	9-10	57	312	2

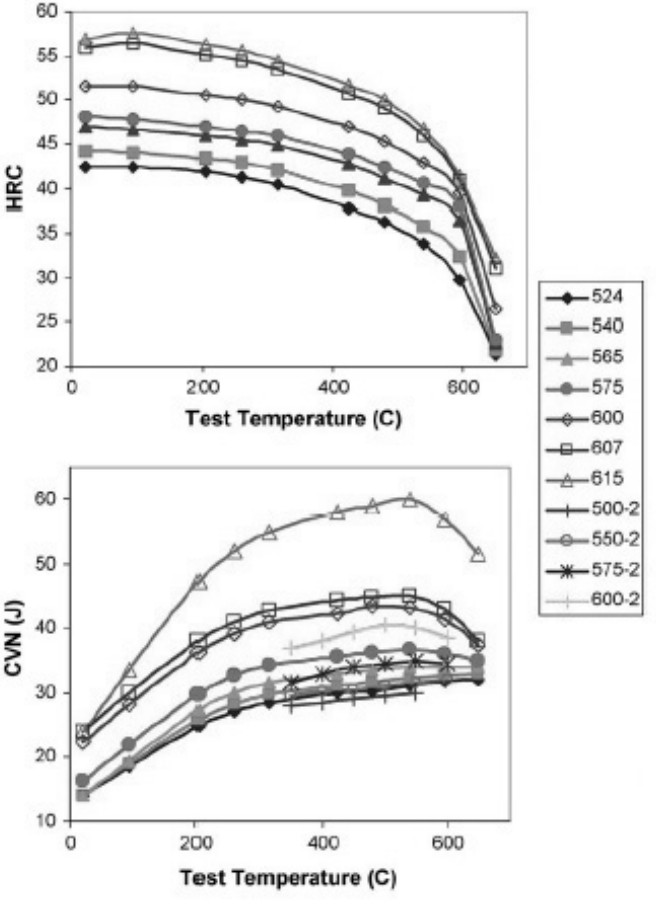

3.3.7.2.4 *[Figure]* Variation of HRC hardness and CVN Charpy V-notch values of heat treated H13 steel as a function of test temperature: H13 steel samples austenitized, quenched, and tempered to a room temperature hardness of 56-42 HRC at tempering temperatures given in insert (Ref. 80)

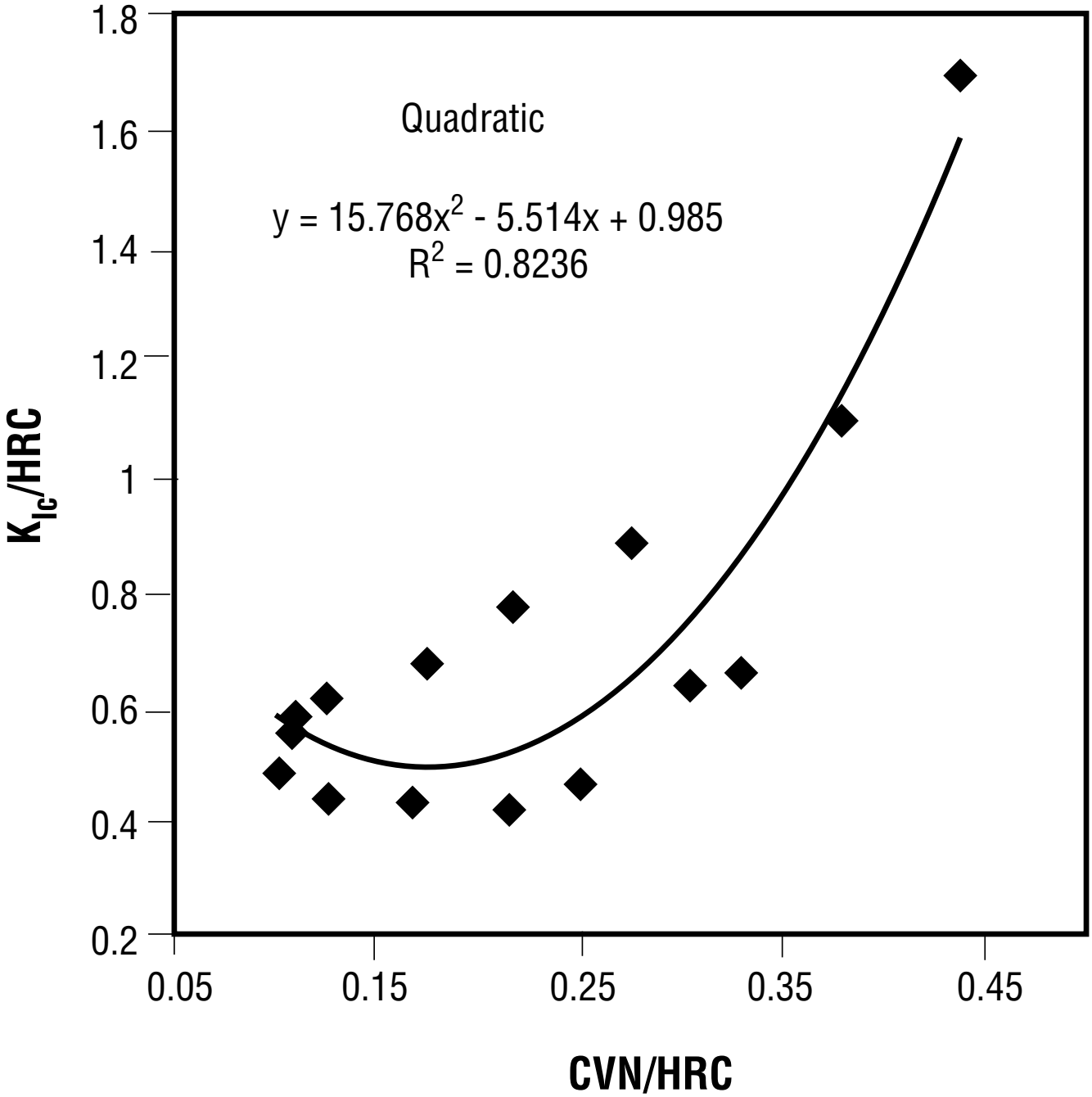

3.3.7.2.5 *[Figure] R*egression analysis showing quadratic fit of K_{Ic}, HRC, and CVN room temperature data for H13 steel heat treated by austenitizing, quenching, and tempering at various temperatures to a room temperature hardness of 56-42 HRC – assumed to hold at high temperatures if high temperature values of HRC and CVN are used instead (Ref. 80)

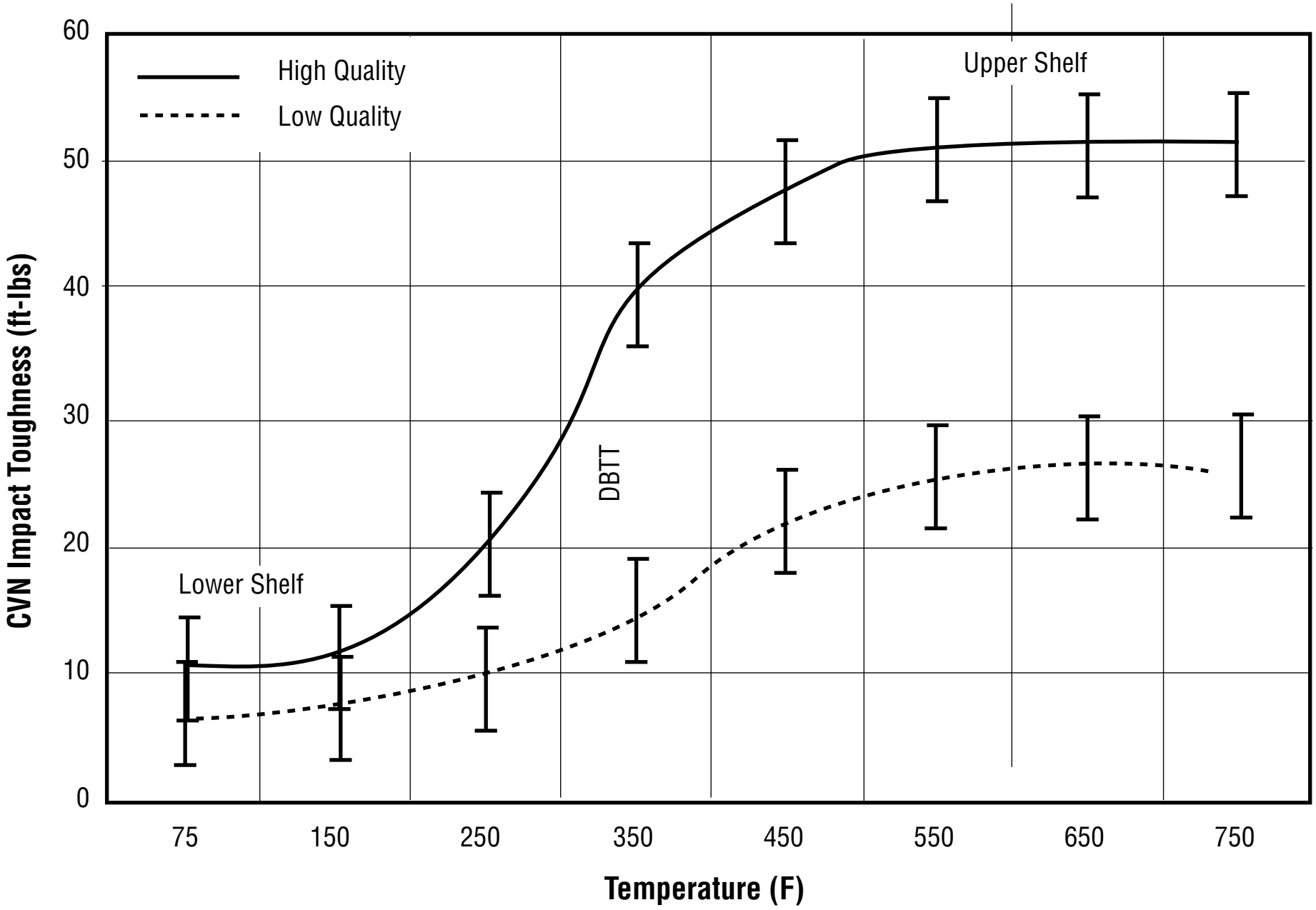

Figure 3.3.9.1 Representation of DBTT curves based on Charpy V-notch (CVN) tests of low quality and high quality H-13 tool steels heat treated as per NADCA 207-97 (3.1.1) (Ref. 60)

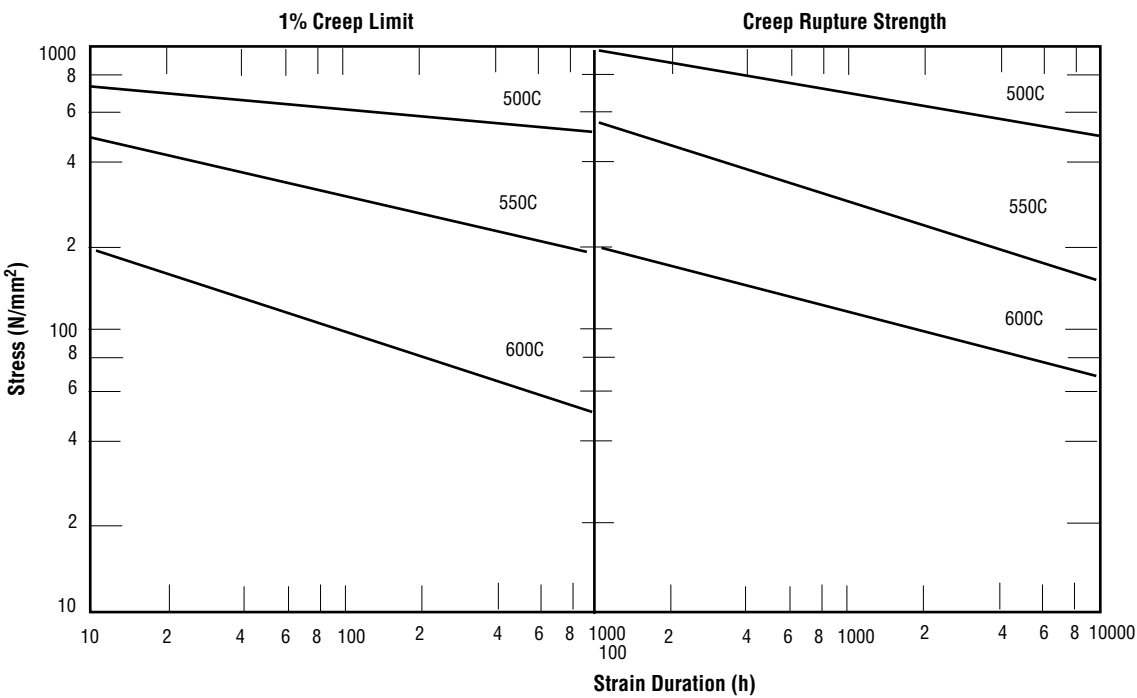

Figure 3.4.1 Creep characteristics of H-13 steel heat treated to 216 ksi room temperature tensile strength (~44-46 HRC): strain duration in h (to 1% creep limit – left or creep rupture – right) as a function of stress (N/mm^2 x 0.145 = ksi) at temperatures (C x 1.8 + 32 = F) indicated (Ref. 17)

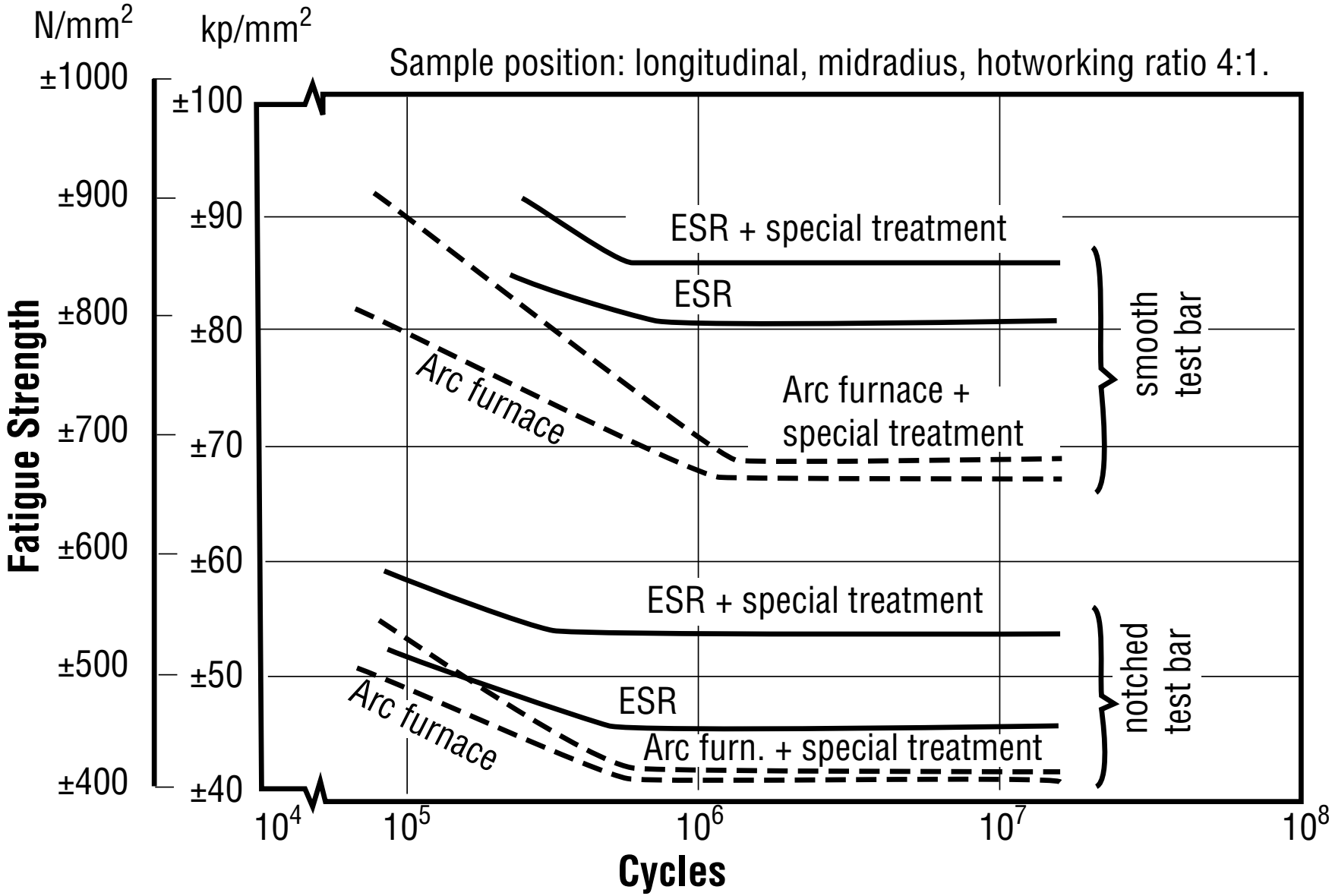

Figure 3.5.1.1 Fatigue strength (N/mm^2 x 0.145 = ksi) of smooth and notched specimens tested at room temperature in fully reversed tension-compression (R = -1) of hardened H-13 steel in relation to microstructural homogeneity achieved by electric arc air melted, ESR, and special treatment (patented Isodisc process) (Ref. 38)

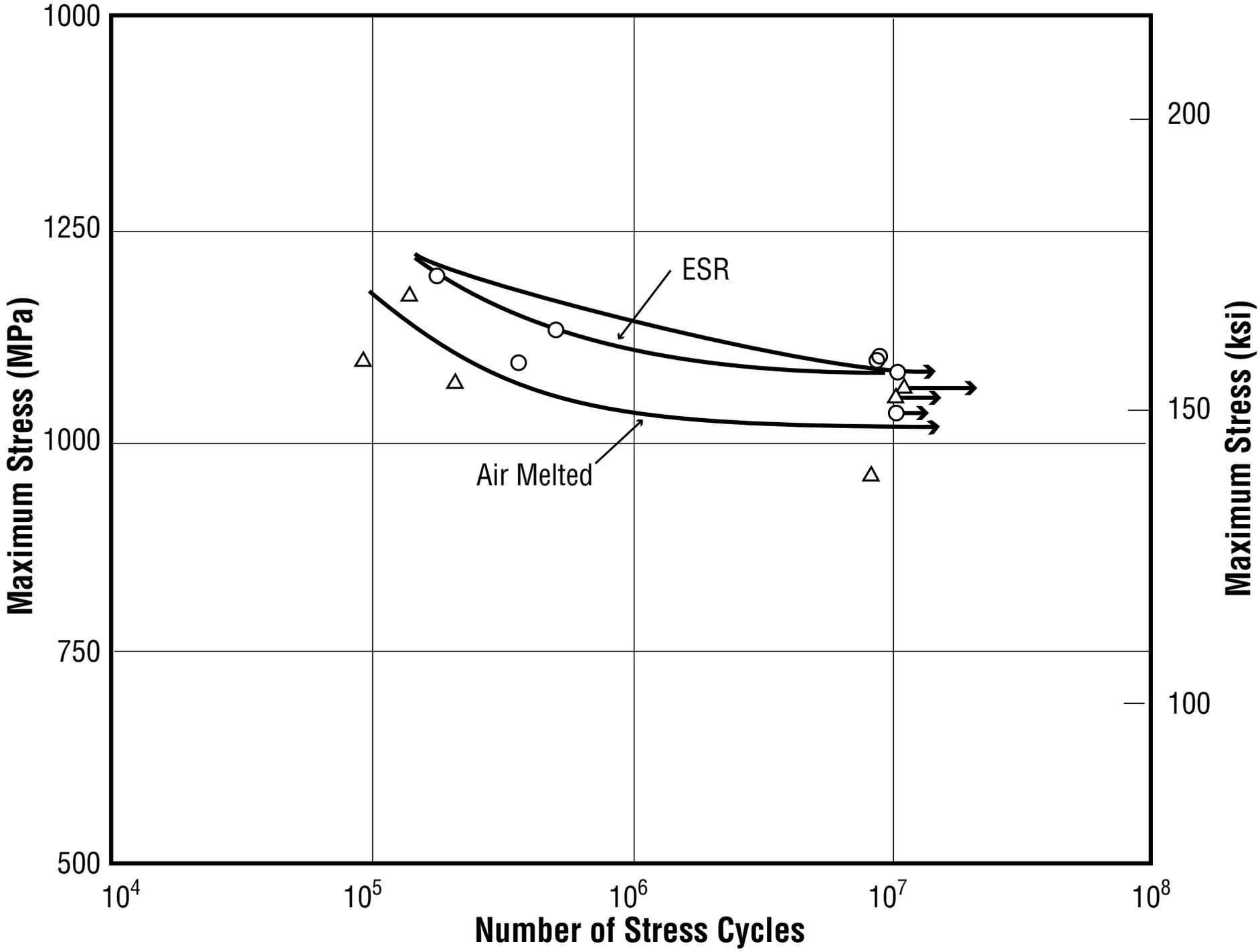

3.5.1.2 *[Figure]* Tension-tension (R = +0.2) fatigue curves determined at 60 Hz for longitudinal specimens of air melted (△) and ESR (❍) heats of H-13 steel in the hardened condition (austenitized at 1850F, oil quenched, and double tempered 2 + 2 h at 1090F to 48 HRC hardness) (Ref. 62)

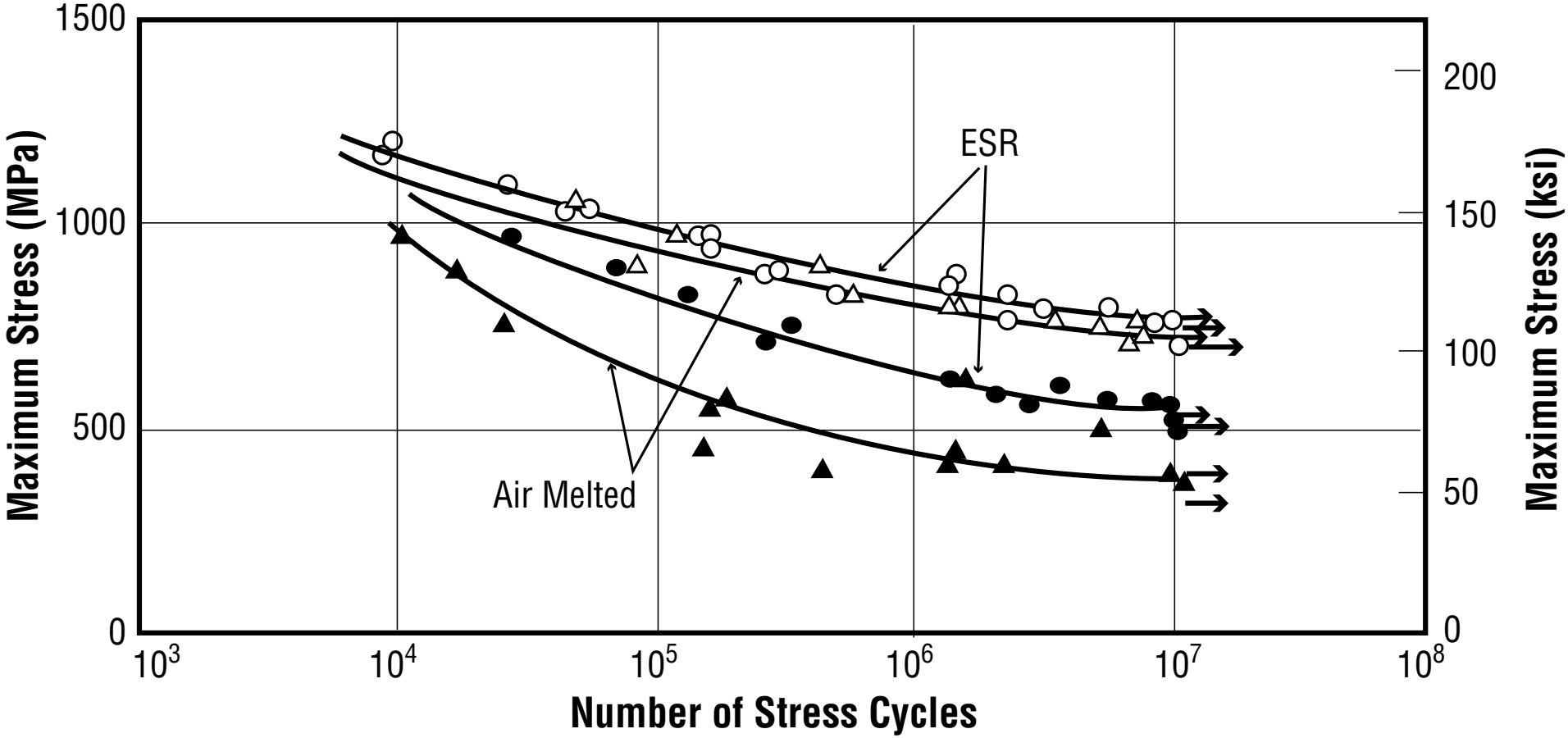

Figure 3.5.1.3 Fully reversed tension-compression (R = -1) fatigue curves determined at 60Hz for longitudinal (❍ – ESR, △ – air melted) and transverse (● – ESR, ▲ – air melted) H-13 steel in the hardened condition (austenitized at 1850F, oil quenched, and double tempered 2 + 2 h at 1090F to 48 HRC hardness) (Ref. 62)

Table 3.6.2.1 Modulus of elasticity of Thyrotherm 2344 ESR Magnum premium grade H-13 steel as a function of temperature (Ref. 18)

Temperature (F)	Modulus of Elasticity (ksi x 1000)
70	31.3
400	29.7
800	27.7
1200	24.8

Table 3.6.2.2 Modulus of elasticity of VDC H-13 steel as a function of temperature (Ref. 16)

Temperature (F)	Modulus of Elasticity (ksi x 1000)
70	30.0
200	29.0
400	27.0
600	28.5
800	27.5
1000	23.0

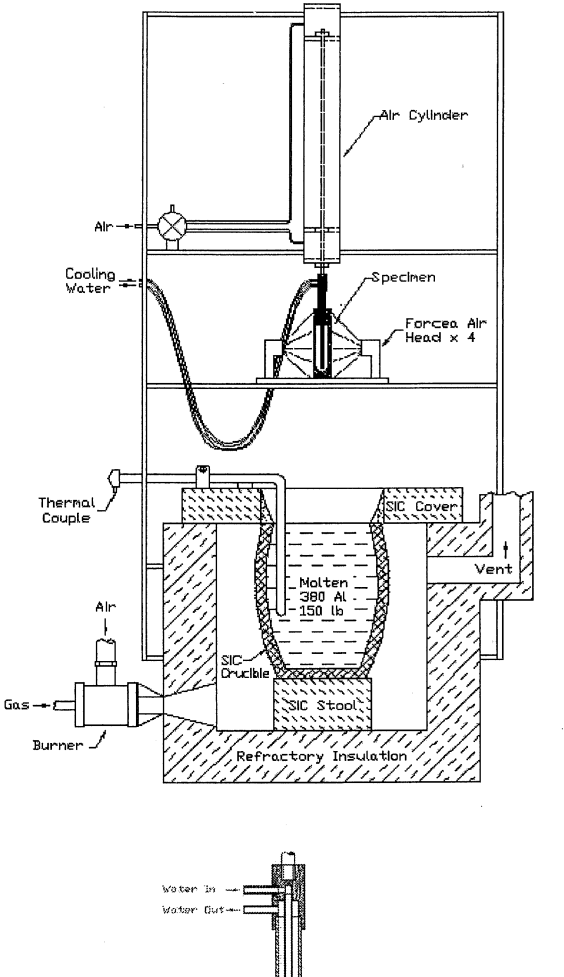

Figure 3.7.1.1 Schematic drawing of CWRU thermal fatigue test used in studying H-13 thermal fatigue and heat checking resistance showing apparatus used to dip specimen into molten A380 aluminum at 1300F (upper) and water cooled H-13 steel test specimen (lower) (Refs. 22–24, 48)

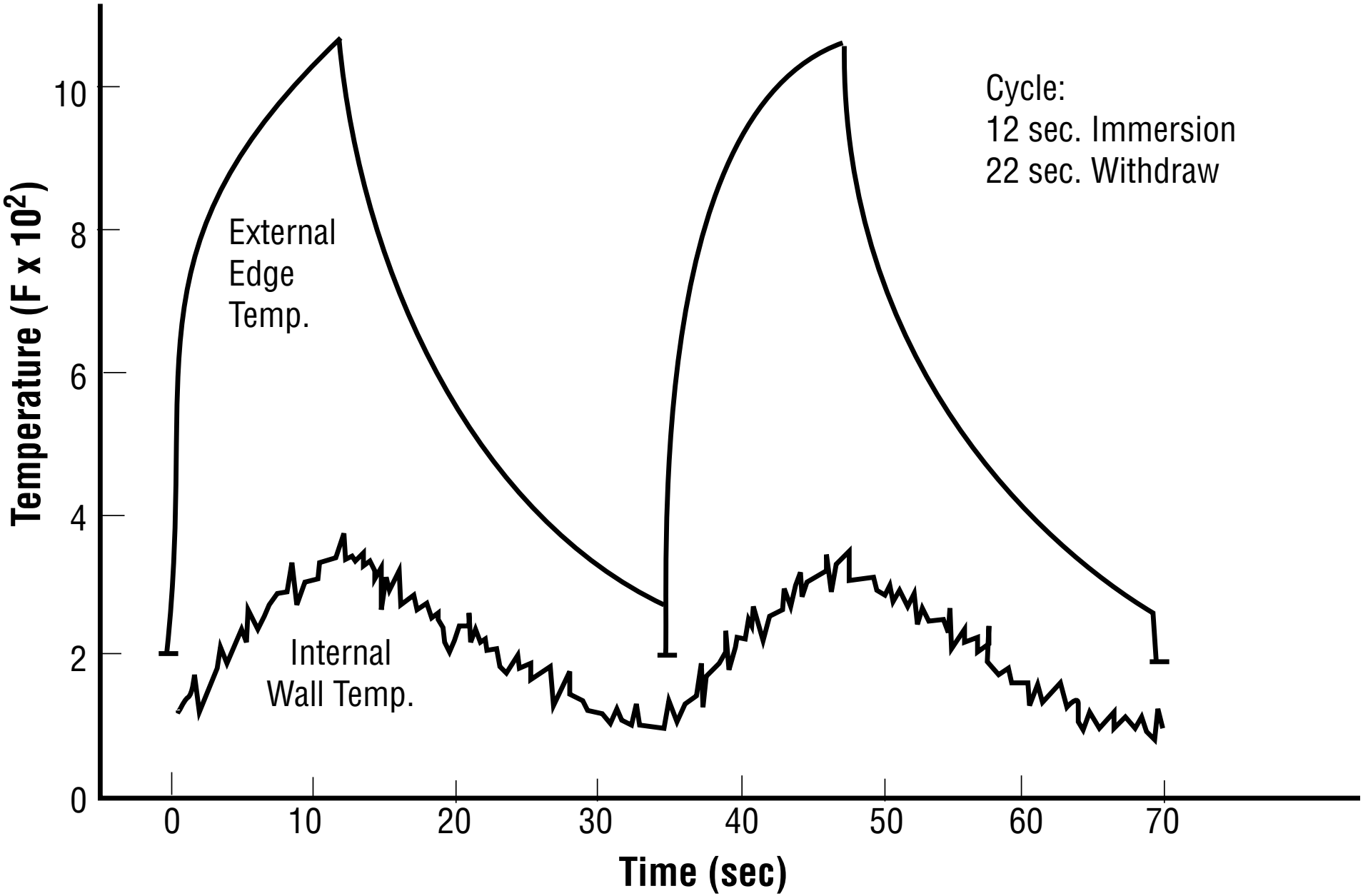

Figure 3.7.1.2 Thermal cycle used in determining thermal fatigue resistance of H-13 steel in the CWRU test for different austenitizing temperatures (Figure 3.7.1.3) and various types and grades of H-13 steel (Figure 3.7.1.4) (Refs. 22–24)

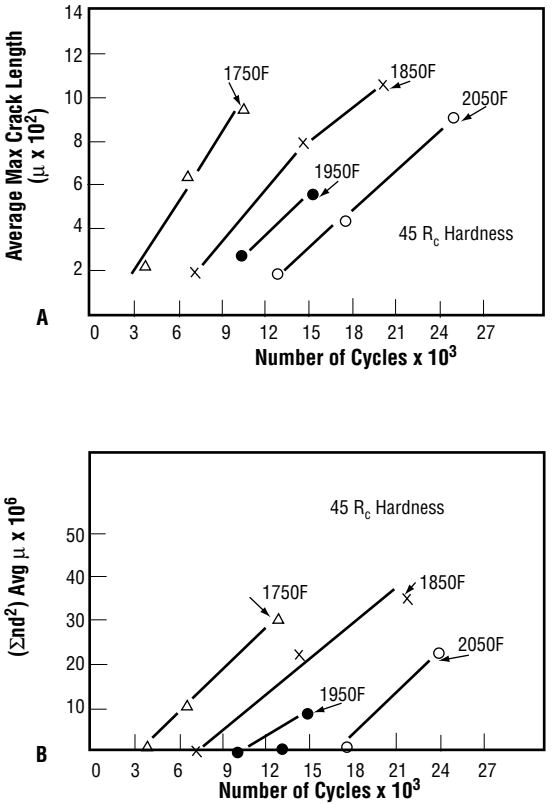

Figure 3.7.1.3 Thermal fatigue behavior in the CWRU test (Figure 3.7.1.1) of H-13 steel austenitized at 1750, 1850, 1950, and 2050F, air quenched, and all tempered to 45 R_c (HRC) showing average maximum crack length in microns (μ) (upper) and summation of total crack area (lower) as a function of number of cycles (Refs. 22–24)

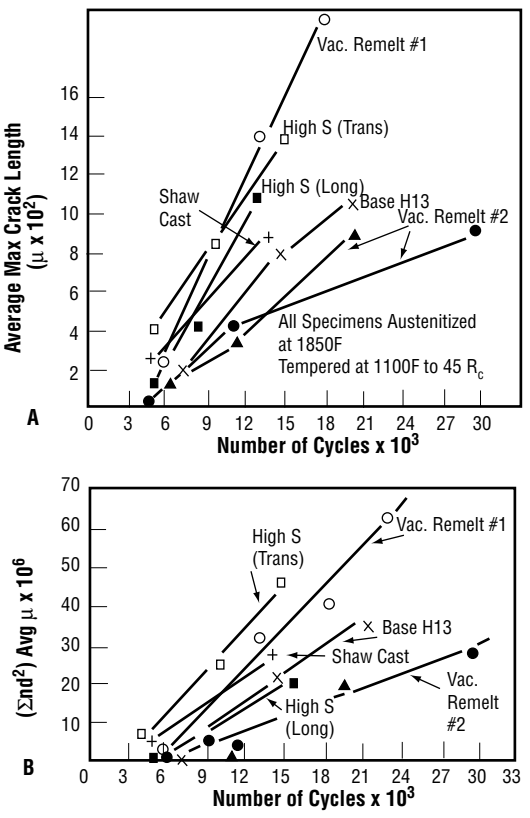

Figure 3.7.1.4 Thermal fatigue behavior in the CWRU test (Figure 3.7.1.1) of various types and grades of H-13 steel austenitized at 1850F, air quenched, and all tempered at 1100F to 45 R_c (HRC) showing average maximum crack length in microns (μ) (upper) and summation of total crack area (lower) as a function of number of cycles (Refs. 22–24)

Table 3.7.1.5 Chemical composition and inclusion ratings of H-13 steel materials tested for thermal fatigue resistance in the CWRU test (Figure 3.7.1.1) (Refs. 22–24)

H-13 Steel Type	Composition (wt. %)								Inclusion Rating per ASTM E 45-63			
	C	Mn	P	S	Si	Cr	Mo	V	Sulfide	Al_2O_3	Silicate	Globular Oxide
Base H-13	0.39	0.40	0.020	0.012	1.28	5.33	1.67	1.30	0.50	0.25	0	1.50
High Sulfur H-13	0.38	0.31	0.015	0.100	0.95	5.15	1.13	0.93	3.25	0.25	0	1.50
Vacuum Arc Remelted H-13	0.38	0.30	0.015	0.003	1.04	5.16	1.29	0.99	0.25	0	0	0.75
Cast H-13	0.38	0.37	0.018	0.015	0.85	5.63	1.68	1.21	0.50	0.25	0	1.75

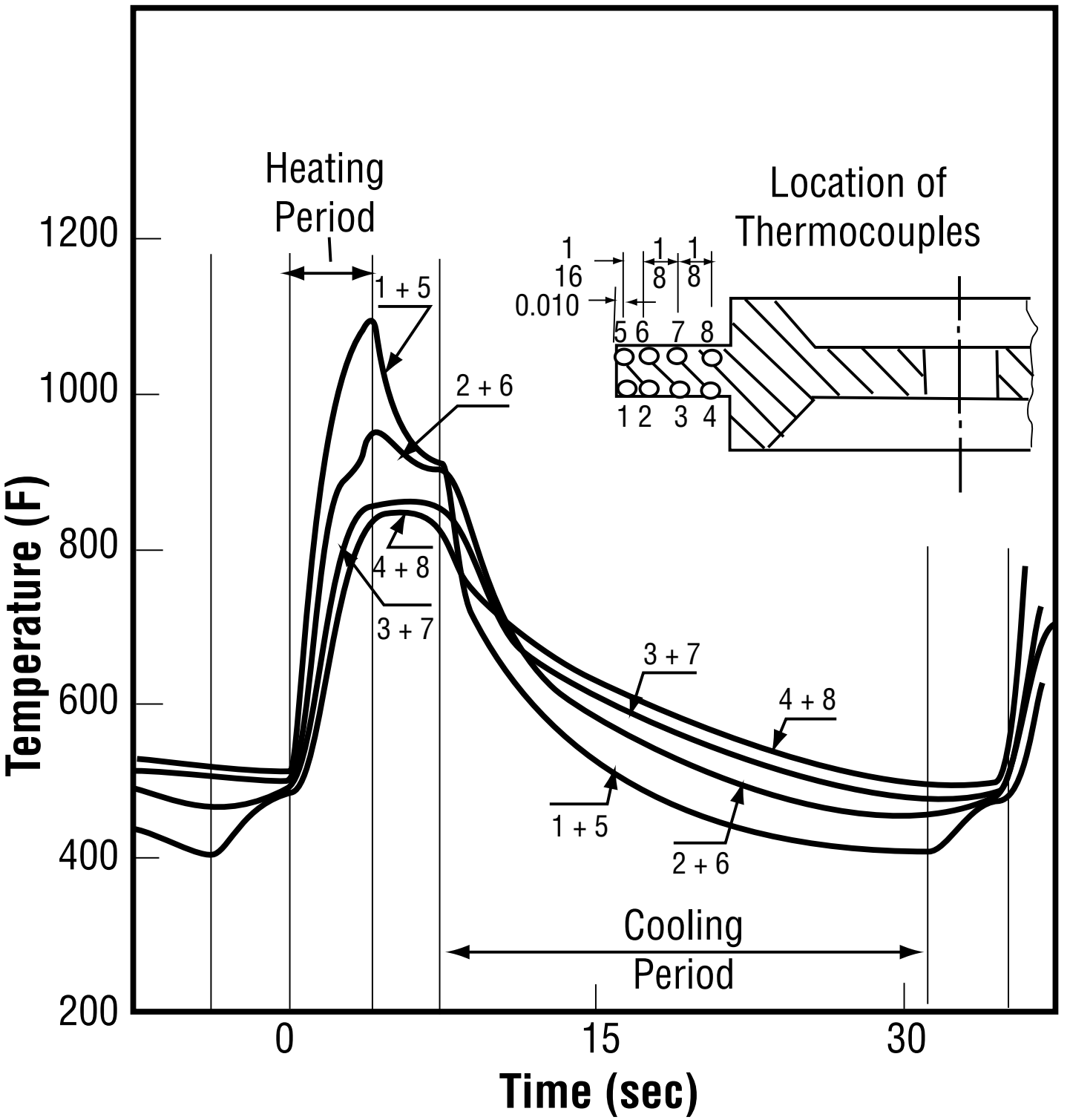

Figure 3.7.2.1 Heating and cooling curves for H-13 steel during a short cycle of thermal cycling between 1100 and 400F in the IITRI thermal fatigue test (Refs. 25, 66)

Table 3.7.2.2 Influence of initial tempered hardness of H-13 steel on thermal fatigue resistance measure in the IITRI thermal fatigue test according to the cycle shown in Figure 3.7.2.1 (Ref. 66)

Hardness (HRC)	Crack Initiation (No. Cycles)	Crack Growth to 0.08 in. (No. Cycles)
27	5,500	8,000
37	8,000	11,000
46	7,000	9,000

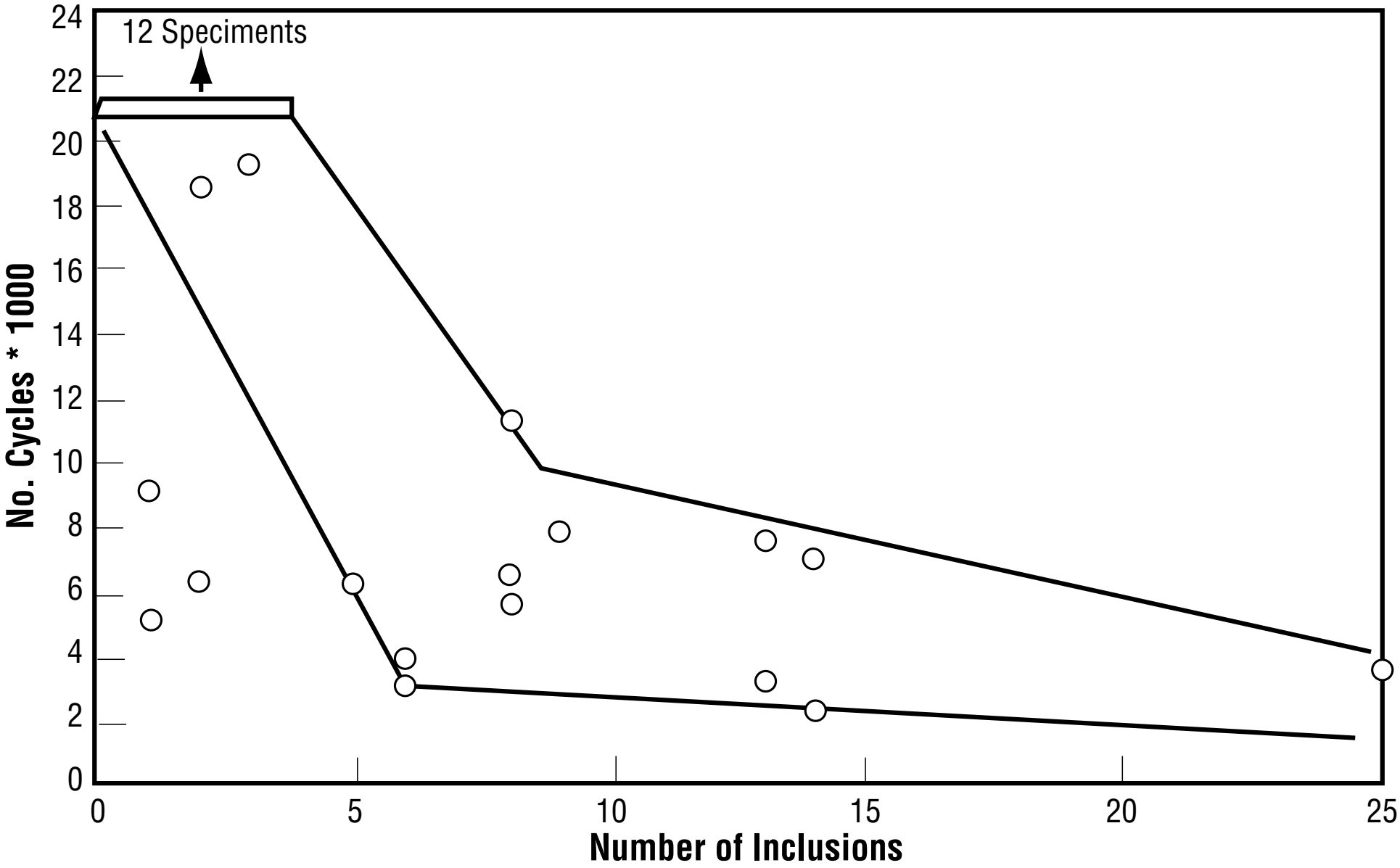

Figure 3.7.2.3 Number of cycles to crack initiation of H-13 steel in IITRI thermal fatigue test according to the cycle shown in Figure 3.7.2.1 as a function of cleanliness of the steel as rated by the number of +4 mm oxide inclusions at 320x magnification in 40 random fields (Ref. 66)

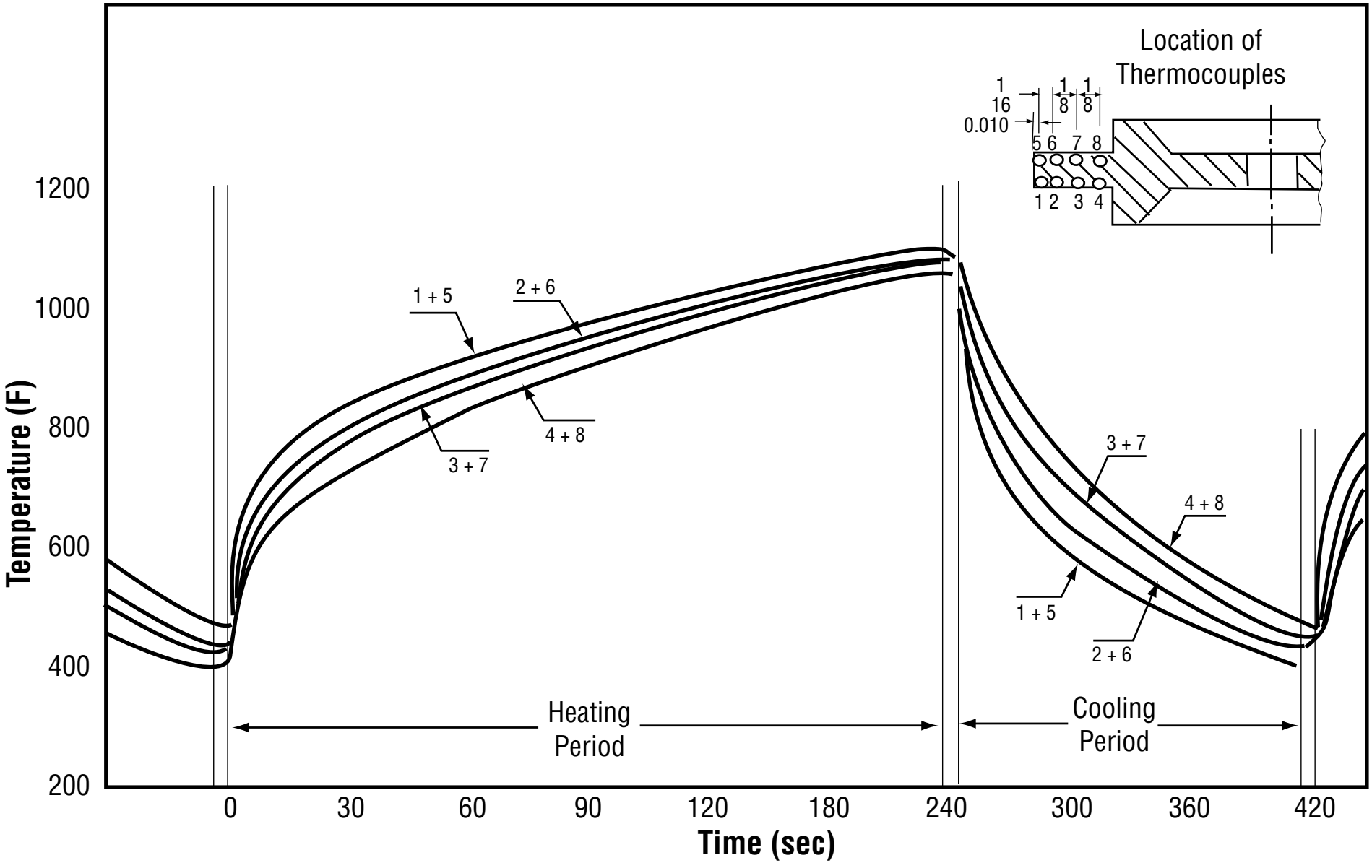

Figure 3.7.2.4 Heating and cooling curves for H-13 steel during a long cycle of thermal cycling between 1100 and 400F in the IITRI thermal fatigue test (Ref. 25)

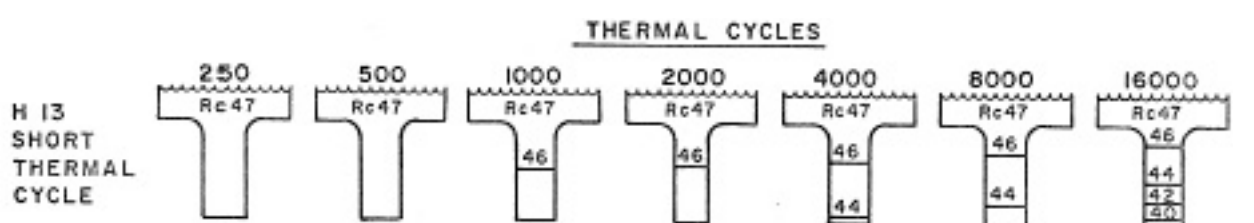

Figure 3.7.2.5 Tempering of IITRI thermal fatigue fins (HRC hardness noted on fins) during short and long thermal cycling for 250–16,000 cycles (Ref. 25)

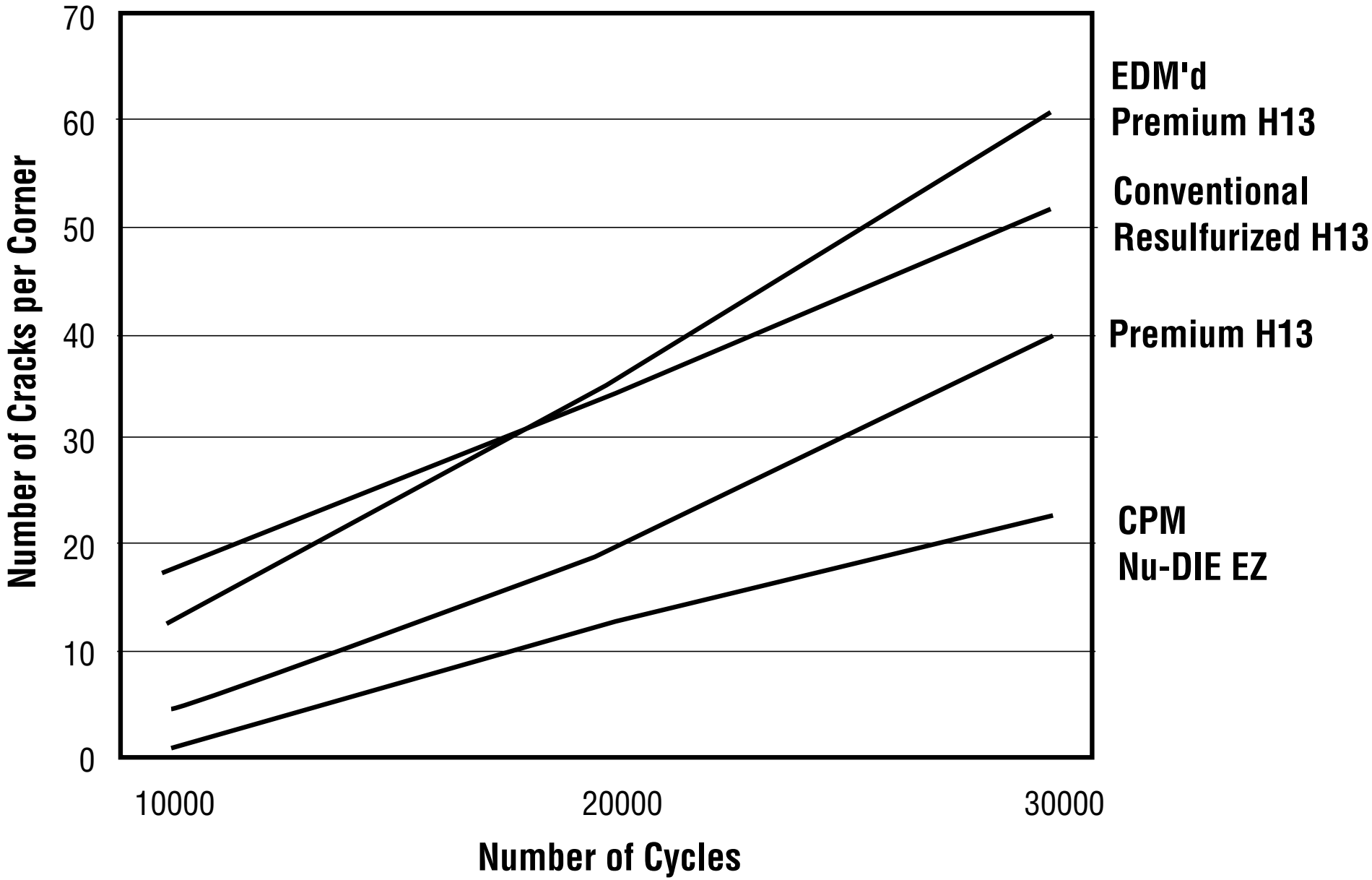

Figure 3.7.3.1 Thermal fatigue data from Crucible Steel Co. test (alternate immersion of square specimens in molten A380 aluminum at 1250F and quenching in a water bath at 200F with examination for cracks every 10, 000 cycles) (Ref. 43)

Table 3.7.3.2 Thermal fatigue/heat checking comparison of AISI H-13 and premium H-13 steel specimens (1.75 x 2.38 in.) heat treated to 47 HRC tested at 1,500 cycles of alternating heating at 1300F and quenching into hot water (Ref. 67)

H-13 Steel Grade	No. of Cracks	Avg. Crack Length (in.)	Max. Crack Length (in.)	Sum of 10 Longest Crack Lengths (in.)
AISI H-13	1,000	0.0020	0.0154	0.0626
Premium H-13	800	0.0014	0.0031	0.0256

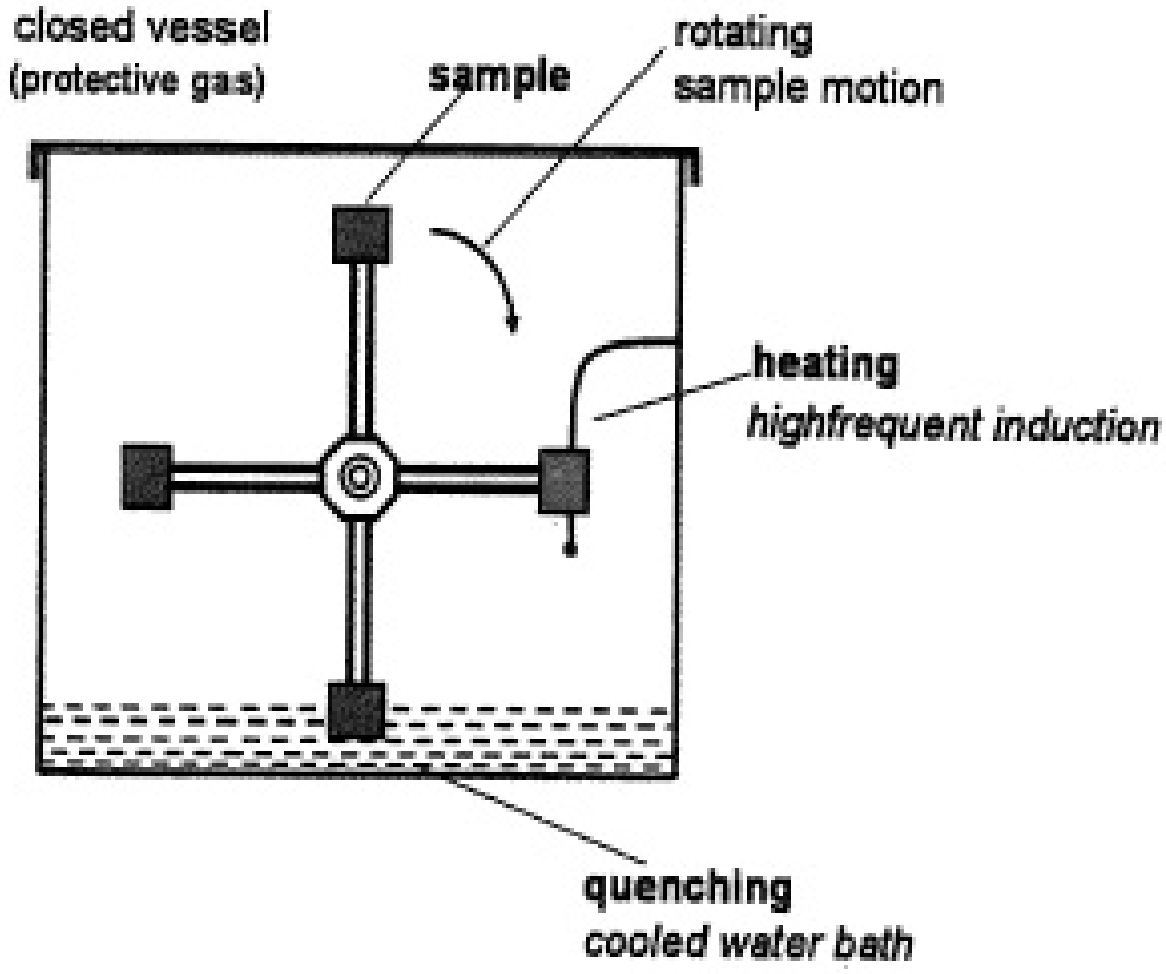

Figure 3.7.3.3 Thermal fatigue testing apparatus of EWK/Thyssen Krupp Specialty Steel: Ar atmosphere to avoid corrosion, induction heating to 1200F, water bath maintained at or near room temperature and at a pH = 10.5 to improve wetting, 2 x 2 x 0.40 in. H-13 steel samples cut from 30 x 8 in. forged slabs in transverse direction and rough machined, samples were hardened and tempered to 44-46 HRC and ground to a fine finish (Ref. 68)

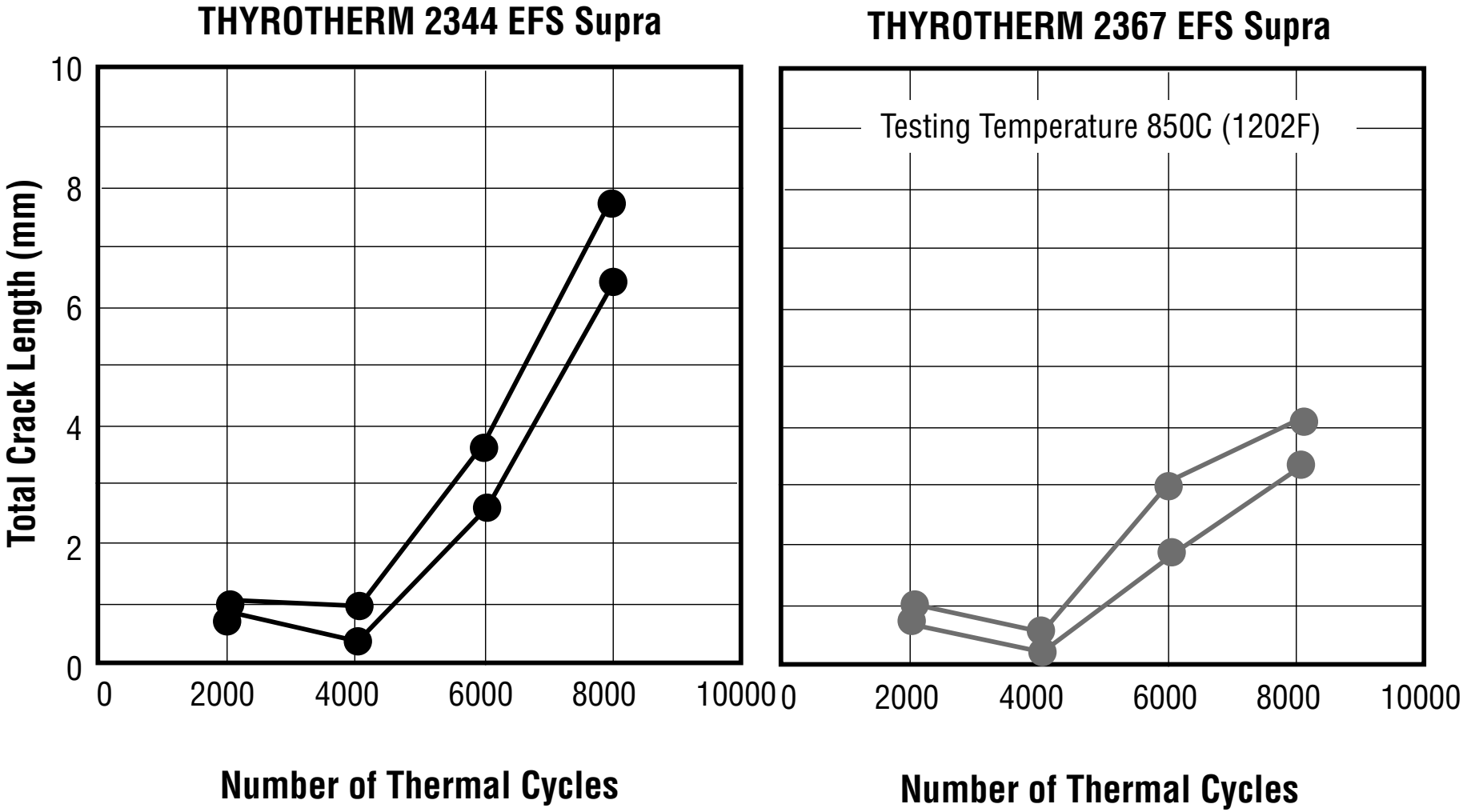

Figure 3.7.3.4 Total crack length measured on samples of a superior grade of AISI H-13 (Thyrotherm 2344 EFS Supra) and a modified grade of H-13 (Thyrotherm 2367 EFS Supra) heat treated to 44–46 HRC and tested in the EWK/Thyssen Krupp Specialty Steel thermal fatigue apparatus shown in Figure 3.7.3.3 (Ref. 68)

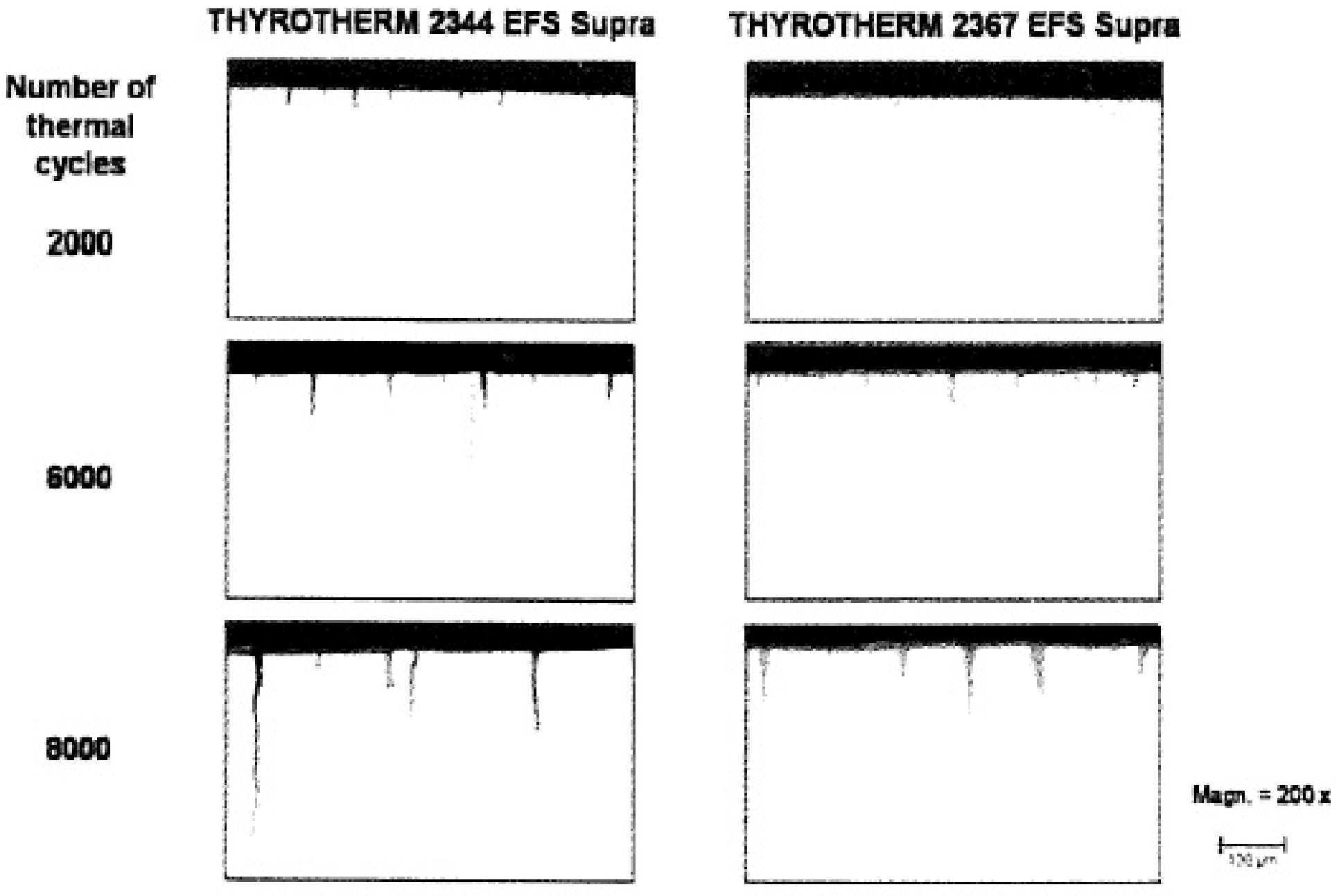

Figure 3.7.3.5 Microscopic evaluation at 200x of some thermal fatigue cracks developed in samples (Figure 3.7.3.4) from the EWK/Thyssen Krupp Specialty Steel thermal fatigue test (Figure 3.7.3.3) (Ref. 68)